

Review

A Comprehensive Review on Fly Ash-Based Geopolymer

Ismail Luhar ^{1,*}  and Salmabanu Luhar ² 

¹ Department of Civil Engineering, Shri Jagdishprasad Jhabarmal Tibrewala University, Jhunjhunu 333001, India

² Centre of Excellence Geopolymer & Green Technology (CEGeoGTech), Universiti Malaysia Perlis (UniMAP), Perlis 01000, Malaysia; ersalmabanu.mnit@gmail.com

* Correspondence: jprraj2017@gmail.com

Abstract: The discovery of an innovative category of inorganic geopolymer composites has generated extensive scientific attention and the kaleidoscopic development of their applications. The escalating concerns over global warming owing to emissions of carbon dioxide (CO₂), a primary greenhouse gas, from the ordinary Portland cement industry, may hopefully be mitigated by the development of geopolymer construction composites with a lower carbon footprint. The current manuscript comprehensively reviews the rheological, strength and durability properties of geopolymer composites, along with shedding light on their recent key advancements viz., micro-structures, state-of-the-art applications such as the immobilization of toxic or radioactive wastes, digital geopolymer concrete, 3D-printed fly ash-based geopolymers, hot-pressed and foam geopolymers, etc. They have a crystal-clear role to play in offering a sustainable prospect to the construction industry, as part of the accessible toolkit of building materials—binders, cements, mortars, concretes, etc. Consequently, the present scientometric review manuscript is grist for the mill and aims to contribute as a single key note document assessing exhaustive research findings for establishing the viability of fly ash-based geopolymer composites as the most promising, durable, sustainable, affordable, user and eco-benevolent building materials for the future.



Citation: Luhar, I.; Luhar, S. A. Comprehensive Review on Fly Ash-Based Geopolymer. *J. Compos. Sci.* **2022**, *6*, 219. <https://doi.org/10.3390/jcs6080219>

Academic Editor:
Francesco Tornabene

Received: 28 April 2022
Accepted: 18 July 2022
Published: 27 July 2022

Publisher's Note: MDPI stays neutral with regard to jurisdictional claims in published maps and institutional affiliations.



Copyright: © 2022 by the authors. Licensee MDPI, Basel, Switzerland. This article is an open access article distributed under the terms and conditions of the Creative Commons Attribution (CC BY) license (<https://creativecommons.org/licenses/by/4.0/>).

Keywords: geopolymers (GP); geopolymerization; fly ash (FA); fly ash-based geopolymer (FGP); ordinary Portland cement (OPC); greenhouse gas (GHG); setting time; drying shrinkage; efflorescence; alkali-aggregate reaction; hardening chemistry; three-dimensional (3D) structure; supplementary cementitious materials (SCM); CO₂ sequestration

1. Introduction

A burgeoning world population and the titanic development of global infrastructures have generated an exigency for colossal quantities of construction materials across the planet. For these reasons, the manufacturing of concrete is estimated to reach greater than one ton per annum per head [1]. This escalating demand for concrete, in turn, has resulted in an energetic demand for ordinary Portland cement (OPC), a primary binder of the concrete. Disappointingly, the existing course of action for the production of OPC is not merely a costly, user-hostile and energy-intensive process of looking for calcinations, but it is also not an eco-benevolent one, since it emits embodied CO₂ (carbon dioxide), a primary greenhouse gas (GHG), into the atmosphere, which is liberated from the decomposition of fossil fuels and limestones—the chief raw material of OPC [2,3]. Unfortunately, 1 ton of OPC production emits an almost equal quantity of CO₂ into the environment [4]. In simple statistics, “more is the production of OPC, more will be the emissions of CO₂, and at the same time, more will be the degradation of confined natural resources” [5–8]. By and large, CO₂ emissions alone are answerable for 65% of global warming, out of which OPC production is single-handedly accountable for roughly 6% of the total emissions of carbon dioxide [9]. This has created a great dilemma for environmentalists and a red signal to the breathing communities on the earth [10].

All these negative impacts have twisted the arms of researchers, concrete technologists and scientists to search for alternate materials for construction, which must certainly be user and eco-benign, durable, sustainable, affordable, essentially cost-effective, and can lend a helping hand in the saving of limited natural resources [11–14]. These are the root causes of the attraction by many researchers towards innovative geopolymer technology and geopolymer composites such as GP-cements, GP-pastes, GP-mortars, GP-concrete, etc. Geopolymers can be synthesized using low energy, a lower temperature, by expending low cost and by utilizing diverse profuse wastes as either precursors or supplementary cementitious materials (SCM), offering a solution to the systematic disposal of materials such as fly ash, metakaolin, ground granulated blast furnace slag, etc. Of these, FA is the key solid waste generated as a by-product from coal-firing power plants, for which thermal electricity stations seek ways in which to dispose it in an economical and environmentally beneficial way, along with CO₂ sequestration [15,16]. A deeper understanding of the physical–chemical and mechanical properties of the fly ash is, therefore, essential for its review in both natural and modified forms.

Geopolymer is a novel production of inorganic alumino-silicate polymer with a network structure that is similar to zeolite in three-dimensional (3D) form, which comprises an Al and Si tetrahedral network and can be produced through the process of geopolymerization. This means the activation of either material, geological or industrial origin in the form of by-products, as a precursor that is rich in alumina and silica [17–21]—such as fly ash with alkali activators, most commonly, silicate, carbonate and hydroxide of sodium, etc. [22,23]. Globally, researchers are inclined towards this novel technology on account of its key benefits such as the simple process of production with lower energy consumption, and the efficient use of industrial and other diverse wastes [24–26]. Consequently, geopolymer is known for the mitigation of CO₂ emissions and its brilliant engineering properties viz., resistance to sulphate [27–31] and acid attacks [30–34]; excellent freeze–thaw cycle [35]; resistance to chloride penetration [27,36,37], etc. These properties will establish it as a potential substitute of OPC. By and large, the display of geopolymer performances is found to be analogous or sometimes even better than OPC properties [38–44], on account of their dissimilar products of hydration and microstructure [41–43]. Activator dosages and curing conditions, along with the kind and attribute of raw material, have a momentous influence on the microstructure and hydration attributes of geopolymers, making the study of them thornier. Firstly, well-known past researchers of concrete [44–50] have summarized the achievement of research in the context of investigating geopolymeric cement, as well as geopolymer concrete, prior to 2005 quite methodically. The past couples of decades have witnessed scores of scientific advancements in the technology of geopolymer, and insights into the fly ash-based geopolymer performance. The rapidly developing knowledge of this innovative technology has, in turn, resulted in several amendments of methods to noteworthy enhance the performances and manufacturing of the geopolymer that is based on fly ash. The wide-ranging application of fly ash-based geopolymer in the construction and infrastructure industries has proved to be assuring. Preceding studies have revealed that, in comparison to the conventional OPC, GP cement is a modern inorganic polymer with a low carbon footprint [45], fewer energy necessities, as well as the low consumption of resources [46,47]. Moreover, GP is a grouping of cement, ceramics and polymers, with the characteristics viz., early higher strength, superior resistance to acid, sulphates, fire, heat, ample raw material resources, a simple process of production, cost-effectiveness, etc. [51,52]. Over the past three decades, these brilliant attributes have made GP viable to be employed extensively as edifice materials, to immobilize nuclear wastes, for use in aerospace fields, as emergency mends, for resource utilization and for the protection of the environment, etc. [53–55]. Recently, emerged GP is viable to be employed extensively as edifice materials. Based on the research papers on GP; a summary of the assessment of the development of fly ash-based geopolymers; their benefits, properties, applications, and existing challenges in the pathway of these novel construction composites, etc., a scientometric review of them has endeavoured, besides essential future works, to promote

them as acceptable building composites, providing a reference for the potential advance in research and utilization of this GP-material [56,57].

The current manuscript comprehensively reviews the fly ash-based geopolymers with respect to the most recent advancements and developments in these most attractive, innovative, low-carbon footprint geopolymer composites, with their rheological properties, setting behaviour, structural characterization, dimensional stability, durability, mineralogy, chemistry of geopolymerization, hardening mechanism, classification, structure and terminology; as well as their applications, advantages, opportunities, micro-structures, Si/Al ratios, constituents, conditions of curing, setting time, strength attributes of their compression, split tensile as well as flexural strength; and their durability properties, such as chloride ion resistance, sulphate, thermal, acid, efflorescence freeze–thaw, drying shrinkage, etc. All of the above, together with workability, flow ability water absorption, and significant characteristics such as the immobilization of toxic or radioactive wastes, etc.; micro-structures—namely, SEM images, XRD, EDS Spectrum, and FTIR, along with thermogravimetric analysis and mercury intrusion porosimetry (MIP), are reviewed and discussed. Not only this, but diverse scientific research on said composites (namely, digital geopolymer concrete and 3D-printed fly ash-based geopolymers with its reaction kinetics and compressive strength) has also been taken into account for the review. Moreover, inhibiting efflorescence development on fly ash geopolymers, hot-pressed and foam geopolymers, besides the acoustic attributes of fly ash-based geopolymers, has been assessed systematically. All the existing insights into these materials have been included to create a complete, state-of-the-art review in all respects, with greater focus on the most significant cutting-edge data that have been obtained in the recent past, since these are draw increasingly more attention as essential parts of the ‘toolkit’ of optional cementitious materials with eco-munificence. Not only this, the benefits of geopolymer technology and its up-to-date status are taken into consideration, and how more potential research can be employed to study their mechanical performance in much detail, in order to further expand production and explore new applications. The review is grist for the mill to establish the viability of geopolymer based on fly ash as a most promising, durable, sustainable, affordable, cost-effective, green, user and eco-benevolent composite. It extends not merely a systematic solution for the disposal of fly-ash wastes, meticulously protecting the environment, soils, and waters from pollution, but also for conserving confined natural resources. Fly ash-based geopolymers have a crystal-clear role to play in extending a sustainable prospect for global construction, as part of the accessible toolkit of binders, cements, mortars, concretes, etc.

Research Methodology

A comprehensive literature review was conducted to identify and appraise the allied available information on record, which are the pedagogic ideas and referenced examples of the fusion work. Recently, one of the rapidly expanding study disciplines in recent years has become a crucial sub-discipline of geopolymeric inorganic composites, polymers of inorganic origin, or revolutionary geopolymer technology. To comprehend in-depth the most recent and emerging drift of geopolymer as an edifice material, the keywords “geopolymer”, “fly ash based geopolymer”, “fly ash in geopolymer”, “alkali activated concrete” and “fly ash in concrete” were methodically recovered, using bibliographic databases of “Springer”, “Elsevier”, “Taylor and Francis”, “Wiley” and “Hindawi”, as well in the interest of congregating an absolute gathering of data. Furthermore, comprehensive data analysis and categorization were carried out based on a thorough understanding of titles, graphical abstracts, highlights, abstracts, keywords, entire texts, conclusions, and impressions. Several synthesis procedures were depicted in figures, graphs, and tables, which were used as references in the current study. The cited literature data represent a comprehensive description of the progress, portrayal, and application of fly ash by geopolymer composites. The present review text includes microstructural techniques such as XRD, SEM, FTIR, and NMR. The aforementioned methodologies are useful for a

better understanding of the inherent linkages of structure, micro-, and pore-structures in geopolymer building composites.

2. Geopolymers

The innovative geopolymer technology contributes a novel, excellent, as well as green solution to the application of different wastes such as fly ash, GGBF Slag, meta-kaolin, fibres [58], volcanic ash [59], glass wastes [60,61], farming wastes [62] etc., avoiding its negative impact on the environment and ecosystem [58]. The materials that were employed for the formation of geopolymers were of geological origin, and the course of action was akin to the process of polymerization of organic compounds, validating its nomenclature. Consequently, geopolymers are the results of geochemistry or the geological synthesis of mineral polymers of rock-forming minerals with a geo-origin [53]. The referred to geo-synthetics are similar to natural rocks on compaction, i.e., they are formed in the course of a quite analogous synthesis, which is found to occur in nature for the formation of natural rocks.

In 1978, the French scientist, Joseph Davidovits, unearthed that alternative binders could be produced through the process of “Geopolymerization”. He invented a novel kind of inorganic alumina silicate oxide through this exothermic chemical process, among the hydroxide and silicate of alkalis under an extremely alkaline medium at a lower temperature, and just at atmospheric pressure. He termed this a “Geopolymer (GP)”. In other words, geopolymerization takes place through alkaline activation, i.e., dissolution at high pH under higher alkaline conditions and just by using atmospheric pressure, and at considerably low temperatures, from room temperature to slightly elevated temperatures—usually below 100 °C or 150 °C. Geopolymerization also occurs, significantly, with nine times fewer emissions of primary GHG gas—CO₂ [63–65], consuming up to a 60% smaller quantity of energy in comparison with the present production method for OPC [66–69], making it approximately 10–30% cheaper than OPC. This exothermic polymeric chemical reaction or the alkali activation occurs between alkaline activators such as NaOH, KOH, Na₂SiO₃ or K₂SiO₃, and jointly or independently with alumina, plus silica-rich source material that originates from either geological origins (such as meta-kaolin, etc.) or industrial origins (such as fly ash, etc.) at a lower temperature and atmospheric pressure only.

Prof. Davidovits coined the resultant product as a geopolymer (GP)”, i.e., a mineral polymer that was achieved from the geochemistry or geo-synthesis of abundant rock-forming minerals, or wastes that were generated from industries analogous to natural rocks formations. Principally, GP is the alkaline activation product, along with a three-dimensional network structure of any aluminosilicates with an empirical form of $Mn [-(SiO_2)_z-AlO_2]_n, wH_2O$, wherein “z” is the Si/Al molar ratio, which may be equal to 1, 2, 3 or maybe higher; “M” is monovalent alkali cation viz., potassium (K⁺) or Sodium (Na⁺); “n” is the degree of polymerization (“n” is a degree of polycondensation or polymerization, and the “-” symbol suggests the existence of a bond); and w is the content of water [70]. Significantly, this novel GP possesses the analogous binding performances, as in the case of OPC. This means, unlike OPC, high energy or elevated temperature reactions are no longer essential. The word “Geopolymer” implies their geological origin and the products of geopolymerization [53] can efficiently be thought of as synthetic rock. Fly ash is a by-product from the industry of thermal plants for electricity and is mainly found as a finely grained powder in the form of a residue from burning pulverized coals. These pulverized fuel ashes comprise the remnants of sands and clays, along with organic matters that are present in the parent coal with higher alumina and silica.

Consequently, geopolymer is a pozzolan that is found in profusion in the form of an industrial waste by-product. For these reasons, the production of fly ash appears to remain momentous and, accordingly, the economical and green-concept technology of fly ashes is highly desirable through their applications. Consequently, the application of fly ash in geopolymer production has attracted engineers and researchers, owing to its appropriateness and universal ubiquity as a redundant residue. Specifically, fly ash is more

preferable to other precursors on account of its massive accessibility [71], reasonably lower down cost and higher reactivity, which is due to its finer particle size. In recent times, research on fly ash-based geopolymers has evolved to mitigate the carbon footprint of concrete, providing a simple way to dump a few of the several million tonnes of the fly ash that is generated universally every year, filling useful lands and creating not only health hazards, but also environmental crises.

2.1. Constituents of Geopolymers

Geopolymer production necessitates raw materials possessing plenty of silica and alumina content viz., fly ash, slag, kaolinite, clays, silica fume, spinel, andalusite, micas, rice husk ash, red mud, etc., as precursors. Commonly, alkali activators such as hydroxide and silicates of Na and K are also used for activation. It is a notorious fact that calcined precursors such as fly ash and slag demonstrate more enhanced compressive strength than non-calcined materials [53,72]. Barbosa et al. [73], and Xu and Deventer [74], accounted that calcined fly ash and non-calcined materials could be combined for the enhancement in their compressive strength, and for mitigating the reaction time. The potential use of fly ash to manufacture geopolymers was also identified by Van Jaarsveld et al. [75].

2.2. Mineralogy

Geopolymers are similar to feldspathoids and zeolites with respect to their mineralogical characteristics, and they are largely found in amorphous to semi-crystalline form with three-dimensional (3D) structures of silico-aluminate, i.e., a poly sialate $(-\text{Si-O-Al-O-})_n$ and poly sialate siloxo $(-\text{Si-O-Al-O-Si-O-})_n$ kind of chemical bonding that results from conditions of hydrothermal setting. "Sialate" is a short form of "Silicon-Oxo-Aluminate", in accordance with Davidovits [53], and a glassy or an amorphous structure symbolizes their hardening at ambient temperatures. Despite their exceedingly smooth surfaces and glassy look with a semi-vitreous to vitreous lustre, geopolymers are competent enough to exhibit a hardness of 4 to 7 on the Mohs scale of hardness [53]. They are mostly found with a non-crystallised form, and this is the reason for the X-ray diffraction outcomes in a wide diffuse halo, as well as for the sharp shape peaks of diffraction [53,76]. This is also why XRD or FTIR spectroscopy alone is not proficient to investigate their structures. This ceramic sort of material not only reveals thermal stability, but also a precise mould capability, justifying its utilization to a great extent as an essential building material.

2.3. Chemistry of Geopolymerization, Hardening Mechanism, Classification, Structure and Terminology

Geopolymers are the novel, inorganic class of solid inorganic complex materials and a product of green chemistry through "Geopolymerization" [53,77]. Contrasting the OPC process of production, this exothermic progression liberates very little (about 90% less) CO_2 , providing evidence that it is an eco-benevolent yield. This simply means that nine times more manufacturing of geopolymer cement is feasible for the sake of the equal amount of CO_2 emissions in comparison with OPC production. Not only this, the reaction kinetics of geopolymerization are also possible, even starting at room temperature to up to $150\text{ }^\circ\text{C}$ at only atmospheric pressure, as well as autoclaving pressure [78] in extremely alkaline conditions, confirming that geopolymers consume lower energy (yet again contradicting OPC production, whereby the restricted natural mineral coals are burnt to attain an elevated temperature for limestone calcinations). For this reason, highly energy intensive and higher temperature reactions are no longer necessary. It is known that geopolymerization necessitates reactive precursors with plenty of alumina and silica, as well as a higher concentration of the reagent activators—particularly, of the alkali hydroxide (OH^{2-}) group [79]. In other words, it is a yield of a chemical reaction among alkali-polysialates and alumino-silicate in the presence of a highly alkaline medium, i.e., at an elevated pH. The attributes and structure of geopolymers are identical to ceramics and can polycondense at a temperature of less than $100\text{ }^\circ\text{C}$ [80], akin to organic polymers. Geopolymers are "polymers,"; therefore, they can be rapidly polycondensed, transformed,

and formed at lower temperatures (i.e., at 30 °C, for just a few hours, at 85 °C for only a few minutes, and with microwave ovens for only a few seconds). Accordingly, geopolymers are hard and weather-resistant mineral materials with enough capacity to resist elevated temperatures. They are utilized just like thermo-setting organic resins and are steady up to 1000 °C to 1200 °C, which is suggestive of their nature to resist high thermal and catastrophic fire conditions [80]. Geopolymerization produces the formation of a disordered alumino-silicate gel phase of alkali, which is called the geopolymer gel binder phase. In this phase, non-reacted solid particles of source materials can be found, and the structure of the gel pore encloses the water, which is used in mixing the precursors. In contrast, water does not become an integral component of a geopolymer binder's chemical structure, as in the case of a calcium silicate hydrate (C-S-H) gel. Apart from the negative charge due to Al^{3+} 's four-fold coordination in one or more of the bridging oxygen particles in every aluminium tetrahedron, the fundamental framework of the gel is closely connected to three 3D setups of the silicate and the aluminium tetrahedra, and balanced by cations of alkali metal that are provided by the activator solution. Geopolymer gel binder shows structural similarities with zeolites on an atomic scale to a nanoscale. This is occasionally extended to the point where the formulation of the nano-crystallites within the geopolymer gel becomes obvious, especially in the presence of abundant water, high temperature for synthesis and a lower Si to Al ratio [81]. The geopolymer structural analysis is simple, since it covers a mix of amorphous X-ray phases and is developed under corrosive reaction conditions that make an in situ analysis complicated. Joseph Davidovits coined three types of geopolymers based on their kinds of chemical bonding, which result from the conditions of a hydro-thermal setting [29,53,82–85]:

- I. "Sialates" (-Si-O-Al-). This is a short form of the chemical title that is provided to "Silicon-Oxo-Aluminate";
- II. "Poly sialate" (-Si-O-Al-O-)_n. This is a contraction of the chemical heading for "Silico-Aluminates";
- III. "Poly -sialate siloxo" (-Si-O-Al-O-Si-O-)_n

The poly sialate has been categorized into three kinds—namely, poly(sialate) (-Si-O-Al-O-) or "PS"; poly(sialate-siloxo) (-Si-O-Al-O-Si-O-) or "PSS"; and poly(sialate-disiloxo) (-Si-O-Al-O-Si-O-Si-O-) or "PSDS". Poly (sialates) are polymers of the chain and ring type Si^{4+} and Al^{3+} , which show a discrepancy in shape from amorphous to semi-crystalline, with four co-ordinations with oxygen. One hardening mechanism among others encompasses the alumino-silicate oxides chemical reaction (Al^{3+} in four-fold coordination) [83–85].

Poly (sialates) can be symbolized chemically by employing a tetrahedral configuration with a form of empirics [86]:



wherein "z" is equal to 1, 2, 3 or maybe higher;

"M" is a cation monovalent viz., potassium (K^+) or sodium (Na^+);

"n" is a degree of polycondensation or polymerization; and

the "-" symbol suggests the existence of a bond.

The alumino-silicate set-up consists of AlO_4 and SiO_4 tetrahedral structure units that link with each other by sharing their oxygen atoms. The negative charge of "Al" is balanced by positive ions viz., Na^+ , Li^+ , K^+ , Ba^{2+} , NH_3^+ , Ca^{2+} , and H_3O^+ [53,77,82].

A supposition is made that the fusions are carried out by the oligomers (dimer, trimer) that compose the specific unit 3D structures with macro-molecular edifices. While under acidic conditions, the alumino-silicates do not interreact or are disgraced, under alkaline conditions, they alter to form tremendously reactive silico-aluminates, which polycondense with each other to develop a 3D framework. It is possible that iron polycondensation, i.e., ortho-sialate and ortho(sialate siloxo), is caused by hypothetical monomers.

Currently, only the sodium-poly(sialate); potassium-poly(sialate); (sodium, potassium)-poly(sialate-siloxo); and potassium-poly(sialate-siloxo) are employed for geopolymers.

Precisely, the chemistry of geopolymerization forms geopolymers through alkali dissolution by the hydrolysis of dissolved units Al^{3+} and Si^{4+} , with the resultant condensation of aluminium and silicate [87]. The complications of the referred reaction kinetics need a model compound to be used to make clear the mechanisms that are involved. An alkaline aluminium silicone gel—in which the aluminium and silicone ions are joined in a 3D tetrahedral gel frame, which is relatively resistant to water dissolution—constitutes the distinctive feature of a geopolymer [88,89].

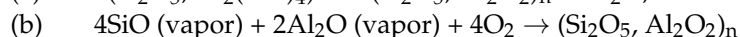
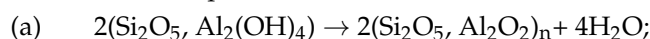
Looking at the terminology of geopolymers, Davidovits introduced the ‘sialate’ classification to depict the structure of aluminosilicate [83]. The kind of link “Si-O-Al” was termed as a “Sialate” bonding, with “Si-O-Si” as a “Siloxo” bond. This provides a way of portraying the chemistry of geopolymers as per their ratio of Si to Al, with a ratio of 1.0 being a “Poly-Sialate”, while 2.0 is a “Poly-Sialate-Siloxo”, and 3.0 is a “Poly-Sialate-Disiloxo”.

Binder Amorphous Poly(Sialate-Siloxo) (-Si-O-Al-O-Si-O-)

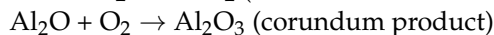
The chemical precursor reaction for geopolymers such as aluminosilicate oxide (Al^{3+} in four-fold coordination) with polysilicates from polymer-produced Si-O-Al bonding is one of the hardening mechanisms. In order, the four-fold co-ordination of Al, commonly represented as $(\text{Si}_2\text{O}_5, \text{Al}_2\text{O}_2)_n$ should be highlighted for the particular, meticulous oxides of aluminosilicate, in place of $(2\text{SiO}_2, \text{Al}_2\text{O}_3)$.

A production of $(\text{Si}_2\text{O}_5, \text{Al}_2\text{O}_2)_n$ is made through:

- (i) Aluminium–silicate hydroxide calcination $(\text{Si}_2\text{O}_4, \text{Al}_2(\text{OH})_4)$, or;
- (ii) SiO and Al_2O vapours condensation [90]:



Also, by forming:



The exothermic process of geopolymerization can be schematized as follows:

It might be considered as the upshot of the poly-condensation of hypothetical monomers, including the ortho-sialate ions [90,91].

The synthesis is performed throughout oligomers (dimers, trimers) that represent the exact unit structures of the 3D macro-molecular formation.

2.4. Properties of Geopolymers

Geopolymers demonstrate excellent characteristics, such as high early strength; brilliant thermal stability at elevated temperatures [92,93]; little shrinkage; excellent resistance against freeze–thaw cycles, corrosion, fire, sulphate and acid attacks; autoclave curing, etc., proving them to be eye-catching alternatives to conventional concrete technology. Moreover, they offer a noteworthy cost-effectiveness of 10% to 30% in comparison to the cost of a traditional concrete system [94,95]. They are non-combustible and non-flammable, and that is why they exhibit exceptional resistance to fire and heat. Not only this, but the CO_2 that is emitted per volume unit of geopolymer cement is roughly nine times lower than the OPC system, endorsing it as an eco-benign material. This simply means that developing countries can have nine times more cement for constructional developments for the same quantity of CO_2 emissions [94]. Moreover, the enhanced polymerization augments the amorphous content and relatively escalates the fly ash-based GPC strength [68]. At a room temperature of only 20 °C, geopolymer cement toughened fast and provided a 20 MPa compressive strength after four hours, while testing as per the norm used hydraulic binder mortars, in accordance with Badami et al. [96]. The ultimate compressive strength 28 days later was found between 70 and 100 MPa [96]. As stated earlier, geopolymeric cement performs similarly to feldspathoids and zeolites [97]. This is why they are capable enough to immobilize even radioactive hazardous wastes into a matrix of geopolymer and perform as a binder to alter partially solid wastes to the adhesive solids. Zeolites are hydrated crystalline aluminosilicates [97]. Zeolites that are suitable for use can be either

naturally occurring or synthesized. Natural zeolites that are preferred include, but are not limited to, analcime, chabazite, gmelinite, mordenite, natrolite, faujasite, phillipsite, sodalite, nepheline, scapolite, cancrinite, erionite, and clinoptilolite [97]. Feldspathoids are chemically and structurally similar to Zeolites, with open holes inside the aluminosilicate structure that are capable of containing alkali metals [97]. Feldspathoids are pozzolanic and have exchangeable alkali ions, making them comparable to zeolites. Examples of feldspathoids include, but are not limited to, nepheline and leucite [96,97]. Feldspathoids are chemically related to clay minerals. Zeolites, on the other hand, differ in their crystalline structure. Unlike many clays, which have a layered crystalline structure and are subject to shrinking and swelling as water is absorbed and removed between the layers, zeolites have a rigid, three-dimensional crystalline structure consisting of a network of interconnected tunnels and cages [97]. Although water flows freely through these holes, the zeolite structure stays stiff. Another interesting feature of this structure is that the pore and channel diameters are essentially consistent, allowing the crystal to function as a molecular filter [96,97].

2.5. Applications of Geopolymers

Geopolymers are useful in many industries such as automobiles, aerospace, non-ferrous foundries, metallurgy, plastic industries, and especially in civil construction engineering because of their sustainability under violent environmental conditions and the unique properties that they possess. Their applications include fixing carbon fabrics to the surface of structural concrete beams [98]; the development of sewer pipeline products, railway sleepers, masonry units, and high performance fibre-reinforced laminates; building parts, together with chemical and fire-resistant coatings and wall panels [99,100], fire-resistant wood panels, high-tech resin systems, and insulated panels and walls; fibre-proof high-tech applications; interiors; decorative stone art; low-energy ceramic tiles; fireproof composites; infrastructure repair; foamed geopolymer panels for thermal insulation; thermal shock refraction and refractory items; and the manufacturing of geopolymer paste, mortar, cement and concrete, etc.

Davidovits categorises a variety of applications based on the silicon and aluminium atomic ratio of a low Si to Al atomic ratio of 1, 2, or 3, demonstrating a 3D network which is very stiff (whereas Si to Al atomic ratios beyond 15 designates a polymer nature).

Geopolymers are attractively useful as they exhibit properties of self-binding for concrete, improved durability, enhanced performance, cost-effectiveness [86], a mitigated negative impact on the environment, lower energy consumption, user and eco-friendliness, excellent resistance to fire, outstanding hardness, and toxic chemical, radioactive and industrial mining wastes immobilization, since their capacity to absorb water, like zeolites, shows a stability of up to 1000 to 1200 °C.

Geopolymer technology is more advanced in precast applications because of the relative simplicity of regulated requirements in handling delicate materials, as well as the controlled high-temperature curing environment, all of which are advantageous to geopolymers. As a result, geopolymer concrete was previously used to make railway sleepers and sewage pipes. Geopolymer concrete may be used to make structural elements such as columns, beams, and even tunnel segments. High durability and resilience to harsh environments, which are typical of geopolymer concrete, are highly required in the manufacturing of sewage pipes. Many soils are rich in corrosive acids. These acids are corroding concrete and steel members that are installed underground.

Geopolymer concrete, according to Dawczynski et al. [101], is an excellent alternative to Portland cement concrete, especially in situations where steel reinforcements are employed. Geopolymer concrete has been found to meet the concrete requirements in hostile conditions such as sulphate soils. Thus, geopolymer concrete may be utilized as a sustainable option in the construction of long-lasting structures, as well as in a variety of maintenance applications. Since geopolymer concrete is resistant to chloride, it sustains less damage during the winter months when salt is used to melt the ice layer. Geopolymer

concrete, because of its strong resistance to chloride corrosion, can be utilized for concrete structures such as piers, coastal bridges, and undersea concrete supports that are constantly attacked by seawater.

2.5.1. Application of GP Binder as a Sustainable Repair Material

The use of GP binder has been widely researched due to its low shrinkage, high early strength, resistance to sulphate attack and corrosion, and high resilience to thawing and freezing. When used in civil engineering, it may significantly reduce stripping time, accelerate the template operation cycle, and increase building speed. A novel form of geopolymeric binder, one-part GP mixes, can be utilized to ease the process of activating GPs in silicate solution. Thermally treated low-quality kaolin at 950 °C, and the strength of the associated binders is up to 47MP, which is equivalent to the strength of two-part mix systems [102].

2.5.2. Application of GP as Multi-Layer Walls

Ma et al. [103] presented an analytical model based on the finite variations approach to predict the thermal impact of buildings with multi-layer walls, composed of a phase change materials layer and a layer of geopolymer concrete that was mixed with microencapsulated phase change materials. Geopolymer concrete GPC was chosen as an ecologically benign material with minimal CO₂ emissions, as well as suitable mechanical and thermal qualities [104,105]. Furthermore, it is ideally suited for integration with microencapsulated phase change materials (MPCM) to provide concrete with a massive heat storage capability, and that meets the mechanical strength requirements for building operations [106,107].

2.5.3. Application of GP as a Coating Material

The GP may be linked into the network structure of film material via the aluminium tetrahedral and silicon tetrahedral, resulting in a type of inorganic coating with non-toxic environmental protection, low cost, fireproof and waterproof properties, and so on. A. Khosravanihaghighi prepared GP-type paints with various amounts of -SiC, and the findings revealed that increasing the fraction of nano-SiC reduced porosity, while improving corrosion and wear resistance. Furthermore, a reflective heat insulation GP coating was created using metakaolin and sodium silicate solutions as the primary starting materials, with talcum powder, hollow glass microspheres, and sericite powder added as fillers [108,109].

2.5.4. Application of GP as a Self-Cleaning Material

Severe air pollution is mostly the result of industrial output, natural disasters, engineering construction, and automotive emissions, among other things. As a result, when exposed to polluted air, building amenities become filthy. This issue has compelled industry to find alternate materials to aid in sustainable development. Due to their unique qualities, GP-based self-cleaning concrete materials provide a green solution to the problem. In addition, the self-cleaning capability of GP-based concrete is being investigated using photocatalytic elements such as ZnO and TiO₂ [110].

2.5.5. Application of GP as a Geopolymer Foam

Geopolymer foams have various uses in industries and construction because of their light weight. TROLIT was the brand name of one of the earliest reported materials of this sort. TROLIT was a type of inorganic geopolymer foam that was composed of three main components: solid silicon and aluminium sources that were obtained as by-products of industrial processes involving high temperatures; a liquid activator that was composed of alkali metal aqueous solutions; and expanding agents such as peroxides and perborates. This substance had unusual features that few scientists had before achieved, and then only on a laboratory scale. The thermal conductivity of the material was 0.037 W/mK, which is comparable to polystyrene.

2.5.6. Application of 3D Printed Geopolymer

The explorations of the attributes of geopolymer products through innovative 3D printing processes are quite promising and are the reason why the field is growing significantly, and why relevant various studies are also focused on the topic contemporarily in the construction and infrastructure industries. For instance, Panda et al. [111], shed light on the development and examination of the processes' directional influence on the compressive strengths of geopolymer mortar based on fly ash, as well as some other industrial by-products viz., silica fumes, slag, etc. The mechanical characteristics and the reaction kinetics of the mixtures that exhibited a good-quality recovery aptitude were reviewed before the 3D printing process in the context of concrete. The heat of the reaction, produced through isothermal calorimetry, was regarded as an indicator of the overall reaction of hydration inside the pastes that were made [112].

2.5.7. Application of Porous Geopolymer

To adapt their use to diverse practical applications, fly ash-based porous geopolymers are often manufactured in a variety of forms such as bulk, membrane, and spherical. This section discusses both the fabrication of bulk/membrane and sphere-shaped components, with bulk and membrane components grouped together, since their preparation processes are typically identical. Previous studies have well detailed the manufacturing processes for geopolymer mortar, concrete, and composites with porous structures that are made from fly ash [113,114].

2.6. Advantages and Disadvantages of Geopolymers

- An innovative, noble and revolutionized material which cuts carbon footprint by mitigating GHG emissions, providing relief from global warming;
- Thermal and fire-resistant materials [115];
- Can immobilize the hazardous, radioactive wastes [116];
- Exhibit excellent strength and durability [117,118];
- High early strength contributing to sustainable composites [119];
- Excellent resistance to chemicals and freeze–thaw conditions [120], etc.;
- No water curing, because water is released during the chemical reaction in the geopolymerization process of geopolymer concrete, and this water tends to evaporate as the specimens are heated during the curing phase. Similarly, drying shrinkage in stiff specimens is low due to the little amount of water in the pores [18,116–121];
- Several studies have been conducted [122,123] to determine the effect of curing conditions on the physical and mechanical characteristics of geopolymer paste and concrete. Curing temperatures ranged from 40 °C to 85 °C for near-perfect geopolymerization [18];
- Hardening mechanism is quicker and at low temperatures [124];
- Much lower creep, as well as shrinkage [116–121];
- Low permeability [125,126];
- User and eco-friendly [125,126];
- Systematic disposal of diverse waste is possible through their consumption in their manufacturing, otherwise, filling land spaces and pollutes the environment, soils, surface, sub-surface and supply waters, etc [125,126];
- Structurally a stable and intact material even under severe conditions because of the special 3D network structure of aluminosilicate [7,116];
- Brilliant mechanical properties on account of typical structure and framework of $[-Si-O-Al-O]_n$ bonding, since this structure does not depend upon lower strength bonds, as found with the OPC system, and thus results in comparatively higher strength [125,126];
- Excellent durability because geopolymers are inorganic materials and generally contain massive minerals of zeolite nature viz., sodalite, analcime, etc. [118,119];

- Noteworthy resistances to chemical, fire and thermal conditions. Mostly, the Si-O and Al-O bonding of geopolymers hardly ever react with other acids, except for hydrofluoric acid (HF). Moreover, the structure of the oxide network of geopolymers is stable at high temperatures, and the lower thermal conductivity of 0.24 to 0.38 W/(m·K) altogether prove it as an exceptional heat-insulated material [127];
- Faster curing rate and higher force for internal binding with the quicker formation of gel and rapid dehydration enable its high early strength as compared to the OPC system;
- Contrary to different cement structures, the geopolymer is found to be strongly bonded to aggregate, enabling it to be employed as a possible mend for a concrete product;
- Lower cost in addition to a widespread source for natural and industrial precursors that are available in plenty to synthesize geopolymer. The requisite elements for geopolymer are silicon, oxygen and aluminium, which exist in the earth's crust in a proportion of 26.3%, 48.6% as well as 7.73%, respectively, in that order. The precursors are kaolinites and industrial wastes such as fly ashes [128,129].
- Potential applications of special kind of geopolymer structure of silicon tetrahedral and aluminium tetrahedral form ring chain structures such as the cage cavity are favoured its utilization as a building material for immobilization of heavy metals, the disposal of nuclear waste, as well as novel making of inorganic membranes [30,69,70].

Disadvantages of Geopolymers

While geopolymer concrete looks to be the superior concrete to replace regular Portland concrete, it has numerous drawbacks, including:

- Geopolymer concrete needs specific handling and is exceedingly difficult to produce. It necessitates the use of potentially hazardous chemicals such as sodium hydroxide [129];
- Due to the hazards that are connected with its production, geopolymer concrete is only available as a pre-cast or pre-mix material [129];
- The geopolymerization process is sensitive—research in this sector has been inconclusive and exceedingly volatile. There is no consistency [129];
- Transporting the primary material, fly ash, to the needed site;
- Excessive cost of alkaline solution [115];
- Safety concern linked with high alkalinity of activating solution [115];
- Practical challenges in implementing steam curing/high-temperature curing procedure [115].

Significant research is being conducted to build geopolymer systems that can overcome these technological challenges.

3. Coal Fly Ash

Coal fly ash, together with the flowing gas in coal-fired power plants, is the fine particulates residue that is expelled by the boiler. It may typically be extracted by any suitable action; for instance, through electrostatic precipitation, cyclone separation, or other particulate filtration equipment before the flue gases reach the chimneys, from flue gasses of sprayed or crusher-powdered coal and lignite-fired boilers [130,131]. According to the projections of the Energy Information Administration (EIA), U.S.A., the quantity of electricity generation will rise with a growth rate of 2% per annum up to 2040, which implies that coal will constitute a major portion in the development [132]. The incessant exigencies for coal as fuel will pilot a generation of more coal ash (CA) production. During coal combustion, 80% coal fly ash (CFA) and 20% coal bottom ash (CBA) are produced as by-products, and disposal from sites will have a hazardous impact on health and, in particular, on eco-systems. In 2016, the planet generated around 1.143 billion tonnes of fly ash. China generated approximately 600 million tons, with a utilization rate of 68–70 percent; the United States produced approximately 44 million tons; and Japan produced approximately 12 million tons, with a utilization rate of nearly one hundred percent. The European Union

produced 40 million tons (all coal-fired solid wastes in the 15 European Union nations), and the utilization rate was ninety percent (completion of 36 million tons); India consumed 169 million tons, with a usage rate of sixty-three percent [133]. The quality of CFA depends mainly on the chemical constitution of the coal that is used for burning, as well as the combustion conditions, i.e., the rate of pulverization and oxidation. CFA not only contains a variety of trace elements (such as As, Se, Cd, Cr), but also encloses oxides of Ca, Si, Fe, Al, Na, K, Mg, and Ti [134,135], which make it potentially toxic. Consequently, the direct application of CFA leads to perilous effects on the environment [136]. The mineralogical and chemical constituent of CAF permits its use in plenty of fields. The utilization rates of 50% of CFA in the US, 60% in India, 67% in China, and 90% for the EU, were estimated [137]. Other developed nations, such as the United States and Europe, have substantially greater usage rates. It is a fundamental reality that fly ash is no longer seen as trash, particularly in the industrialized world. It is presently a very popular and frequently utilized raw material in building [138]. According to the European Coal Combustion Products Association, Europe generated about 40 million tonnes of CCW in 2016 and reused more than ninety percent of it in the building and reclamation industries [138]. In the same year, the United States generated over 107 million tonnes of CCW, of which nearly sixty percent was re-used [139]. By 2020, their entire CCW had been decreased to 40 million tonnes, with over fifty-eight percent being re-used [140]. Since CFA is used directly as a raw resource or additive material in the building and construction sector, it contributes considerably to CFA recycling. The volumes that are disposed of, however, continue to be a serious management problem. CFA is also a potentially low-cost adsorbent material, either directly or by functionalized production [141,142]. It has also been discovered as a potential source for the metallurgical recovery of high-purity products such as alumina [143,144]. In the field of building materials, its future is frequently debated, as developed European countries are currently dealing with the cessation of coal combustion in power plants and its replacement by other raw materials, raising concerns about the possibility of construction without coal ash, confirming the fact that fly ash is currently very desirable as a raw material.

Interestingly, CFA is a pozzolanic material, and this is the core reason for its prevalent application as a supplement in manufacturing cement, in order to save the natural resources that are used to produce cement. The upshots of research also indicate its capability to adsorb metal ions from solutions, because of its alkaline attributes with the negatively charged surface. Moreover, the application of CFA as a low-priced source of aluminosilicate has become the centre of attention for scientists in the last couple of years, who have successfully transformed this waste by-product material to zeolitic geopolymers for diverse uses [145,146]. In addition, the implementation with CFA of synthetic products has succeeded in removing toxic elements from both contaminated soil and water [147–149]. If not adequately controlled, the enormous volume of fly ash that is created by municipal solid waste incineration plants might fast become one of the country's major sources of heavy metal pollution [150]. By 2020, their entire CCW had decreased to 40 million tonnes, with over fifty-eight percent being re-used [140]. Since CFA is used directly as a raw resource or additive material in the building and construction sector, it contributes considerably to CFA recycling. The volumes that are disposed of, however, continue to be a serious management problem. Table 1 shows the chemical composition of fly ash from past studies. Although fly ash is a popular source material for geopolymer, there are certain drawbacks to using it. For example, the quality of fly ash can impair the quality and strength of geopolymer concrete. Poor quality fly ash can increase the permeability of geopolymer concrete and cause structural damage. The use of fly ash causes a slower strength increase and can prolong the time it takes for geopolymer concrete to cure.

There are several forms of fly ash produced by the coal supply and combustion method. They are classified into two types: high-temperature fly ash and fluidized bed combustion ash. Fluidized bed combustion ash is a by-product of coal-fired power stations that must decrease air emissions cheaply in order to fulfil Clean Air Act regulations. The concept of fluidized bed combustion technology is the burning of coal with sorbent, which is

introduced to the combustion chamber based on the sulphur level of the coal. Ground limestone is commonly used as a sorbent, which is why these ashes have a greater CaO concentration. The combustion process begins at around 850 °C [151,152]. Although the physical and chemical composition of fluidized ashes is comparable to that of Portland cement, the resultant materials have poor compressive strengths and are thus employed exclusively as pozzolan in concrete applications. The primary distinctions between these kinds are increased SO₃ concentration, highly reactive free CaO, and potentially larger loss on the ignition of ash, following fluidized bed combustion. While standard high-temperature FA primarily contains pozzolanic action, fluidized ash may set and harden by just combining it with water, without the any additional additives or chemicals. The binding capabilities of fluidized ash are primarily determined by the quantity of present anhydrite and free lime, which is gently burned during the coal combustion process and is thus highly reactive [151–154].

Currently, nitrogen oxide reduction strategies that allow meeting NO_x emission standards include methods that are based on the injection of ammonium compounds [155–157]. This procedure is often carried out in one of two ways: selective catalytic reduction (SCR) or selective non-catalytic reduction (SNCR). The authors Michalik et al. [158] concentrated on the properties of fly ashes that were produced by the SNCR process of flue gas denitrification. The study focused on silica fly ash from flue gas denitrification and ash from a traditional boiler that did not go through the flue gas denitrification process. The research focused on the physicochemical and structural properties of ashes, as well as slurries and cement mortars containing ashes. Research has shown that fly ash from flue gas denitrification is characterized by a higher value of losses on ignition and ammonia content in comparison to ashes without denitrification; it has also been shown that the ammonia content in the analyzed range does not limit the use of fly ash as an additive to cement and concrete. Procházka et al. [159] explained the influence of fly ash denitrification on the properties of hybrid alkali-activated composites. The purpose of this study was to evaluate the effect of SNCR denitrification on fly ash for usage in hybrid alkali-activated materials that were based on blast furnace granulated slag. In the experiment, a potassium water glass with a silicate modulus of one was utilized as an activator. So far, the results suggest that using fly ash after denitrification in hybrid alkali mixtures does not significantly impair the reported attributes when compared to using standard fly ash without denitrification. The experiment findings demonstrated that there was no significant change in the characteristics of the mixes that were formed from fly ash after and without denitrification.

The alkali activation of waste material is a chemical method that allows the user to convert glassy structures into highly compact well-cemented composites. The major reaction result of fly ash alkali activation is an amorphous, three-dimensional alkaline inorganic polymer known as NASH (Na₂O-Al₂O₃-SiO₂-H₂O) gel. Na-chabazite, zeolites A and P, and faujasite are examples of secondary reaction products [160] Fly ash alkali activation is a unique process in which this powdered grey material is blended with alkaline activators and then cured at a moderate temperature to generate solids. The FA’s glassy ingredient turns into a well-compacted cement. The major reaction product that was generated in alkali activated fly ash was discovered to be an amorphous aluminosilicate gel with zeolite precursor characteristics.

Table 1. The chemical composition of fly ash in previous research.

Reference	Type of Fly Ash	CaO	SiO ₂	Al ₂ O ₃	Fe ₂ O ₃	SiO ₂ + Al ₂ O ₃ + Fe ₂ O ₃	Na ₂ O	K ₂ O	MnO	MgO	SO ₃	TiO ₂	LOI
[161]	Class F	0.87	61.89	28.05	4.11	94.05	0.4	0.82	-	0.38	1.32	-	0.49
[162]	Class F	2.24	57.2	24.4	7.1	-	0.38	3.37	-	2.4	0.29	-	1.52
[163]	Class F	2.38	50.7	28.8	8.8	88.3	0.84	2.4	-	1.39	0.3	-	3.79
[164]	Class F	5	49	31	3	83	4	1	-	3	0	2	0

Table 1. Cont.

Reference	Type of Fly Ash	CaO	SiO ₂	Al ₂ O ₃	Fe ₂ O ₃	SiO ₂ + Al ₂ O ₃ + and Fe ₂ O ₃	Na ₂ O	K ₂ O	MnO	MgO	SO ₃	TiO ₂	LOI
[167]	Class F	10.58	17.57	36.37	12.43	66.37	-	1.77	-	3.05	1.39	0.88	1.19
[168]	-	3.6	58.0	29.08	3.58	-	2.0	0.73	-	1.91	1.8	1.75	2.0
[165]	Class F	1.55	53.5	28.8	7.47	89.77	-	-	-	0.81	0.14	-	3.11
[166]	-	3.05	52.3	28.0	6.32	-	-	2.51	-	-	-	-	-
[169]	-	5.41	27.35	50.85	2.01	80.21	0.04	0.33	0.02	0.28	-	2.12	7.74
[170]	Class F	5.31	54.72	27.28	5.15	87.15	0.43	1	0.1	1.1	1.01	1.82	6.8
[171]	Class F	0.2	57.6	28.9	5.8	92.3	-	0.9	-	0.9	0.2	-	3.6
[172]	Class F and Class C	14.14	50.67	18.96	6.35	75.98	0.69	-	-	3.12	0.74	-	0.17
[173]	Class F	1.64	66.56	22.47	3.54	92.57	0.58	1.75	-	0.65	0.1	0.88	1.66
[174]	Class F	2.58	63.13	24.88	3.07	91.08	0.71	2.01	0.05	0.61	0.18	0.96	1.45
[175]	Class F	3.81	47.87	28	14.09	89.96	0.41	0.62	0.21	0.93	0.27	1.99	0.43
[176]	Class F	4.3	51.1	25.7	12.5	89.3	0.8	0.7	0.2	1.5	0.2	1.3	0.6
[177]	Class F	12.92	52.75	18.05	5.92	76.72	1.11	2.09	0.14	3.86	1.76	1.01	1.6
[178]	Class F and Class C	1.29	54.48	27.72	8.14	90.34	0.67	-	-	-	0.11	-	4.11
[179]	Class C	17.16	35.86	15.05	17.31	68.22	1.58	3.12	-	2.34	5.94	-	0.1
[180]	Class F	7.32	58.4	23.8	4.19	86.39	1.43	1.02	-	1.11	0.44	-	0.5
[181]	Class F	-	50.83	23.15	6.82	80.8	1.29	2.14	-	1.7	1.24	1.01	0.55

3.1. Sources of Fly Ash:

Electricity and heat production in power plants contribute a titanic quantity of minerals matters, which are associated with the original coals that are brought for combustion as a waste by-product in most areas of the world [182]. Nearly 80% of by-products from coal combustion are represented by fly ash. Bottom ash is also found to be associated with the pulverized fuel ash that accumulates at the bottom of the boiler through some proper practices. However, the bottom ash from the boilers is not mixed with the fly ash. The fly ash that is collected in the beginning is coarser than the fly ash that is later gathered in the stages of electrostatic precipitators. Flue gas desulphurization material is a residue from a coal-fired boiler, resulting from the falling emits of SO₂ (sulphur dioxide). It is a wet sludge or a dry powder consisting of CaSO₃ or CaSO₄ sulphate (calcium sulphate). As a hazardous solid waste, municipal solid waste incineration fly ash includes harmful compounds such as heavy metals and dioxin, making its disposal a global public health problem. With the growth of urbanization and the improvement of people's living conditions, the amount of municipal solid waste (MSW) that is created grows year after year.

3.2. Properties of Fly Ash

3.2.1. Chemistry and Morphology

Fly ash is industrial by-product dust from thermal coal plants of a fine-grained nature and comprises mostly spherical to subrounded melted vitreous particles that range in size from 0.5 to 300 µm with a smooth surface [183]. As mentioned earlier, the key component of most of them is silica (SiO₂), ferric oxide (Fe₂O₃), calcium oxide (CaO) and alumina (Al₂O₃), along with minor quantities of Na₂O, MnO, SO₃, MgO, K₂O, TiO₂ and non-burnt carbon, which are present in some of the fly ash. Fly ash with properties such as low calcium, a high vitreous phase, 80 to 90% of particle sizes that are less than 45 µm [184], unburned material at less than 5%, reactive silica of 40% to 50%, and less than 10% Fe₂O₃ results in the optimal binding characteristics [184]. A momentous amount of calcium can hinder the polymerization setting rate resulting from an alteration of the microstructure [185]. For this reason, low calcium fly ash is preferable for making fly ash-based geopolymers. The value of a loss on ignition depends on the kind of working regime and the type of power station. An immense discrepancy in the key composition of silica (25 to 60%), ferric oxide (5 to 25%) and alumina (10 to 30%) was found [186]. Fly ash is technically considered as siliceous when the three key constituents total 70% or more and the reactive calcium oxide is less

than 10%. This sort of fly ash is a product that is obtained through the burning of anthracite coal or bituminous coal, which possesses pozzolanic attributes [187]. If the combination of these three constituents is equivalent to or greater than 50% and the reactive calcium oxide is not lower than 10%, then calcareous fly ash generates the types of sub-bituminous or lignite characteristics of coal and has both hydraulic, as well as pozzolanic characteristics. The chemical composition of the fly ash is consistent with natural pozzolans, such as volcanic ashes, whereas the calcareous ashes include hydraulically active mineral phases and pozzolanic materials. The pozzolanic reactivity is a unique characteristic of siliceous fly ash, i.e., its aptitude to act in response with water and lime at ambient temperature to formulate strength-furnishing mineral phases that are analogous to OPC. Other than Si, Al, Fe and Ca, fly ash is customarily found to be associated with many other trace elements of metal, such as Ti, Cr, V, Mn, As, Co, Sr, Pb, Mo and Hg [188,189]. Fly ash could produce 4–10 times more toxic trace elements than those in coal [187–189]. Moreover, it may possess smaller dioxins concentrations, along with organic compounds of polycyclic aromatic hydrocarbon [190,191]. Therefore, fly ash is regarded as a perilous material, and this is why offensive fly ash disposal will not only merely accelerate the land occupation, but also pollute the environment, ecology, soils, surface and subsurface waters. Concerning its particle size distribution, fineness and the reactivity of pozzolan, CFA is frequently utilized in cement composites to enhance their technical attributes and substitute OPC. The glassy materials that are present in fly ash are found to be reactive with the hydroxides of alkali and Ca, which are obtained from fly ash cement systems and develop a cementitious gel that contributes supplementary strength.

3.2.2. Morphology

Looking to the morphology and its impact on the reactivity of fly ashes, the size of their spherical to subrounded particles and their fineness are the key factors [192] deciding the appropriateness of their use in the manufacturing of concrete, because they significantly influence the attributes of ultimate fly ash-based products [193]. Chindaprasirt et al. [194–196] exhaustively investigated the impact of fineness on chloride penetration [194], drying shrinkage, strength, sulphate resistance [196], etc., and improved compressive strength, mitigated shrinkage, and expansion, etc. by employing finer fly ashes. On the other hand, coarse fly ash is less reactive and requires more water from more porous mortar with a greater vulnerability to sulphate attack. However, the negative effects of coarse fly ash are often referred to as the reason for reduced strength, accelerated drying shrinkage and excellent sulphate resistance, etc. [196]. On the other hand, a diminution in the particle size of fly ash accelerates the content of amorphous SiO_2 and tends to reduce the quantity of SO_3 , which can hinder the hydration of dangerous ions in mortar or concrete [197]. The positive impact of fly ash fineness on the mechanical characteristics of the concrete on improving the compressive strength is repeatedly accounted [198]. The finer fraction of lesser than 63 μm of fly ash particles in manufacturing concrete and cement can improve the pozzolanic reactivity. Nevertheless, the removal of coarser particles may suppress certain cementitious characteristics [199]. Finer particles of fly ash are greatly desirable for the development of strength because they contribute more hydration nucleation sites. However, coarser particles of fly ash cannot be eradicated totally as they possess definite positive performances when employed in diverse composites. This is why both fine and coarser particles of fly ashes, employed in the proper ratio, would display improved outcomes concerning the strength and durability of ultimate composite.

3.3. Types or Chemical Classification of Fly Ashes

As stated earlier, the contents of fly ash differ significantly depending on the coal source being fired. By and large, the components of fly ash characteristically include SiO_2 , Al_2O_3 , CaO and Fe_2O_3 , which are found in amorphous and crystalline form as oxides or a variety of minerals. In accordance with the American Society for Testing and Materials (ASTM) standard C 618 [200], chemically, fly ashes can be classified as Class C fly ash, as

well as Class F types, on the basis of their contents of calcium oxide (CaO), which generally decides how fly ash performs when it is employed. Fly ashes are classified primarily according to the EU Standard (EN-450—1) standard or the American Society for Testing and Materials (ASTM—C-618) standard. The American Test and Material Society (ASTMs) has two classes of fly ash, “C” and “F” fly ash [200].

A. Class C fly ash:

It possesses a higher content of calcium, which is chiefly found in the burning of sub-bituminous or inferior quality coal, i.e., lignite deposits from coal sources. It contains an overall content of SiO₂, Al₂O₃ and Fe₂O₃ ranging from 50% by weight to 70% by weight, whereas the content of CaO is greater than 20% by weight.

B. Class F fly ash:

It has a lower content of Ca, which is produced from the burning of superior quality coal, namely, anthracite or sometimes bituminous—the second highest quality of coal. It has a total content of SiO₂, Fe₂O₃ and Al₂O₃ beyond 70% by wt. and less than 10% by weight of CaO content [201,202]. It is classified as a normal type of pozzolan, i.e., a silicate glass material that is altered by Al and Fe.

The above-referred Standards govern the physical and chemical characteristics of the fly ash that is employed. The key dissimilarity among these standards depends upon their chemical composition, fineness and loss on ignition (LOI). Commonly, non-burnt residues of carbon are described as LOI. Consequently, the chemical constituent of the fly ash that is employed influences the performance of the ultimate composites [203].

Fly ashes that contain low calcium slowly react, especially during the early hydration stages, because of the presence of more crystalline, chemically inert phases. Due to the progress in characterization techniques, the hydration products that are developed at various stages can be analyzed. The images of SEM are more helpful to recognize the chemical constituents, as well as the morphology of developed hydrated products. SEM images of fly ash-based composites, along with a dispersive energy spectrum, exhibit the composition of a variety of hydrated products in the alike image at dissimilar spots. On the other hand, high-calcium fly ashes are less sensitive to insufficient curing and react more swiftly to contribute an improved early-age strength.

Nevertheless, fly ashes with a high calcium content are commonly less competent in suppressing the distribution because of sulphate attack [204] and alkali-silica reaction (ASR) [205], in comparison with those containing low-calcium. In addition, calcium replacement during the glass phase is believed to usually speed up the reactivity of high calcium-possessing fly ash. For this reason, it enables the development phases of the silicate and aluminate of calcium without an outside source of lime.

Furthermore, fly ashes of Class C differ from those of Class F concerning the content of lime and the lime depolymerized glass phase. The content of CaO in the glass phase of fly ashes with high calcium shows higher reactivity because of the condensed degree of SiO₄ polymerization [206]. Diamond [207] accounted that the pore solution alkalinity was on account of the presence of hydroxide of calcium, which was developed from the hydration of cement, beside ions of Na and K in cement, as well as fly ash. The fly ash-based composites augment the resistance to corrosion through densification of concrete when appropriately proportioned and sufficiently cured [208].

3.4. Nature of Fly Ash—Crystalline or Amorphous

Fly ashes are the by-product that is derived from coal-combustion, possessing an intrinsic heterogeneous property. In general, it contains three dissimilar kinds of constituents such as crystalline minerals, non-burnt particles of carbon and non-crystalline aluminosilicate glass—each one with exceptional reactivity while employed. The process of eliminating this non-burnt carbon through calcination [209] partly converts the amorphous phases that exist with fly ashes into crystalline phases. This contains the distinctive crystalline phases such as quartz, hematite, mullite, ferrite anhydrite, spinels, melilite,

periclase, merwinite, lime and tricalcium aluminate [210]. Mostly, fly ashes are comprised of glassy shape material possessing a weak atomic structure. On account of the amorphous nature, the ingredients, by and large, take part in the chemical reaction [211]. As a result, highly amorphous fly ashes are more effectual in improving the pozzolanic reaction. Sakai et al. [212] accounted for the impact of the amorphous-type content of fly ashes on the pozzolanic reaction at later stages. Moreover, in the case of fly ash containing lower calcium, an alkaline environment favours less reactivity because of the inert nature of most of these crystalline phases. Further, because of a few reactive crystalline phases, fly ash containing higher calcium is more reactive. Tkaczewska [213] added the benefit of employing a finer sized particle of fly ash in accelerating the grade of SiO_4 depolymerization, which escalates the pozzolanic reactivity.

3.5. The General Applications of Fly Ashes

The applications of coal-fired fly ashes have drawn the attention of vast numbers of researchers in recent years. The most significant fields for the applications of fly ashes that are accounted are concrete production, road basement, waste solidification/stabilization, cement clinkers, asbestos, the construction of roads and embankments, mine reclamation, the recovery of precious metals, ceramics and glass ceramics, the synthesis of zeolites, low-cost adsorbents for waste removal, soil amendment, nutrients, a silica and alumina source for producing zeolites, etc. [214–220], and quite recently for geopolymer binders, pastes, mortars and concretes [221]. Its significant use has also recently been found in the production of diverse fly ash-based geopolymers with a state-of-the-art binder or cement, which is more or less comparable to hydrated cement in appearance, properties and reactivity, as either raw or as a supplementary cementitious material (SCM) [221,222].

The reusing of coal ash has been considered by the United States Environmental Protection Agency [132], which has resulted in moves to save the environment and economy, besides product gains such as mitigated emissions of greenhouse gas CO_2 , the lowered necessity of dumping them in landfills, along with the conservation of restricted natural resources. The declined costs of coal fly ash have enabled cheaper construction materials on one hand, while on the other hand, the escalated revenue from the sale of coal fly ash substituting costly cement has altogether benefited the economy. The enhancement of the strength, durability, and workability of fly ash-based construction materials has proved them to be the ultimate product of quality. Therefore, it can be noted that economic values and the improvement of the environment do not undermine the quality of the final finished geopolymer products, indicating the sustainability of industrial production that uses coal fly ashes.

The fly ash application strategies can be classified into three major groups based on their usefulness and economic value, i.e., non-advantageous, advanced and straightforward [223]. The best fly ash utility rate is based on their simple use for construction and building objectives. Although, their use for the production of building materials necessitates very cautious consideration of global levels of environ-safety and financially reasonable standard parameters, based on cost gain calculations and socio-economic aspects entailing the GDP of particular nations [224]. However, industrial technologies are not available for the advanced use of fly ash. In accordance with the European Coal Combustion Products Association, 51.7% of the entire by-products of coal combustion viz., fly ash, bottom ash, fluidized bed combustion ash, boiler slag, FGD-gypsum, etc., are employed for building, agricultural and road pavements, while 39.8% are used for restoration and reclamation. The rate of total use is 91.5%. As per ASTM standard, the potential end application of fly ash entails soil amendment; waste treatment, as well as stabilization; hazard waste treatment; and the production of slurry walls, mineral fillers, pozzolanic liners, cement, concrete, as well as gypsum products.

3.6. Opportunities of Coal Fly Ash

Researchers investigate the possible transformation of CFA into a sequence of effective products such as geopolymers, catalysts, zeolites, and photo-catalysts. Since the CFA contains aluminosilicate, it is preferably used for the manufacturing of more competitive cost-effective products than the costly commercial types of products. Processes of physical, chemical, quality control, packaging and final distribution can be used for the manufacturing of CFA-based adsorbents. A golden prospect for both the coal-fired power plants and the coal factories is their employment and support of lucrative plans by instituting a lateral or autonomous unit for the production of value-added products from CFA.

4. Fly Ash Based Geopolymers

In the last couple of years, greater than ever attempts have been made for the utilization of profuse fly ashes in a competent way—particularly, with green concept. The application of the profuse waste of fly ash for the production of fly ash-based geopolymer is found with nine times lower CO₂ emissions as compared to the OPC system [225,226]. These up-to-date composites largely demonstrate closely equivalent durability and mechanical strength as with hydrated Portland cement, and they can be used to preserve natural resources as a class of inorganic green cement [227]. The use of fly ash as either a precursor or SCM not only enhances the workability and mitigates hydration heat, as well as thermal cracking in concrete at early periods, but also increases the mechanical and durability attributes of concrete (particularly at later stages) [228].

4.1. Production of Fly Ash based Geopolymers

The manufacturing of fly ash-based geopolymers is possible through an exothermic and complex chemical process that was coined by Davidovits as geopolymerization, which includes stages such as dissolution, precipitations, restructuring, gelation and eventually poly-condensation [229]. The genetic mechanism of fly ash-based GP can be explained in three steps [229,230]. The initial step includes the dissolution of the alumino-silicate of fly ash, which takes place by an alkaline activation at a low temperature and at atmospheric pressure, and hydrolysis, which forms the monomers of aluminate and silicate. Then, the Al³⁺ and Si⁴⁺ ions are transformed into oligomers that generate a gel with comparatively big networks through condensation. Lastly, the emergent gel continues to restructure, and the amorphous structure gives rise to the development of an alumino-silicate network via poly-condensation reactions. However, the reaction kinetics that occur in the series, of course, are much more complicated and remain hard to pin down. The reactions that occur among fly ash, as well as alkali activator solutions, include Na₂SiO₃, NaOH, KOH, K₂SiO₃, etc., whereby Si-O-Si- or Si-O-Al- bonds of alumino-silicate break and liberate active Si⁴⁺ and Al³⁺ ions. Subsequently, the condensation of these released Si⁴⁺ and Al³⁺ ions takes place, which is followed by other complex reactions such as nucleation, oligomerization, and polymerization, which finally lead to a novel polymer that is based on aluminosilicate with a novel amorphous 3D network structure with a SiO₄ and AlO₄ tetrahedra. For testing or applications, the geopolymer paste that is produced with fly ash is additionally cast into a mould and placed into an oven at a necessary temperature, or it can be left to cure for a certain time to develop geopolymers based on fly ash. The chains of alumino-silicate oligomers can be a form of polysialate –Al-O-Si- chain, polysialate disiloxo –Al-O-Si-Si-Si- chain and polysialate siloxo –Al-O-Si-Si- chain, depending on the Si: Al ratio. In alumino-silicate monomers, Si⁴⁺ is partly replaced by Al³⁺, and the negative charge results in the alumino-silicate chain being balanced with alkali cations such as K⁺ or Na⁺ [231,232]. In this framework, the Si: Al ratio derives notably from the ultimate structure of the resultant geopolymers [233]. For instance, it was found that the Si to Al ratio in the fly ash reactant had a noteworthy effect on porosity, which is one of the significant parameters for controlling geopolymer mechanical strength [234,235].

In addition to the Si/Al ratio, the alkaline solution strongly influences the microstructure of the produced fly ash geopolymer. When fly ash comes into contact, it starts to be

discharged and transferred with alkaline activators such as NaOH, KOH, Si^{4+} , Al^{3+} and other ions. For illustration, the amount of Si^{4+} and Al^{3+} that is released is affected by NaOH concentration. A high concentration of about 10 mol/L of NaOH solution is advantageous for the decomposition of the aluminosilicate of the fly ash, and then the discharge of Si^{4+} and Al^{3+} takes place. For instance, the solubility of Al^{3+} and Si^{4+} that are present in NaOH liquid is more than in KOH activator liquid with an identical concentration [236].

Moreover, the transfer of Al^{3+} and Si^{4+} ions and the poly-condensation of aluminosilicate oligomers could also be escalated by an alkaline liquid with a higher concentration [237].

Furthermore, diverse alkaline cations have dissimilar charge density and sizes, and they also hydrate differently. This has a definite impact on the alumina silicate chain nucleation, the charge density of the chain, the chain development, the degree, and the polymerization process rate [238]. The leaching rate of Al^{3+} and Si^{4+} ions determine the actual obtainable Si to Al ratio in a series of reaction kinetics to produce geopolymers, and consequently act for the fly ash-based geopolymer structure. Fascinatingly, a recent investigation by Ma et al., 2013 [239] uncovered that the addition of Na_2SiO_3 to a solution of alkali could augment such a Si to Al ratio, resulting in a low porosity and a finer pore network in a geopolymer matrix.

The setting time for fly-ash geopolymer is generally taken into account for the workability of the final products of fly ash-based geopolymer. Usually, the ultimate setting can be achieved in 1 to 2 h at room temperature, while the higher CaO and calcium additive Class C fly ash content, as CaCl_2 , reduces fly ash-based geopolymer paste setting time [240]. During the course of geopolymerization, Al^{3+} and Si^{4+} ions react with Ca^{2+} , either into the fly ash or from the outside calcium additives, to produce gel of calcium-silicate-hydrate, gel of calcium-aluminate-hydrate or gel of calcium-aluminium-silicate-hydrate (CASH) [$\text{C}^{1/4}\text{CaO}$, $\text{S}^{1/4}\text{SiO}_2$, $\text{A}^{1/4}\text{Al}_2\text{O}_3$, $\text{H}^{1/4}\text{H}_2\text{O}$] in the presence of water [241]. Ca^{2+} ions lend a hand to accelerate CASH gel and CSH gel, and the nuclei development and agglomeration of Ca^{2+} ions lend a hand in accelerating CASH gel and CSH gel nuclear development and agglomeration [242]. The swift development of amorphous of CASH gel and CSH gel results in less setting time, creating ultimate products and diminishing the porosity, whereas a quick setting time has a negative effect on the development of more geopolymeric gel. The higher concentration of NaOH could lengthen the time for setting by restricting the leaking of Ca and permitting the usual process of geopolymerization to manage the setting time of geopolymeric paste [243].

Nevertheless, the fly ash dissolution at room temperature is incomplete, and the lower fly ash reactivity increases the time that is needed to set up a geopolymer based on fly ash. Curing is, thus, essential, i.e., that geopolymer paste must be kept within a practical range of humidity and temperature, and the prolonged duration of the cure promotes the growth of a more crosslinked bond and denser microstructure. It has been recorded that the reactivity of fly ash becomes high while the temperature for curing is from 30 °C to 50 °C [244].

To enhance the performances of geopolymer and the reactivity of fly ash, slag, fibre, chitosan, red mud and rice husk-bark ash (RHBA) can be supplemented with fly ash to synthesize geopolymer. Captivatingly, the addition of blast furnace slag (BFS) [245] can improve fly ash reactivity while geopolymerizing. Idawati et al. [246] studied the fly ash plus slag-based geopolymer with dissimilar ratios of fly ash to slag and revealed that the geopolymerization of geopolymer based on slag was dominated by CASH gel, whereas fly ash-based geopolymer was dominated by gel of sodium-aluminosilicate (NASH). Kumar et al. [247] replaced fly ash with 5–50% slag to produce geopolymer at 27 °C and noted that the reaction was obtained through the dissolution and precipitations of the gel of CSH. Likewise, Yang et al. [248] discovered that the initial setting period for fly ash plus GBFS-based geopolymer was boosted and the level of polymerization of geopolymer declined due to the higher calcium content of GBFS. The rice husk-bark ash (RHBA) contains around seventy-five percent SiO_2 , enhances the pozzolanic content of the matrix of

geopolymers and increases the quantity of geopolymer –Si-O-Si- bonds in the geopolymer gel (NASH). Red mud is a highly alkaline material consisting essentially of Fe, Al and Si, as well as minor CaO and TiO₂ oxides and hydroxides. Its addition can control the Si: Al ratio and lower alkaline activator consumption [249]. Fly ash-based geopolymer can solidify the heavy metals trace and is capable of immobilizing them.

4.2. Fly Ash Based Geopolymer: Properties

The properties of geopolymers may differ not merely in accordance with the origin, morphology and size of a particle of fly ash, but also with the metal, alkali and amorphous contents. The properties of geopolymers also depend on various parameters such as sodium hydroxide NaOH concentration, an alkaline solution to FA ratio, sodium silicate to sodium hydroxide ratio, alkaline liquid to fly ash ratio, curing duration, curing temperature, superplasticiser dose, added water content and rest period. Fly ash-based geopolymers are very useful materials for green constructions in the form of paste, mortar, binder and concrete. Hence, they should essentially exhibit the acceptable mechanical attributes—especially of strength, as well as durability—to establish them as promising sustainable building materials of the future [250].

4.2.1. Compressive Strength

The value of the compressive strength of fly ash-based geopolymers depends upon Si/Al ratios, alkali activator solutions, the content of calcium, a choice from a variety of additives and curing conditions such as temperature, as well as period.

The concentration, as well as the alkaline activator solution, affects the release of Si⁴⁺ and Al³⁺ ions from fly ash during geopolymerization reaction kinetics. It is established that alkaline activator solution with a higher concentration is usually advantageous for achieving elevated compressive strength; however, there exists an optimum limit [251]. Gorhan and Kürklü [252] have manufactured fly ash-based geopolymer by using dissimilar concentrations such as three, six and nine mol/L of NaOH. The best possible compressive strength figuring of 22 MPa was attained on activation of the geopolymer paste-based on fly ash with the concentration of 6 mol/L of sodium hydroxide, and subsequently cured at a temperature of 85 °C for 24 h. The solution of sodium silicate (Na₂SiO₃) is generally employed with NaOH to boost the compressive strength of resultant geopolymer based on fly ash [253]. This is because of the greater viscosity of sodium silicate, which can help to form geopolymeric gels and achieve a compact, eventual micro-structure of a fly ash-based geopolymer.

Additionally, the course of separate activation also affects the compressive strength of geopolymer based on fly ash. For illustration, Rattanasak and Chindaprasirt [254] first attempted to add NaOH activator liquid to fly ash to release the Si⁴⁺ and Al³⁺ ions for 10 min, which was followed by employing Na₂SiO₃ activation to favour the formation of a homogeneous geopolymer paste for another minute. This type of separate activation has contributed to the higher strength of fly ash geopolymer. While fly ash was mixed separately and activation was made with 10 mol/L concentrated NaOH plus sodium silicate with a molar ratio of 1.0, followed by a curing temperature of 65 °C for 48 h, the resultant compressive strength value of geopolymer based on fly ash was found to range from 60 to 70 MPa.

The ratios of Si: Al are confirmed by precursor materials, and the alkaline solution that was employed was Na₂SiO₃. Higher ratios of Si/Al enhance the quantity of –Si-O-Si- bonds, giving them the elevated compressive strength of an entirely consolidated structural matrix of geopolymer, because the –Si-O-Si- bonds are stronger than that of –Al-O-Al- and –Si-O-Al- bonds. For instance, Yang et al. [255] produced high magnesium-nickel slag and fly ash geopolymer by activation through a solution of Na₂SiO₃. They revealed that the key phase in fly ash plus high magnesium-nickel slag (HMNS)-based geopolymer was a sort of sodium magnesium aluminosilicate gel. The addition of high magnesium-nickel slag (HMNS) boosted the content of silica. Furthermore, the particles

of HMNS played the role of micro-aggregates and mitigated the entire volume of pores that were present in the geopolymeric pastes. On employing 20% of HMNS in the said manufacturing process, the geopolymer exhibited an improved compressive strength of more than 60 MPa. However, the elevated quantity of slag (like slag/binder was greater than 70%) escalated the compressive strength of geopolymer based on fly ash plus HMNS. Regrettably, it caused a quick setting and cracked on account of the autogenous shrinkage of the slag [256]. Moreover, Wang et al. [257] produced fly ash plus slag-based geopolymer by using unlike ratios of fly ash/slag such as 0, 20, 40, and 60 wt.% and similarly dissimilar NaOH activator solutions with 0.5, 1 and 1.5%, and subsequently cured them for one, three, seven and twenty-eight days. The increase in the quantity of slag enhanced the value of the resulting geopolymer's compressive strength, and the best possible value of compressive strength that was obtained in this case was 93.06 MPa. Deb et al. [258] utilized a fusion of Class F type fly ash addition of slag to obtain a blended geopolymer of slag plus Class F type fly ash in a ratio of 0, 10 and 20% by activating with Na_2SiO_3 plus NaOH activator solutions, correspondingly. The value of the compressive strength of the resultant product was enhanced with a boost of the ratio of slag/Class F fly ash. The geopolymer concrete is manufactured by fly ash of 80% and 20% slag, and having used 40% NaOH plus Na_2SiO_3 activator solutions and cured subsequently at a temperature of 20 °C, achieved the optimal compressive strength value of 51 MPa. Xu et al. [259] employed slag and fly ash to produce geopolymer through activation by activator that was made from Hanford secondary waste, with the concentration of 5 mol per 1L sodium hydroxide liquid with solid binders. In this case, the best possible value of compressive strength that was obtained was 52.5 MPa when the ratio of fly ash to GBFS by mass was kept as 5/3. The addition of rice husk-bark ash enhanced the silica content of the geopolymer composite and escalated the quantity of bonds (-Si-O-Si-) in the geopolymer, and the value of the compressive strength [259]. Nazari et al. [260] supplemented rice husk-bark ash added with fly ash to manufacture geopolymeric paste with oven curing at 80 °C for 28 days. The study achieved geopolymer with a compressive strength value of 60 MPa. Likewise, Songpiriyakij et al. [261] synthesized geopolymer based on fly ash by employing the fusion of fly ash with rice husk-bark ash with NaOH as the activator solution, subsequently curing it at 27 °C for 24 h, and then again at 60 °C for up to 24 h. Here, the optimum ratio of $\text{SiO}_2/\text{Al}_2\text{O}_3$ to achieve the best possible value of compressive strength of 73 MPa was recorded as 15.9. Zhang et al. [262] manufactured fly ash plus red mud blended geopolymer at a curing temperature of 23 °C. The values that were obtained for the highest compressive strengths were found to vary from 11.3 to 21.3 MPa, while the Si to Al ratio was 2. Calcium hindered the gelation of alumina and silica in the course of geopolymerization and modified the microstructures of geopolymer based on fly ash, hence, altering the compressive strength value [263]. The coexistence of NASH gels and CSH gel generally enhances the compressive strength of ultimate yields. One of the reasons for this is that the CSH amorphous gel mitigates the porosity factor [209]. In addition, temperature curing and duration also influence fly ash-based geopolymer compressive strength. Prolonged periods of curing that range from 6 to 28 days display the enhanced value of fly ash-based geopolymer compressive strength. The elevated temperature curing enhances the compressive strength through eliminating water from the early formed geopolymer and achieves the collapse of the capillary pores through a denser structure [264]. Geopolymer can be cured at a lower, i.e., even room, temperature, but the development of compressive strength takes place gradually and slowly, which forever necessitates a long and drawn out curing period [265]. Nasvi and Gamage [266] uncovered that the crack commencement and sealing of the thresholds of geopolymer based on fly ash cured at higher temperatures, varying from 60 °C to 80 °C, in comparison with those that were cured at an ambient temperature of 23 °C and 40 °C. Nonetheless, the lengthened elevated temperature curing shatters the geopolymer granular structure, causing dehydration, as well as excessive shrinkage, and at last mitigating the value of its compressive strength [70].

The conventional heating technique such as “Steam curing” depends upon the heat conductivity from the exterior to the interior surface fly ash-based geopolymer paste through steam. This heating is inconsistent and necessitates a prolonged period of heating to obtain the desired temperature. On the other hand, microwave heating works based on internal energy dissipation, which is accompanied by the excitation of molecular dipoles in electro-magnetic areas, and it conveys swiftly with more consistent heat [267]. Chindaprasirt et al. [268] synthesized the paste of geopolymer based on fly ash with 10 mol per 1 L concentrated Na_2SiO_3 with NaOH solutions, and subsequently cured it in the 90W radiation of a microwave for five minutes. After that, supplementary heating occurred at a 65 °C curing temperature for a curing period of 6 h, resulting in a similar compressive strength to that which was obtained with a 65 °C curing temperature for 24 h of fly ash-based geopolymer. The radiation from the microwave accelerated the fly ash dissolution in an alkaline liquid and developed a denser microstructure. Given that, the microwave radiation reduced the requisite curing period and further improved the geopolymerization kinetics.

Altogether, boosting the Si/Al ratio largely augments the value of fly ash-based geopolymer’s compressive strength. The improvements in the Si to Al ratio can be seen in addition to the outer slag, red mud and rice husk–bark ash, but the intrinsic causes are difficult and complex. The progress in the synthesis signalled that one of the prominent reasons could be attributed to the escalated quantity of -Si-O-Si- bonds to a certain extent, rather than -Al-O-Al- and -Si-O-Al- bonds. To sum up, the application of K_2SiO_3 or Na_2SiO_3 along with sodium hydroxide as activators for fly ash activation can augment the Si to Al ratios and, in this way, pilot a structure which is more compact and which displays elevated compressive strength. Not only this, the existence of calcium within fly ash or employed as an additive is advantageous for synthesizing the amorphous gel of CASH, as well as CSH, and mitigates the available porosity and attains the higher compressive strength of geopolymer. Curing demonstrated a remarkable impact by modification of the product density and porosity on the value of the compressive strength of the fly-ash based geopolymer.

4.2.2. Flexural and Splitting Tensile Strength

No doubt, geopolymers based on fly ash perform extremely well under compression strength examinations. Their performance is controlled by the start of cracks in mass; however, this is under tensile loads. Lee et al. [269] accounted for the investigational upshots of the tensile performance of geopolymeric concrete. With an increase in the sand to fly ash ratio, a gradual drop in tensile strength was monitored. Zhuang et al. [270] recorded a comparison between ACI standard design strength and the results of experiments that examined geopolymer concrete tensile performance. They observed that the splitting tensile strength of geopolymer concrete was likely to be similar to the design values that were provided by the ACI standard. Zhang et al. [271] noted that the geopolymer concrete performed more than the OPC-based concrete in the context of tensile strength. Adak et al. [272] unearthed that the supplement of 5 to 6 percent of nano silica enhanced the geopolymer concrete’s tensile strength with standard curing. Al-Majidi et al. [273] uncovered the findings through experiments on geopolymer concrete that employed fly ash plus GGBFS. The outcomes demonstrated that the application of slag in the geopolymer concrete had an optimistic impact on the direct tensile performance. The impact of slag on the tensile attributes of geopolymer concrete, whereby an enhancement of up to 30% can be monitored, leads to the augmentation of its tensile strength. Moreover, the review of past research revealed that the tensile performance of geopolymer concrete is more magnificent than OPC concrete, possessing identical compressive strength [274,275]. Nath and Sarker [276] provided an idea for a geopolymer concrete and OPC concrete mix, manufactured through various proportions, as well as additive materials of GGBFS, OPC and calcium hydroxide, for investigating fly ash-based geopolymer concrete’s flexural strength at an ambient curing temperature. The flexural strength of geopolymer concrete based on

fly ash is affected considerably by the kind of additive that is employed, accompanied by fly ash. In comparison with calcium hydroxide and GGBFS additives, the addition of OPC with fly ash enhances the flexural strength of geopolymer concrete.

4.3. Durability Properties

The significant parameters for the durability of fly ash-based geopolymers such as resistance to sulphate, chloride, thermal, acid, efflorescence and freeze–thaw, must be taken into consideration to establish it as a potential construction material. The durability property is strictly associated to the microstructure, as well as the migratory ions conduct from geopolymer based on fly ash, which, consecutively, could be regulated by the alkali activator, the supplement of composite materials of calcium, as well as by silica fume, along with curing through its synthesis.

4.3.1. Resistance against Chloride

Resistance against chloride is one of the key aspects for the durability of fly ash-based geopolymer composites. The penetration of chloride encourages the corrosion of the entrenched steel bars in reinforced geopolymer concrete. The chloride ions infiltrate into the geopolymers through capillary pores absorption, ions diffusion and hydrostatic pressure. The comparatively higher concentration of sodium hydroxide facilitated the leaking of additional Si^{4+} and Al^{3+} ions from fly ash precursor and produced a superior level of poly-condensation, resulting in a dwindling of fly ash-based geopolymer porosity. The chloride penetration depends upon the porosity of the material. For instance, Chindaprasirt and Chalee [277] synthesized a geopolymer based on fly ash utilizing Na_2SiO_3 plus sodium hydroxide mix activator solutions. In this case, dissimilar concentrations of NaOH were used such as 8, 10, 12, 14, 16 and 18 mol/L, but the molar ratio of $\text{SiO}_2/\text{Al}_2\text{O}_3$ was kept as a constant. The rate of chloride penetration reduced with the boost in the concentration of NaOH, which was employed in the course of geopolymerization on account of the refinement of the pore structures, due to the reaction of polycondensation. Ismail et al. [278] studied the chloride permeability of an infusion of Class F type fly ash plus slag-based geopolymer by the chloride accelerated technique and the ponding technique. AgNO_3 was useful to disclose the depths of chloride penetration. The upshot displayed that a slight development of silver chloride (AgCl) was found for the geopolymer based on slag. They reported that the slag favoured the development of a denser gel of CASH, offering to enhance the durability and mechanical strength when exposed to chloride, while fly ash encouraged the production of additional porous NASH gels, reducing the chloride ions' resistance transportation.

Even though a greater porosity was monitored in the case of the geopolymer in comparison with the OPC- system samples, still, the geopolymer exhibited greater chloride resistance. Yang et al. [279] manufactured a fly ash addition with a slag-based geopolymer, with a ratio of slag to fly ash of 0, 0.25, as well as 0.50, along with the exposure of the precursor materials to a 3% NaCl solution for 72 h. The CASH gel in the fly ash plus slag-based geopolymer led to a lower diffusion of chloride than the NASH gel. Moreover, the fusion of slag with fly ash-based geopolymers led to the enhancement of the pore structure.

4.3.2. Resistance against Sulphate

The migration of sodium-ion (Na^+) into the sulphate solution from the fly-ash-based geopolymer results in vertical cracks. Not only this, the solution of sulphate generally causes the breakdown of the bond $-\text{Si}-\text{O}-\text{Si}-$ in geopolymeric gel with the leaking of silicon. Bakharev [280] produced geopolymer based on fly ash, utilizing solutions of KOH, NaOH or Na_2SiO_3 as activators, and studied the durability subsequent to exposing them to sulphate media, which consisted of 5% solutions of MgSO_4 alone, Na_2SO_4 alone and MgSO_4 plus Na_2SO_4 combined for five months. Subsequent to immersion, the geopolymer based on fly ash specimens were found to be slightly altered. The production of the geopolymer that was activated by NaOH displayed the highest resistance to sulphate on account of an

additional steady cross-linked structure. A mixture of silty clays plus fly ash was used by Sukmak et al. [281] to synthesise a geopolymer and to examine its resistance by five percent Na_2SO_4 plus MgSO_4 in solutions by weight. The decline in the compressive strength that was observed for the clay plus fly ash-based geopolymer subsequent to exposure for 240 days was in 10.8% solution of Na_2SO_4 and 21.6% solution of MgSO_4 . The ettringite, brucite and gypsum were noticed after being subjected to sulphate conditions. Due to the reaction to the development of ettringite and sulphates, the CSH phase disappeared. The magnesium sulphate degraded the GPC significantly in the calcium-rich geopolymer that was produced in the end products. By replacing the calcium in the structure, it breaks the CSH link and creates the Mg-SH. The magnesium-formed structure increased the volume, causing fracture development in the GPC. At the same time, sodium sulphate does not significantly degrade the GPC. The mechanical properties of GPC-mixed specimens are reduced by magnesium sulphate [282]. The high-calcium BA geopolymer mortar has exceptional resistance to sodium sulphate [283].

4.3.3. Acid Resistance

The acidic conditions can rigorously reduce the life-cycle period of composites. Acid attack is found to be accompanied by the depolymerization of an alumino-silicate structure, as well as the release of silicic acid in the geopolymer based on fly ash. While submerged in a solution of a strong acid, K^+ and Na^+ of fly ash-based geopolymer might be replaced by H_3O^+ or H^+ , the breakdown of bonds $-\text{Si}-\text{O}-\text{Al}-$, as well as $-\text{Si}-\text{O}-\text{Si}-$, along with a release of silicic acid.

Diverse solutions of alkali such as NaOH , Na_2SiO_3 and KOH were employed by Bakharev [284] to produce a fly ash-based geopolymer, following their immersion into 5% solutions of CH_3COOH and H_2SO_4 for five months. The fly ash-geopolymers were been manufactured by activating them with 8% NaOH solution. They displayed a steadier structure and higher resistance against both solutions of CH_3COOH and H_2SO_4 acid, in addition to the fly ash form geopolymer that was produced by activation through KOH (which demonstrated an enhancement in the average pore diameter and the active sites in the geopolymeric gels lying on the surface, leading to inferior durability).

In addition, there is an emphasis on the impact of silica and calcium on the acid resistance of the geopolymer based on fly ash. In acid solutions for nitric acid HNO_3 and sulfuric acid H_2SO_4 , Lloyd et al. [285] studied corrosion rates in a Class C fly ash plus slag-based geopolymer. The calcium content of Class C fly ash or slag was found mitigate the mass transport rates by developing tortuous pores and fine networks in the geopolymer. Not only this, because of the enhancement in the content of alkali in the form of Na_2O , the layer that underwent corrosion became more robust, and further vulnerable to the formation of cracks. The high content of alkali is advantageous for the release of more aluminium and calcium, as well as for producing geopolymeric gels. When it was removed upon exposure to acids, the structure of the geopolymer was more susceptible under acid exposure conditions. Chindapasirt et al. [277] supplemented silica fume in the proportion of 1.5, 3.75, as well as 5.0% with fly ash to synthesize geopolymeric mortars. A resistance to acid by the said mortars was examined in three volumetric percentages of H_2SO_4 acid. The best possible addition of 3.75% silica fume improved the strength of fly ash-form geopolymer and exhibited the optimum resistance to acid because of the boost in CSH gels, resulting in a denser structure.

With higher temperature curing, resistance to acid by a fly ash-form geopolymer is advantageous. Nguyen et al. [286] maintained a curing temperature of 80°C for curing period of 10 hours for the fly ash-based geopolymer at and after that the immersion in a solution of 1, 2 and 4 mol/L of concentrated HCl . They noticed that the fly ash-form geopolymer maintained a value for compressive strength of roughly 20 MPa, greater than OPC in the 1, 2 and 4 mol/L HCl solution. Furthermore, Chindapasirt et al. [287] cured fly ash-form geopolymer with a 90W microwave for five minutes and observed that the microwave radiation escalated the process of geopolymerization and provided improved

densification that was analogous to the traditional curing. The fly ash-form geopolymer that was cured with a microwave had a dip in the 3 volume % of H_2SO_4 and recorded that it merely had a little strength loss when subjected to the acid exposure.

4.3.4. Resistance against High Temperatures

Although the geopolymer based on fly ash is subjected to higher temperatures, the amount of water that evaporates from its structure results in shrinkage [288]. Some of them demonstrate an enhancement in strength, subsequent to their exposure to higher temperatures, proving themselves fit to use for constructions as concrete, thermal barriers, fire-resistant structures, refractory and thermal insulators, etc.

It has been made known that heat can travel more swiftly in geopolymer concrete than its counterpart from the OPC system during fire exposure, resulting in a lower temperature gradient within geopolymer concrete [289]. The OPC concrete exhibited average residual strengths of 90, 52 and 11 to 16%, subsequent to its exposure to fire at 400, 650 and 800 to 1000 °C, respectively, while in the context of geopolymer concretes, the average residual strengths were 93, 82, and 21 to 29%, i.e., higher than OPC concrete, following the same kind of treatments. Furthermore, the OPC concrete underwent rigorous spalling and widespread surface cracking, subsequent to the exposure to temperatures of 800 to 1000 °C, whereas there was an absence of spalling and merely negligible surface cracking in the case of geopolymer concrete. Guerrieri and Sanjayan [290] exposed the fly ash plus slag-form geopolymer, maintaining the ratio of fly ash to slag as 100, 65/35, 50/50, 35/65 at 800 °C. Their outcomes evidenced that the geopolymer samples with very low early strengths of less than 7.6 MPa displayed an enhancement in the residual compressive strength of up to 90%, following exposure at 800 °C, whereas the samples with an early strength of 28 MPa—along with samples with an initial strength of 83 MPa—lost roughly 70 and 90% in residual strength, following 800 °C thermal exposure, correspondingly. These dissimilar residual strengths of fly ash plus slag-formed geopolymer, subsequent to its exposure at a temperature of 800 °C, were the result of sintering of the non-reacted fly ash-slag and further hydration. Geopolymer has high early strength and is less able to permit thermal incompatibilities among the internal and external parts of the sample on account of uneven temperatures during the heating period. Rickard et al. [291] studied the thermal attributes at a temperature of more than 500 °C for Class F fly ash-formed geopolymer. The peak shrinkage was about 3%, which was found at 900 °C thermal exposure temperatures. The Fe_2O_3 that was present with fly ash at 15% by weight directly influenced the thermal characteristics of the geopolymer, by impacting the thermal expansion, modifying the composition and altering the morphology, following the course of heating.

The density and pore structure of the geopolymer based on fly ash encourages escape from the moisture and facilitates damage protection during heating. Kong et al. [292] synthesized and exposed a fly ash-based geopolymer to heating at a temperature of 800 °C and found that a little quantity of moisture fled from the fly ash matrix, as well as the pores creating furnished routes to escape moisture in the matrix, thus, reducing the possibility of damage to the matrix at very high temperatures. Bakharev [293] compared the influences of the course of thermal temperature at 800 to 1200 °C on the geopolymer that was composed of Class F type fly ash, activated by sodium hydroxide, as well as potassium hydroxide, correspondingly. The geopolymer that was activated by sodium hydroxide activator solution showed a quick strength drop, in addition to a higher shrinkage at temperature 800 °C because of the theatrical enhancement of the average pore size, whereas another geopolymer that was produced with activation by potassium hydroxide displayed a noteworthy escalation in the value of compressive strength on heating course (whereby the strength deterioration was only initiated at 1000 °C). The supplement of low-concentrated foaming agent led to a lower density through the cellular structure. Rickard and van Riessen [294] also developed the foamed Class F type fly ash geopolymer, maintaining a ratio of Si to Al of 2.5, and exposed it to a simulated fire for 60 to 90 min, resulting in its considerable loss of strength. Foaming notably diminished the strength of Class F type fly ash-formed

geopolymer, whereas the thermal insulating characteristic was also enhanced, since their thermal conductivities are mitigated by more or less half.

The use of $\text{Ca}(\text{OH})_2$ in the production of geopolymers based on fly ash led to the development of the CSH gel and the different mineral developments and changes at high temperatures. Fly ash-based geopolymer was produced, and the effect of calcium on the thermal resistance was examined by Dombrowski et al. [295]. While the geopolymer was subjected to temperatures that were greater than 600 °C, the formation of amorphous aluminosilicates and mineral sodalite took place, and this was converted into nepheline, afterwards exhibiting a denser structure. The nepheline transformed into mineral albite with its additional temperature increase. The fly ash-based geopolymer with a production of eight percent $\text{Ca}(\text{OH})_2$ showed optimum strength and the lowest shrinkage with a maximum nepheline content of 800 °C and of feldspar at 1000 °C. Geopolymer, when subjected to fire, demonstrated not only the propensity to shrinkage, but also to crack. In accordance with the standard that was fixed by the International Standards Organization, Sarker et al. [296] tested the fire resistance by the fly ash of the geopolymer and OPC system through exposure of the specimens to heating through fire at 400, 650, 800 and even at 1000 °C. However, when the exposure to heat through fire was made of fly ash-formed geopolymer at 1000 °C, it showed only slight cracks on the surface and a mass loss of 4.8%, whereas that of the OPC-system had a mass loss of 90%, proving fly ash geopolymer as an excellent fire and thermal resistant.

4.3.5. Freeze–Thaw Resistance

In regions with severe environmental conditions, the freeze–thaw attack generally accounts for the expansion of cement, as well as concrete, in-house cracking, and mass loss [297]. It can be considered as a severe attack on composites next to chloride attack. Remarkably, geopolymer based on fly ash has not exhibited any sign of deterioration, even with 150 freezing cycles.

Temujin et al. [298] synthesized a geopolymer using Class F type fly ash, activated by a $\text{NaOH} + \text{Na}_2\text{SiO}_3$ activator solution, and afterwards cured it with a curing temperature of 70 °C for 22 h. The supplement of Na_2SiO_3 solution did not enhanced the durability criterion of the freeze–thaw of geopolymer based on fly ash. The amorphous Ca-compounds, such as lime and anhydrite in fly ash, and the existence of crystalline negatively impacted the resistance to freeze and thaw. The solution of Na_2SiO_3 reacted with compounds of calcium viz., CaO , amorphous calcium aluminosilicate and CaSO_4 that were present in the fly ash, as well as developed a CASH gel or $\text{Ca}(\text{OH})_2$. The development of $\text{Ca}(\text{OH})_2$ weakened the internal structure and increased the water penetration, as well as demonstrated a negative effect on freeze–thaw resistance. Air entrainment has been evidenced as an efficient technique to raise the OPC system's resistance to freeze–thaw.

Sun and Wu [299] made a comparison of both the geopolymer based on fly ash and the OPC system with or without air entrainment for three hundred freeze–thaw cycles. OPC without air entrainment suffered deterioration most gravely, displaying a loss in strength of roughly 20% following 300 cycles, while 5% strength loss was seen for the OPC with air entrainment. In the case of the geopolymer based on fly ash, without air entrainment, this was found with an ultimate loss of 8.4%, with 300 cycles. Fly ash-based geopolymer with the air entrainment exhibited a loss in strength of 6.8%. Undoubtedly, the air entrainment did not show much of an optimistic impact on the fly ash geopolymer.

The influence of air entrainment on the scaling rate of fly ash-based geopolymer was investigated by Brooks et al. [300]. Air-entrained geopolymer based on fly ash demonstrated minor scaling after 40 cycles of freeze–thaw, whereas the geopolymer based on fly ash sans air-entrainment was found without scaling. The compressive strength of fly ash-formed geopolymer declined considerably through air entrainment from 10 to 30%, compared to the sans air-entrained fly ash-based geopolymer, as well as the homogeneous, steady pore structure, which is supposed to boost durability in the context of resistance to freeze–

thaw. This was not found to be absent in the case of fly ash-based geopolymer that was not air-entrained.

4.3.6. Resistance against Efflorescence

Particularly, a geopolymer with higher alkali, as well as lower calcium contents tends to be porous with an open micro-structure. The water solution is captured or linked with the network in the pores, while the geopolymer 3D structure is finally developed [53]. Inside the pore structure, the surplus sodium oxide is movable. In addition, this is susceptible to producing crystal in a white colour, i.e., efflorescence, while contact with carbon dioxide that is present in the atmosphere causes the degradation of the geopolymer [301]. The efflorescent nature of fly ash-formed geopolymers is highly reliant on the kind of alkali activator solution, the calcium that is present and the curing temperature. The application of KOH in place of NaOH as an activator solution reduces the efflorescence of the geopolymer [302]. The higher concentration of alkali in the pore solution and the low connection of Na^+ in the geopolymeric structure are the root causes of moving Na^+ in pore solution and lead to a severe geopolymer efflorescence [303].

On the other hand, K^+ represents a stronger bond to the alumino-silicate gel framework and crystals of K_2CO_3 are generally visually less evident than their sodium counterparts. Zhang et al. [304] activated fly ash with sodium hydroxide to produce geopolymer. In addition, they maintained a curing temperature of 23 °C and 80 °C. They revealed that geopolymer displayed greatly inferior efflorescence at an elevated temperature, compared to those that were manufactured at the lower temperature. The curing was beneficial to crystallize and restructure NASH gels, as well as to reduce the rate of efflorescence. The presence of calcium helps to develop CSH gel in geopolymer based on fly ash and a smaller pore size with lower penetration, which puts stops the diffusion of alkali [305]. On the contrary, in the case of the foamed geopolymer based on fly ash, the foaming resulted in the large pore size and high porosity of the geopolymer based on fly ash, which led to the quick leaking of alkali and, hence, resulted in speedy efflorescence [304].

4.4. Fly Ash-Based Geopolymer for Concrete

The emerging concerns regarding the environment and restricted natural resources have motivated scientists, researchers, engineers and people related to construction and infrastructure industries to seek alternative construction materials [306]. Fly ash is one of the profuse industrial by-product waste materials, employed as either precursor or supplementary cementitious material in manufacturing diverse geopolymers for the concrete industry. Geopolymer concrete based on fly ash differs from OPC production regarding the higher carbon dioxide emissions that are linked to it [307]. In several respects or under specific conditions, fly ash-based cement has sometimes demonstrated a superior performance to OPC. In comparison with OPC concrete, fly ash-based geopolymer concrete has a dense microstructure with a lower diffusion of chloride and low porosity.

Reddy et al. [308] utilized Class F type fly ash as a precursor with Na_2SiO_3 plus NaOH as alkaline activator solutions to produce geopolymer cement. They revealed that the referred geopolymer concrete demonstrated outstanding chloride attack resistance with lesser cracks owing to corrosion, while it was subjected to an induced current and simulated seawater. Alkali-silica reaction is a familiar phenomenon among the OH^- in the pores that are present inside the concrete matrix and the reactive aggregates of the concrete. Alkali-silica reaction is accountable for the loss in strength, the distribution of the concrete structure and, significantly, for cracking. It is well-known that fly ash-based geopolymer concrete is considered to be susceptible to a lesser amount of ASR than OPC concrete. Kupwade-Patil and Allouche [309] manufactured a geopolymer concrete based on fly ash with reinforcement by steel bars using aggregates of quartz, siliceous limestone and sandstone. Afterwards, they compared the cyclic wet and dry chloride medium for chloride ion diffusion for more than 12 months, along with OPC concrete for comparative study. Surprisingly, the outcomes suggested that OPC concrete specimens went beyond

the allowable limit by the ASTM standard for expansion, whereas geopolymer concrete samples were found to be within the permissible range.

Additionally, the leaking and visual cracking were monitored in OPC concrete, while geopolymer concrete-based fly ash demonstrated no such footprint of cracks. Normally, aggregates encircle as high as 85% of the total material that is present in concrete. In the case of fly ash-based geopolymer concrete, the interactions between the aluminosilicate framework, alkali cations, aggregates and additives are key factors which affect the mechanical performances on the whole. The powerful interfacial interactions among the geopolymer matrix and the aggregates in a greater region provide the higher splitting tensile strength amid steel reinforcements and geopolymers [310]. Moreover, the size of the aggregates impacts on the performances of the fly ash-formed geopolymer concrete.

The influence of the aggregate size on the compression strength of fly-ash-based geopolymer concrete with aggregates of crushed old basalt, slag and river sand at elevated temperature was investigated by Kong and Sanjayan [311]. They reported that the thermal incompatibility among the aggregates and the matrix of the geopolymer resulted in a loss in strength for geopolymer concrete samples at very high temperatures. The larger aggregates of more than 10 mm in size demonstrated high-quality performances in the context of strength at both ambient and higher temperatures, whereas aggregates that were less than 10mm in size favoured not only the spalling, but also wide-ranging cracking at the higher temperature. The coarse recycled aggregate was employed to manufacture geopolymer concrete based on fly ash with up to the standard attributes. Sata et al. [312] utilized crushed bricks comprised of clay and structural beams of concrete subsequent to crushing as recycled coarse aggregates to produce geopolymer concrete based on fly ash. The referred recycled aggregate containing fly ash-formed geopolymer concrete displayed inferior compressive strength values ranging from 2.9 to 10.3 MPa than the one possessing natural aggregates.

Moreover, the ratio of the total void was 21.7 to 26.9% of the geopolymer concrete made up of recycled aggregate, which was just analogous to those containing natural aggregate at 24.2 to 27.4%, and the water permeability that was recorded was 0.71–1.47 cm/s versus 1.18–1.71 cm/s. Nuaklong et al. [313] employed high calcium fly ash with recycled aggregates that were obtained from old concrete, possessing the compressive strength of 30–40 MPa to synthesize the fly ash-based geopolymer, and examined the strength criterion. In this case, they monitored the range of values of compressive strengths from 30.6 to 38.4 MPa, less than those of fly ash-formed geopolymer concrete possessing crushed limestone as an aggregate. The diverse superplasticizers such as polycarboxylates and naphthalene (N) as the water reducer admixture were applied by Nematollahi and Sanjayan [314] to enhance the workability of the geopolymer concrete. The polycarboxylates superplasticizer of 3.3 wt.% caused a noteworthy decrease of 54% in strength, regarding concrete with no use of superplasticizer.

On the contrary, N superplasticizer with a 1.19% weight caused a 22% decline in strength. At a higher temperature, the use of superplasticizers is not useful to geopolymer concrete at elevated temperatures. The lower permeability of the geopolymer based on fly ash can effectively stop CO₂ leakage.

Nasvi et al. [315] investigated the apparent permeability of the CO₂ of geopolymer cement based on fly ash. Furthermore, Nasvi et al. [316] synthesized geopolymer cement by employing fly ash with NaOH plus Na₂SiO₃ activator solutions and examined the permeability of CO₂ under three conditions, such as (i) temperatures of 23 to 70 °C; (ii) confining pressures of 12 to 20 MPa, (iii) CO₂ injection pressures of 6 to 17 MPa. The findings exhibited that the apparent permeability of CO₂ for geopolymer escalated with a boost in curing temperature. These outcomes indicated that geopolymer cement based on fly ash possesses an excellent potential for its use in the storage of carbon. Table 2 represents the existing literature based on the properties of geopolymer concrete.

Table 2. Existing literature properties of geopolymer concrete.

Sr. No	Paper	Test Conducted	Observations	
1.	Strength studies	Hardjito [317], Llyod [318], Paniyas et al. [319], Sofi et al. [320] Rangan [321],	Compressive strength	Geopolymer composites based on fly ash exhibited high early strength compressive strength, compared to cement concrete. Higher temperature and higher sodium hydroxide concentration give the highest compressive strength. There is no major reduction in compressive strength with concrete age.
		Sofi et al. [320]	Flexural strength	The flexural strength determines the tensile properties of concrete under internal or external loading. The flexural strength of geopolymer concrete is more privileged than that of cement concrete, which exhibits a decreasing rate of crack propagation due to corrosion of embedded steel bars in the concrete.
		Sofi et al. [320]	Split tensile strength	The split tensile strength of geopolymer concrete decreased as the proportion of rubber tyre waste increased. However, the strength is higher than that of cement concrete due to good bonding between the geopolymer paste and aggregates.
		Sofi et al. [320] Fernande et al. [322] Neville [323] Hardjito et al. [324]	Modulus of elasticity	The modulus of elasticity of geopolymer concrete is dependent on the modulus of elasticity of the aggregate, as well as the microstructure and modulus of elasticity of the geopolymer paste. Geopolymer concrete exhibits good bonding between the geopolymer paste and aggregates. However, geopolymer concrete has a higher modulus of elasticity than cement concrete.
2.	Durability studies	Cheema et al. [325]	Permeability	The coefficient of water permeability is low in geopolymer concrete as compared to OPC concrete. As the alkaline ratio increases, the water permeability of geopolymer concrete decreases.
		Adam et al. [326], Thokchom et al. [327] Mishra et al. [328]	Sorptivity	As the alkaline liquid ratio increased from 0.75 to 1.25, the sorptivity of geopolymer concrete decreased. An increase in Na ₂ O content in geopolymer concrete decreased the sorptivity.
		Song [329] Sathia et al. [330]	Water absorption	The water absorption of geopolymer concrete is lower than in cement concrete.
		Bakharev [331] Wallah et al. [332] Thokchom et al. [327]	Sulphate resistance	Geopolymer concrete exhibits excellent performance against sulphates. Significant changes in mass and compressive strength have been observed in geopolymer concrete, as compared to cement concrete, as a result of alkaline liquid enhancing the stability of the geopolymeric structure. Increased alkaline content in the geopolymer mixture can improve the performance of geopolymer concrete against sulphates.
		Bharkdev [333] Song et al. [334]	Acid resistance	The degradation of mass and compressive strength of specimens after immersion in acid solution is less than observed in cement concrete specimens under an acidic environment.

Table 2. Cont.

Sr. No	Paper	Test Conducted	Observations		
2.	Durability studies	Monita et al. [335]	Corrosion The corrosion of steel reinforcement embedded in geopolymer concrete is similar to that of steel embedded in cement concrete.		
		Adam et al. [326] Roy [336]	Carbonation The carbonation performance of geopolymer concrete is excellent compared to that of cement concrete.		
		Monita et al. [335]	Chloride ion penetration The chloride-ion penetration of fly ash geopolymer was higher than for OPC concrete.		
		Wallah and Rangan [337]	Shrinkage Geopolymer concrete has very little drying shrinkage compared to that of OPC concrete.		
3.	Elevated temperature effect	Rashad and Zeedan [338]	Residual strength of alkali-activated fly ash paste at a different temperature Sodium silicate is more resistant to degradation caused by exposure to elevated temperatures than Portland cement specimens. The compressive strength and thermal shock resistance decreased.		
		Kong and Sanjayan [339]	Residual thermal damage of geopolymer composites Geopolymer strength increased by approximately 53% after exposure to elevated temperatures. Aggregate expanded with temperature. At 800 °C, expansion reached approximately 1.5–2.5%.		
		Luhar et al. [340]	Compressive strength of geopolymer paste Aggregates larger than 10 mm show higher strength at both ambient and elevated temperatures.		
		Zhu pan et al. [341]	Compressive strength of geopolymer mortar The compressive strength of geopolymer mortar decreases in some cases and increases in others after exposure to high temperatures.		
		Ranjbar et al. [342]	Compressive strength, density and TGA of fuel ash-based geopolymer mortar Palm oil fuel ash and fly ash used as source materials. Geopolymer mortar accelerated micropore formation at elevated temperatures.		
		Kong et al. [343]	Compressive strength of fly ash and metakaolin The compressive strength of fly ash-based geopolymer concrete is increased beyond 800 °C but the strength of the metakaolin based geopolymer concrete decreases at the same temperature.		
		Zhu pan et al. [344]	Compressive strength and transient creep of geopolymer and OPC composites At 550 °C, the strength of geopolymer paste increased, whereas the OPC paste exhibited little change.		
		Hussain et al. [345]	Mass loss, compressive strength of blended ash geopolymer concrete In comparison to OPC concrete at high temperatures, geopolymer concrete provides better compressive strength.		
		4.		Fenghong Fan [346]	Thermo-Mechanical Properties Study includes the thermo-mechanical properties of class F fly ash based geopolymer materials prepared using KOH and Na ₂ SiO ₃ alkaline activators with different curing and cooling methods.
				Omar et al. [347]	Compressive strength of lightweight geopolymer paste, mortar, and concrete The unexposed geopolymers have excellent mechanical and microstructural properties. The deterioration of the properties of geopolymers begins at 800 °C.
Sun et al. [348]	Compressive strength, TGA, SEM and FT-IR analysis of geopolymer paste As source material, ceramic waste is used. A compressive resistance of 28 days of 71.1 MPa before and 75.6 MPa after thermal treatment at 1000 °C was presented with the synthesized geopolymer paste.				

4.5. Fly Ash-Based Geopolymer for Mortar

The potential applications of geopolymers based on fly ash as mortar necessitate the study of its significant properties, in order to establish it as a successful building material.

4.5.1. Properties

Workability

The degree of workability of fresh geopolymer mortar is an imperative attribute, which determines the characteristics of hardened geopolymer mortar. Water is usually used to control the fluidity of fresh mortar without decreasing the visible strength [349]. Flow is often used to calculate the workability of the mortar, which can be measured with the flow test. Flow is normally utilized to assess the functioning ability of fresh mortars, that is given away in the percent of the early base diameter. The devices for testing comprise a mould for flow, a trowel, tamper, measuring tape and flow table. During the flow test, the new characteristics of workability can be achieved, as well as the mortar constancy and the filling ability.

Jumrat et al. [350] disclosed that geopolymer mortar's flow value reduced with the increase in $\text{Na}_2\text{SiO}_3/\text{NaOH}$ ratio and fly ash to alkaline solution ratio on account of the higher viscosity of a solution of Na_2SiO_3 . Further, additional water might be supplemented to acquire the geopolymer mortar with a functioning workable characteristic. The enhancement of Na_2SiO_3 constituent resulted in the rapid development and superior viscosity ability of the binder, which was increased with the augment in the level of Na_2SiO_3 and NaOH [351].

The investigations obtained the fluidity at 30s and 30 min, due to the measurement index of the workability property of mortar. Further, the monitored geopolymer mortar fluidity accelerated when the NaOH concentration reduced [352]. Moreover, Patankar et al. [353] had the same opinion concerning geopolymer mortar having dissimilar ratios of activator solution to fly ash.

Bhowmick and Ghosh [354] revealed that the fly ash to sand ratio escalated the flow value percentage of geopolymer mortar, in addition to the ability of flow with the cohesiveness of the geopolymer mortar, which boosts with the escalating the ratio of $\text{SiO}_2/\text{Na}_2\text{O}$. The outcomes of their study also made known that the uniformity of the mortar and flowability are affected by the size of the particle and grading of the aggregate.

Malkawi et al. [355] conducted a flow test and accounted that the flowability of the geopolymer mortar that was synthesized by using fly ash was strongly influenced by the concentration of sodium hydroxide, and the workability was monitored as lessening with the acceleration of NaOH concentration.

Lee [356] manufactured the geopolymer mortars that were produced by slag and fly ash, in addition to employing styrene-butadiene latex and measuring the flow accordance with a flow test, demonstrating that the coarse bottom ash and SB latex dose had more or less no impact on the value of the flow, whereas the supplement of alkali activators enhanced the value of the flow.

Sathonsaowaphak [357] studied the workability performance of geopolymer mortars that were produced by using the bottom ash waste from lignite source. The bottom ash can be used to replace the finer aggregate in the geopolymer mortar; nevertheless, the bottom ash substitution reaches lower flow levels than those where the standard sand is used [358].

The effects of the alkaline solution and calcium to silicate ratio on the flow of the geopolymer mortar were calculated by Huseien et al. [359]. Their results showed that the use as an alkaline-activator solution of sodium silicate could reduce the geopolymer mortar flow without sodium hydroxide, due to the higher Na_2SiO_3 viscosity.

Compressive Strength

The geopolymer mortars based on fly ash were manufactured using 70% of GGBFS and 30% of POFA by Islam et al. [360], who demonstrated the best possible compressive strength of roughly 66 MPa. In high-calcium fly ash-based geopolymers, a significantly

higher concentration of NaOH may gain less compressive strength than low-calcium fly-ash geopolymer mortar [361].

The upshots of Temuujin et al. [362] pointed out the bonding among geopolymer binders with aggregates. Nevertheless, Zejak [363] uncovered that the compressive strength property of geopolymer mortar that was prepared with fly ash was enhanced by the addition of limestone sand. However, the existence of the sand particles with well-combined grains amends the gel phase of the geopolymer structure.

The influence of the ratio of $\text{SiO}_2/\text{Na}_2\text{O}$ and the ratio of water to fly ash on the compressive strength performance of geopolymer mortar. The impact of an escalating $\text{SiO}_2/\text{Na}_2\text{O}$ ratio on the compressive strength property of the geopolymer mortar is not identical with the alkaline liquid ratio [364].

The authors Kotwal et al. [365] illustrated the impact of sand to fly ash ratio on compressive strength. The compressive strength augments with the addition in the ratio of Na_2SiO_3 to fly ash. While the ratio of NaOH to fly ash increases from 0.05 to 0.125, the compressive strength property of the geopolymer mortar also enhances at first, but subsequently declines. Moreover, the ratio of binder/sand influences the compressive strength performance of geopolymer mortars.

Patankar et al. [353] reported that the compressive strength measurement of geopolymer mortars with a curing age of three days was found to be improved with an augment in curing temperature, whereas the strength improved slightly after the curing by oven heating for more than three days.

Gorhan and Kurklu [366] found an accelerating propensity concerning the compressive strength performance of geopolymer mortar that was cured at 85 °C, while the concentration of sodium hydroxide and time for curing increased. The optimal 6 M concentration of NaOH and 85 °C temperature for curing generated the brilliant compressive strength of the referred geopolymer mortar.

The findings of Bashar [367] suggested that the fly ash geopolymer mortar that was synthesized with 100% quarry dust with manufactured sand did not show a visible reduction in strength in comparison with the geopolymer mortar that was produced with 100% conventional mining sand.

Helmy [368] investigated the intermittent curing technique for geopolymer mortars at a curing temperature of 70 °C for four stages, whereby each stage was of 6 h/day, resting afterwards for 18 h. The monitoring indicates that the intermittent curing of geopolymer mortar can enhance compressive strength.

The outcomes of Li et al. [369] for geopolymer mortars synthesized using Class C type fly ash at 70 °C with a curing period for 20 h obtained the best possible compressive strength. Nevertheless, Adam and Horiato [370] accounted that fly ash-based geopolymer mortar attained optimum compressive strength, obtained with a 120 °C curing temperature for up to 20 h.

A comparative study was made by Narayanan and Shanmugasundaram [371] for diverse curing techniques of geopolymer mortars such as oven curing, heat chamber ambient temperature, and autoclave by. They reported that the optimum compressive strength of the geopolymer mortar was observed at an 80 °C curing temperature for 6 h. Increased compression strength with the increment in the fly ash substitution rate with GGBFS was observed for geopolymer mortar [372]. The geopolymer mortar based on fly ash, which employed a different percentage of the colloidal nano-silica supplement [373]. They reported that a 6% fly ash substitution rate was the maximum dose of nano silica that was necessary to achieve agreeable compressive strength at an ambient temperature curing condition.

Tensile Strength

Furthermore, the fly ash geopolymer mortar is commonly recognized to have exceptional performance under compressive loading. Chuah et al. [374] compared the average geopolymers' tensile strength with the design strength of the ACI standard and reported

that the tensile splitting force of geopolymers could satisfy the design requirements of the ACI code, irrespective of sand type.

Guades [375] assessed the tensile attributes of geopolymer mortars via carrying out the experiments. The tensile strength property of geopolymer mortars accelerates gradually with the augment in the sand to fly ash ratio as 7 to 28 days of curing.

Adak [373] upshots revealed that the 6% nano-silica mixture improved the geopolymer mortar tensile strength at ambient temperature curing, and the escalation in the molar concentration of the activator solution increased the tensile strength of the mortar. The kinds of alkaline activator solutions and curing temperature have a significant effect on geopolymer mortar tensile strength. The geopolymer mortar that is cured at 27 °C is stronger than the mortar that is cured at 60 to 90 °C. The sodium hydroxide liquid solution that is employed as the activator results in an enhanced tensile characteristic compared to the sodium alumino-silicate hydrate solution [359].

Flexural Strength

By and large, the cement mortar with higher compressive strength shows a prominent flexural strength performance. Nevertheless, the geopolymer mortar demonstrates higher flexural and lower compressive strength on account of the exceptional bonding of geopolymer paste to the aggregates and the extraordinary fragility of the geopolymer [376]. The kinds of alkali activator solution and temperature for curing considerably influence the flexural strength performance of geopolymer mortar.

Atis et al. [377] studied the discrepancies of the flexural strength behaviour of geopolymer mortars with a variety of contents of Na, which were cured for a period of 24, 48 as well as 72 h at 45 to 115 °C. The findings showed that the geopolymer mortar, which combines fourteen percent sodium when cured for 24 h below 115 °C, had the best possible flexural strength, while the geopolymer mortar with four percent of Na had the least flexural strength, which had been cured at 105 °C for 24 h. While the ratio of bottom ash to fly ash is enhanced from 0 to 3, the flexural strength of the geopolymer mortar improves first, but subsequently tends to mitigate, failing to reach the optimum value at a ratio of the bottom ash to fly ash [358]. The blending of nano-silica in geopolymer mortars has a significant influence on the flexural strength of the mortar. The geopolymer mortar with 6% of nano silica displays elevated flexural strength than the mortar sans nanoparticles. In addition the flexural strength accelerates gradually with the addition of a concentration of molar or alkaline activator solution, irrespective of a supplement of nano silica [272].

Huseien et al. [359] uncovered that geopolymer mortars that were cured at 27 °C had elevated flexural strength, compared to the mortars that were cured at 60 and 90 °C. Moreover, the solution for sodium alumino-silicate hydrate resulted in less flexural bending strength than the sodium hydroxide solution.

Acid Resistance

The structural integrity of the geopolymer mortar relies upon alumina-silicate and not calcium silicate hydrate bonds. Several researchers have conducted experiments on the acid resistance of geopolymer mortars. Satya et al. [378] summed up that the synthesized geopolymer mortars that were incorporated with fly ash and POFA displayed brilliant resistance to acidic water on account of the development a few novel zeolite-type phases.

Moreover, fly ash-based geopolymer mortar showed a very high resistance to acidic peat water, compared to the geopolymer mortar that was incorporated with POFA [379]. Further, the findings of Sreevidya et al. [380] monitored the resistance of geopolymer mortar against muriatic and nitric acids and compared a compressive strength value before and after immersion in acid solutions. Nevertheless, the augment of the content of OPC in the geopolymer mortar led to a higher degree of weight loss of the samples, following their immersion in a 10% solution of sulphuric acid [381].

Thokchom [382] assessed the resistance to acid by geopolymer mortars containing Na₂O of about 5–8%, following the immersion in nitric, as well as sulphuric acids, for

an exposure period of 24 weeks. The author suggested that geopolymer mortar with 8% of Na₂O demonstrated a minor loss of compressive strength. In addition, the loss in the compressive strength of the samples that were immersed in sulphuric acid was superior to the samples that were immersed in nitric acid.

Water Absorption

The water absorption of the geopolymer mortar depends on the pores, especially the apparent porosity value and the pores' size. Adak et al. [272] concluded that geopolymer mortar with 6% of nano silica particles with dissimilar concentrations of molar displayed an inferior absorption of water after the curing of samples for 28 days, compared to the geopolymer mortars with the absence of nano silica particles.

Kurklu [383] synthesized the geopolymer mortars employing fly ash and blast furnace slag (BFS) and assessed the impact of slag dose on the water absorption of the mortars through a heat curing period of 5–168 h. The water absorption values of the mortars containing dissimilar doses of fly ash ranged inconsistently with the increase in BFS quantity, and the least absorption of water was seen in the sample with 100% BFS after 24 h of curing, whereas the optimum absorption of water became visible in the sample incorporating 25% BFS, following curing for 5 h.

Abdollahnejad [381] gauged the water absorption capillarity coefficient of diverse kinds of geopolymer mortars. The authors reported that the single part of the geopolymer mortar enclosing 8% calcined content demonstrated high capillary water absorption on account of a huge quantity of capillary pores.

It was reported by Helmy [252] that the increase in treatment time resulted in the water absorption mitigation of geopolymer mortars, while the specimens were thermally cured at 85 °C, and that NaOH concentrations influenced water absorption.

The water absorption of geopolymer mortar that was synthesized in volcanic ash was examined by Djobo et al. [384]. The water absorption of the sample that was cured below 80 °C was higher than the specimen that was cured below 27 °C, and the maximum value for water absorption was seen before 28 days, while the water absorption was constant, regardless of the curing temperature.

Micro-Structures of Fly Ash-Based Geopolymer Mortar

For geopolymer mortars that were synthesized using class C Fly Ash when examined for micro-structures by Li et al. [352], their SEM micrographs displayed relatively denser reaction product development in the mortars. The amalgamation of nano silica for making the geopolymer mortars is competent enough to modify its morphology. The geopolymer mortar enclosing six percent particles of nano silica is found to comprise a higher amount of crystalline compound transformed from an amorphous material, compared to the one which does not contain nano-particles [373]. The microstructures of the geopolymer mortars with or without exposure at higher temperatures through SEM micrographs were studied by Abdulkareem et al. [385]. They revealed that the appearance of the microstructure of geopolymer mortars altered to some extent when they were exposed to an elevated temperature of 400 °C.

Nevertheless, it was unearthed that the structural water evaporation caused some smaller micro-cracks in the geopolymeric gel, leading to the deterioration of the strength of the geopolymer mortar when subjected to a temperature of 600 °C. The referred deterioration in the micro-structure turned out to be more severe on the elevation of the temperature to 800 °C. The geopolymer mortars that were produced through employing dissimilar activators, along with the incorporation of POFA and fly ash, were studied micro-structurally by Huseien et al. [359]. They found that the FESEM images of geopolymer mortar that was synthesized through employing sodium silicate displayed a fragile matrix, as well as a lower density. They also saw the presence of more non-reacted or partly reacted particles of POFA and fly ash in the composite [359].

4.6. Fly Ash Based Geopolymer Paste

The properties of fly ash-based geopolymers have been examined in the past by many researchers, mainly concerning their workability, flowability, setting time, water absorption, compressive strength and drying shrinkage.

4.6.1. Properties

Workability

The workability property of geopolymer paste was studied by Kumar and Ramamurthy [386], who established that for constant ratios of NaOH and Na-Si to NaOH, as well as an alkaline liquid to fly ash, there is a noteworthy impact on the workability of geopolymer paste and mortar. The mix becomes more workable when the liquid alkaline is used in the mix. While there is an elevated ratio of La/ash such as 0.75 for geopolymer mortar and 0.45 for geopolymeric paste, an enhancement in NaOH contents in terms of molarity results in steep mitigation in the workability of the mixture. This is because of a boost in the solution viscosity with NaOH molarity. However, the mixture was found to be very stiff when the La to ash ratio was maintained as 0.65 for geopolymer mortar and 0.4 for geopolymer paste, regardless of the ratios of Na-Si to NaOH and NaOH molarity.

Flowability

The average slump flow of geopolymeric mixes was determined by Ling et al. [387], who accounted that none of the investigated geopolymer pastes demonstrated notable bleeding during the mini-slump test. The activator concentration affected the flowability of geopolymeric paste more extensively than the module. When comparing them with cement pastes, pastes with a concentration of twenty-five percent significantly reduced the slump flux, while pastes with a concentration of twenty percent significantly increased the slump flux. According to Zuda et al. [388], the augmented silica was probably associated with the high module activator solution, which promoted the precipitation of larger molecular species and led to a stronger gel of improved density. Additionally, a solution with a high module activator presented an elevated quantity of Na_2SiO_3 . Moreover, Chindaprasirt [350] accounted for analogous findings and explained that these owed to an elevated concentration of activator, which would have led to the enhanced viscosity property of the mix. A high module also reduced the slump flow. The mitigation was more rigorous for pastes with a higher concentration of activator. The elevated viscosity of Na_2SiO_3 might also have influenced the flowability of the paste [355]. As per Lee et al. [269], the measurement upshots for the flow and images of the geopolymeric paste in the context of the Si/Al ratio were as follows: The flow measurements were 187.5 mm, 177.5 mm and 167.5 mm on maintaining the Si to Al ratios as 1.5, 3.5, and 4.0, correspondingly, suggesting that the flow reduced the increase in the ratio of Si/Al. When the value of the ratio of Si/Al was fixed as 3.5 and 4.0, the flow possibly diminished on account of the higher viscosity of the activator of $\text{Na}_2\text{SiO}_3 \cdot \text{H}_2\text{O}$, compared to the case whereby the value of the Si to Al ratio was 1.5. For this reason, while $\text{Na}_2\text{SiO}_3 \cdot \text{H}_2\text{O}$ is used as the activator to synthesize geopolymers, it is highly important to observe it for any deterioration concerning the fluidity.

4.6.2. Setting Time

Saha and Rajasekaran [389] observed from their experimental investigations that the setting time for both the early and final stages of geopolymer paste that was prepared with fly ash were found to be considerably lower with the augment of the GGBFS in the mixtures. It was found that a blending of GGBFS in mixtures increases the initial setting time from 420 to 480 min, to 25 to 130 min, and the final setting time from 1425 to 1600 min, to 90 to 355 min. The initial and final setting times of geopolymer paste were observed to change from 73 to 94% and by 77 to 92%, respectively, on the addition of slag from 10 to 50% in the mixtures, in comparison to the setting time of geopolymer paste mixtures with no slag. The discrepancies of geopolymer paste occurred with a variety of GGBFS within the initial setting time and final setting time. The geopolymer paste is found to

rely characteristically upon the production of NASH gel. Since the quantity of calcium oxide is significantly greater in the slag, geopolymer paste mixtures that are developed incorporating slag may also develop CSH gel in association with NASH gel in the initial period. Consequently, geopolymer paste that is incorporated with a higher amount of GGBFS takes considerably less time for both the initial and final settings, according to the findings of setting time by Hanjitsuwan et al. [243]. The initial and final set-up times were both enhanced by NaOH concentration acceleration. The final times were recorded for various samples, including 130, 160, 205, 245, as well as 260 min. The leakage of alumina and silica was also found to be low when the NaOH concentration remained low [254]. The leakage of Ca^{2+} ions into the solution was not disrupted and, therefore, the solution was full of calcium. The referred quantity of calcium was adequate for precipitation and reacted to develop CSH gel and CAH gel that result in the paste setting. Consequently, the setting time became shorter [390,391]. As a result, the geopolymer paste setting time is connected to the quantity of the accessible calcium [240]. When the concentration of NaOH was high, the leaking of alumina and silica was superior to a great extent. The leaking of Ca ions was delayed, and the quantity of Ca in the solution was restricted.

4.6.3. Compressive Strength

The discrepancy in the context of the compressive strength property of aerated geopolymer paste formed with fly ash was studied by Kumar and Ramamurthy [386]. Kumar and Ramamurthy [386] illustrated that (i) for a provided alumina dose, the density and the compressive strength improved with the NaOH molarity value. This may be assigned to the higher fly ash dissolution and increased NaOH concentration with advanced geopolymerization, and that a liquid alkaline/ashes ratio of 0.4 provides a comparatively higher strength-to-density ratio. (ii) On the other hand, an increase of 2 in a ratio of Na-Si to NaOH extends a number of lower densities such as 1250 to 700 kg/m^3 , matching compressive strength mitigation, which is altered in pH by modification in the silicate [224].

Ling et al. [387] confirmed the value for the compressive strength of geopolymeric paste. Ling et al. [387] suggested that geopolymeric pastes possess superior strength to ordinary Portland cement pastes at every age, except the mixtures containing a molar ratio of 1.5 $\text{SiO}_2/\text{Na}_2\text{O}$ at twenty percent concentration for 28 days. On the 7th day, 90% of geopolymer pastes had a 28th-day compressive strength, whereas the strength of cement pastes was more or less established for approximately 60% of their strength after 28 days. Following seven days, the compressive strength property of geopolymer pastes improved at a snail's pace, but that of PC pastes was augmented quickly. The molar mixtures of 1.0 for $\text{SiO}_2/\text{Na}_2\text{O}$ had the best possible concentration compressive strength at the 25% concentration, followed by those of the 1.0 molars at the 20% concentration. Keeping the constant water/binder ratio of 0.33, the fly ash-based geopolymer paste that was synthesized using an activator with a ratio of molar 1.0 $\text{SiO}_2/\text{Na}_2\text{O}$ and twenty-five percent concentration demonstrated the compressive strength value of 76.0 MPa after 28 days, whereas the cement-paste exhibited the value of compressive strength as 59.4 MPa. The impacts of geopolymerization that were encouraged by an increased alkaline concentration could also be determined by the effects on the fluctuating porosity of the ultimate geopolymer products [392]. The referred tendencies correspond with the outcomes of not only Fernandez and Palomo [393], but also Rattanasak and Chindaprasirt [254]. The value of the compressive strength of the geopolymeric pastes with a range of substitutions of fly ash with water glass powder were studied by Liu et al. [394]. The upshots designated that the levels of substitution for both fluorescent lamp glass (FP), as well as ground container glass (CP), had imperative influences on the compressive strength properties of geopolymeric pastes. The best possible presentations for FP, as well as CP substitutions, are achieved from the samples with 10 FP and 20 CP content, with the compressive strength values as 41.1 MPa and 47.6 MPa, correspondingly, whereas the reference paste exhibited the compressive strength value of 45.7 MPa. The value of compressive strength has the propensity to reduce as the echelon of substitution by FP is boosted. Due to its higher silicone content,

the decreasing value of the compressive strength can be assigned to FP substitution and can change the ratio of silicon/aluminium. The higher ratios of silicon/aluminium encouraged the development of lower cross-linked alumino-silicate materials with mitigated strengths, which was intimated by Rattanasak et al. and Fletcher et al. [395,396]. The characteristics of geopolymers are drastically modified with comparatively lower alterations in the contents of aluminium and silicon during geopolymerization of alumino-silicates, as revealed by De Silva et al., [397]. Davidovits [63], as well as Chindaprasirt et al. [390], who found that for a good-quality strength geopolymer, the optimum ratio of silicon/aluminium was among 3.5 to 4.0. Nevertheless, the geopolymer samples employing 10% to 30% FP displayed the values of compressive strength of 87% to 90%, compared to the reference paste, due to the FP-particles being and finer. The finer particles of FP performed as micro-fillers and induced matrix densification to the geopolymeric paste. Moreover, the compressive strengths performance of geopolymer pastes incorporating CP dropped, analogous to those possessing FP, on account of the enhanced ratios of silicon/aluminium. Nevertheless, the compressive strengths measurement of the pastes blended with CP, i.e., CaO as 12.80%, were greater than those that were manufactured with FP, i.e., with 7.43% CaO content, at the identical substitution echelons. The high CaO levels for the geopolymer pastes were considered as a generating factor in the formation of denser structures and enhanced strengths in combination with other rates of geopolymerization, following Saha and Rajasekaran, [389] and Temuujin et al. [398]. The twenty percent CP geopolymer paste represents the best compressive strength value of 47.6 MPa, a little higher than the reference paste. This is possibly attributed to the blending of an appropriate quantity of finer particles of CP with a higher content of CaO. In relation to the ratio of amorphous Si/Al in fly ash, Lee et al. [269] analyzed the results of compressive strength measures in the geopolymer paste. When the compressive strength of the samples was cured at 70 °C for one day, the attained values were 15.0, 23.0, and 9.5 MPa for 1.5, 3.5, and 4.0 as the ratio of Si/Al, correspondingly. After more than one day of age, the values for compressive strength were augmented when cured at 20 °C. The compressive strength values of the samples were 43 MPa following the 28 days and showed the most compressive strength possible for the sample with an Si to Al ratio of 3.5 and with NaOH plus $\text{Na}_2\text{SiO}_3 \cdot \text{H}_2\text{O}$ used as the alkali activator. In the meantime, the value of compressive strength for the samples that were cured at a temperature of 70 °C between one and 28 days at 3 days of age was about 1.29–1.45 times greater than for the samples that were healed 20 °C between the age of two and 28 days. Moreover, for the samples with a ratio of Si/Al as 1.5, the value of compressive strength due to curing at a higher temperature until the age of 28 days was found as 48.1 MPa, which was more than the compressive strength value of the sample that had a ratio of Si/Al as 3.5. The compressive strength of the geopolymer paste that was preserved as cube specimens and at ambient curing temperature by Saha and Rajasekaran [389] was recorded to have an escalating drift, whereas the concentration of the solution of NaOH and the GGBFS quantity percentage in the mixtures were both found to be enhanced. An enhancement in the compressive strength was monitored more while the slag was present in an elevated amount. The compressive strength of the geopolymer paste is assigned to develop a 3D network of silicon aluminium structures through the manufacture of a gel of sodium aluminium silicate hydration (NASH). The elevated concentration of the solution of NaOH helps to produce an adequate gel of sodium-aluminate-silicate-hydrate (NASH) and leads to polycondensation. Consequently, the stable 3D network of silico-aluminates is developed to offer greater strength to the geopolymer based on fly ash. Moreover, the development of CSH gel besides structures of silico-aluminates in the paste mixtures provide a notably improved strength. The compressive strength of geopolymer paste is improved after 7, 28 and 56 days with a various percentage of slag. The best possible compressive strength value of geopolymer paste on the 7th, 28th and 56th days were monitored as 66.4, 78 and 78.2 MPa, correspondingly, for the mixture with a solution of 16 M NaOH and 50% quantity by weight of GGBFS. of the compressive strength value for geopolymer paste mixtures following 28 days is found to be greatly reduced. The mixture that was

manufactured with the solution of 16 molarity concentration of NaOH and 50% by weight of slag demonstrated optimum compressive strength, and exhibited a 14.8% increase in compressive strength after 7 days, and 0.26% growth after 28 days. This is according to the findings of the compressive strength by Hanjitsuwan et al. [243]. The recorded value of compressive strength accelerated with an augment in NaOH concentration such as 43.3, 46.7, 50.0, 54.1, as well as 56.0 MPa of pastes, in that order. The dissolution of Si^{4+} and Al^{3+} ions from fly ash increased, while the concentration of NaOH was higher and the development of sodium-alumino-silicate was augmented, leading to an increase in the compressive strength [251,254,399].

4.6.4. Water Absorption

Kumar and Ramamurthy [386] studied the geopolymer paste and mortar water absorption property. Generally, the absorption of water reduces with an increase in the density of the geopolymer composites (paste and mortar). For an analogous density, an acceleration in the temperature for curing resulted in inferior water absorption. When the ratio of Na-Si/NaOH was elevated, although the mitigation in density could be obtained, the resultant absorption of water was much higher. For an equivalent density, where the curing temperature was 90 °C for a ratio of Na-Si/NaOH as 1, the disparity in the absorption of water among ratios of La/ash as 0.4 and 0.45 was trivial; therefore, the selection of the mixture should be that which contributes superior strength for a required density.

4.6.5. Drying Shrinkage

Ling et al. [387] investigated the drying shrinkage attribute of geopolymers. The drying shrinkage tests of all mixtures were made up of Portland cement (PC) and fly ash-based geopolymer (FG) for a drying period of 56 days. However, the main free drying shrinkage also occurred in the initial 14 days, and the trend in the free drying shrinkage test results was not the loss of paste mass. FG pastes with a high activator solution concentration usually had more drying shrinkage. The pastes with 25% activator concentration suffered high shrinkage, whereas the pastes with a lesser concentration of activator solution of 20% demonstrated less free drying shrinkage than their respective PC pastes.

4.6.6. Microstructures of Fly Ash-Based Geopolymers Composites

The chemistry and microstructure of geopolymer composites based on fly ash are controlled through the particle size distribution analysis and mineralogical composition of the primary fly ash, the type of activator and a few other variables. The microstructure of geopolymer concrete that is formed with fly ash regarding reaction, and the type of activator that is employed have been studied by many renowned scientists [400,401]. In the SEM images of the fly ash, the referred figure shows that the dissimilar, spherical size, shaped series of glass particles vary in length from 10 to 20 μm , and a few of these spherical particles might hold other particles of a lesser size in internals.

Akin to Weir et al.'s models [402], which clarify the microstructure of OPC concrete, as well as its hydration reaction, the reaction that occurs while fly ash is geopolymerized is characterized by Fernández-Jiménez and Palomo [393]. In the commencement, the attack against the chemical initiates at a particular place on the surface of the particle and subsequently forms to manufacture a larger hole; Dissimilar smaller particles either vacate or else are partially filled with other small ashes, toward a bi-directional alkali attack, in accordance with Brouwers and Van [403]. Afterwards, the reaction form is developed in both the exterior and interior of the sphere-shell until the ash particle is entirely or more or less completely utilized. A few significant outcomes regarding the microstructure of geopolymer concrete that is formed with fly ash have been characterized. Nevertheless, the similarity among investigations has been frequently restricted on account of disparities in experimental points of view.

X-ray Diffraction (XRD)

Abdulkareem et al. [385] accounted for a wide hump from 20 to 35 that was indicative of the presence of amorphous geopolymeric yields. On the basis of a precedent investigation, the presence of mullite, as well as quartz, reflected the composition of characteristic fly ash. Fly ash consists of Ca and Fe. Hence, it described the crystalline phases in the geopolymeric paste. A few peaks were made known in nano silica blended geopolymer concrete that designated the development of the novel phases of Albite $\text{NaAlSi}_3\text{O}_8$; silica SiO_2 ; anhydrous aluminium silicate $\text{Al}_2\text{Si}_2\text{O}_5(\text{OH})_4$; mullite $3\text{Al}_2\text{O}_3 \cdot 2\text{SiO}_2$; calcium silicon oxide Ca_3SiO_5 ; and calcium hydroxide $\text{Ca}(\text{OH})_2$ crystalline type compound. After the addition of the alkaline solution, the crystalline phases were exposed, followed by a comparison of the amorphous hump. Zeolite was produced after dissolution, while all of the fly ashes had mullite ($2\text{Al}_2\text{O}_3 \cdot \text{SiO}_2$); quartz (SiO_4); and hematite (Fe_2O_3). The XRD analyses for fly ash-based geopolymers with a ground glass container (CP) for 7 days were explained by Tho-In et al. [394]. The geopolymeric fly ash paste has a broad hump with 25–35 phases and is in the lower calcite phase, which corresponds to the geopolymerization level [404]. Fly ash-CP pastes have the same XRD drifts as 100FA paste. The calcite and quartz spikes were nevertheless monitored, with the higher CaO and SiO_2 presence increasing the percentage of ground CP [405]. At a high percentage of CP substitution, tridymite and cristobalite peaks were noticed.

Fourier Transform Infrared Spectroscopy (FTIR)

Adak et al. [406] endeavoured to determine the geopolymeric structure by means of an FTIR analysis. The distinct intensity band in the vicinity of 460 cm^{-1} was identified for the Si-O-Si vibration bending. Due to the AlO_4 vibration, the band between 750 cm^{-1} and 800 cm^{-1} was monitored. The asymmetrical span of Si-O-T is further enhanced by $T = \text{Al, Si}$; the most powerful band was described and recorded in the area of 950 cm^{-1} to 1050 cm^{-1} [407]. The position, i.e., 1420 cm^{-1} of Si-O-Si in 12GC0H was moved to the exact position, i.e., 1485 cm^{-1} , in 12GC6. Moreover, an important band was situated at just about 3450 cm^{-1} for OH stretching bonding. Tho-In et al. [394] carried out the FTIR analysis on geopolymer with fly ash with container glass pastes and a ground fluorescent lamp (FP). The absorption bands at more or less 3450 cm^{-1} and the band, which is weak at 1650 cm^{-1} , are accompanied by O-H and H-O-H bond vibrations in the molecules of the water. The preceding investigations accounted that the bands were recorded and uncovered [394]. Tho-In et al. [394] stated that the water molecules were incorporated into pores or absorbed on a surface during geopolymerization [393,408,409]. The band at approximately 1450 cm^{-1} was the indication of the expansion of O-C-O in carbonate groups because of the reaction to atmospheric CO_2 of alkali metal hydroxides. Every sample shows an irregular Si-O-X stretch at 1050 cm^{-1} , in which the X represents an aluminium or tetrahedral silicon. The Si-O-X bond assisted the course of geopolymerization with the phases of amorphous alumino-silicates that were developed. Researchers also explained that the sharp absorption band connects to many tetrahedral aluminium particles in the geopolymeric gel [410]. Additionally, the stretching of Si-O-Si and O-Si-O bonds is alike to that of the Si-O-Al group and is located at 450 cm^{-1} [411]. Moreover, the corresponding wide bands accounted for both fly ash that was incorporated with GP and FP, as well as 100 FA specimens. On the other hand, samples of 100 FA evidenced the elevated rate of geopolymerization kinetics because of the absorption band at 1050 cm^{-1} , which was greater than the FP and GP samples.

Thermogravimetric Analysis

In order to measure the mass loss in terms of temperature between $25 \text{ }^\circ\text{C}$ and $800 \text{ }^\circ\text{C}$, a thermal analysis was performed by Abdulkareem et al. [385]. The water loss due to the evaporation of both the geopolymer chemically bound water and free water was confirmed by a fast reduction in mass prior to $150 \text{ }^\circ\text{C}$ [385]. A sharp loss in weight was exemplified by more or less 55 to 60% of the free water in the geopolymeric matrix, which evaporated

ahead of 100 °C in specimens. Nevertheless, it is monitored that the loss rate in weight is steady from 150 °C to 780 °C, because of the disappearance of the hydroxyl groups-OH and chemically bonded water. No added loss in mass was noticed with the augment of at 800 °C temperature. The average mass following the heating at 800 °C was found to be 79.8%, which was depicted. According to Abdulkareem et al. [385], the loss in weight that was found at 250 °C in place of 150 °C was also assigned to the evaporation of hydroxyl group-OH [238]. The modification in weight is somewhat stable after 300 °C. Kong and Sanjayan [311] analyzed the behaviour of fly ash-based geopolymer paste that was subjected to a very high temperature. Kong and Sanjayan [311] hypothesised that the slower rate of shrinkage that was witnessed from 300 °C and beyond was accompanied by a lower rate of weight loss. The average mass that was evidenced following heating at 800 °C was found to be 89. Duan et al. [412] investigated the thermal analysis of geopolymeric paste with iron ore tailing (IOT). The calcium hydroxide content diminished when the IOT quantity that was assigned to the smaller loss in mass augmented, in comparison with the specimen of reference. It is comprehended that the supplement of iron ore tailing (IOT) aided the CSH gel development by employing $\text{Ca}(\text{OH})_2$. Nonetheless, $\text{Ca}(\text{OH})_2$ decomposition was demonstrated to correspond to the endothermic peak, even after making a thirty percent IOT supplement in the mixture. Following Abdulkareem et al. [385], each specimen had an insignificant mass loss rate at high temperatures following 800 °C. In order to investigate the thermal stability for geopolymers, Okoye et al. [413] conducted a thermal analysis. The weight loss for the fly ash geopolymer specimens that were incorporated in kaolin occurred at approximately 100 °C. When the temperature increased, while the fly ash-based geopolymer-incorporated kaolin showed a complex curve type, a relatively sharp dip in weight was monitored. The examination of both specimens made it obvious that the ideal temperature for curing might range from 80 °C to 100 °C. Cai et al. [414] explained that the earliest method of quality deterioration was dehydration. The authors toughened fly ash-based geopolymer by using polyvinyl alcohol (PVA) fibre and powder geopolymer composites. In the temperature range of 0–150 °C, all the samples lost 7–9% of their quality. This process was connected to the evaporation of free water on the sample's surface or in the pores. Then, at around 650 °C, all the samples lost their weight entirely, including the loss of bound water and the disintegration of polyvinyl alcohol, accounting for around 8% of the overall mass.

Mercury Intrusion Porosimetry (MIP)

Das et al. [412] studied the pore structure dimension of geopolymer fly ash ranging from 0.0036 to 10 μm through MIP to endorse the X-ray tomography (XRT) investigations. The cumulative porosity for the geopolymer that was formed with fly ash was more or less 32%. Nevertheless, the bulk of the pores in the geopolymeric matrix were of 0.0036–1 μm dimension. Kaze et al. [415] The assessment of mercury intrusion porosimetry (MIP) and the porosity of hardened geopolymer binders revealed that using a silica modulus of 1.5 and MH as the precursor provided the best performance in terms of porosity, cumulate pore area, and pore size distribution. The reduction in the pore characteristics of geopolymers that were created with a silica modulus of 1.5 can be attributed to the creation of additional aluminosilicate products when compared to bulk density values that were obtained with a silica modulus of 1.3. Higher porosity is predicted to be harmful to the mechanical characteristics of the geopolymer binders; therefore, these results are compatible with the mechanical performance results. Ramli et al. [416] investigated the pore structure of alkali-activated kaolin at various sintering temperatures in this work. The results of the research revealed the presence of open and closed pores in alkali-activated kaolin geopolymer ceramic samples. The distributions of the key components within the geopolymer ceramic edifice were discovered using Si and Al maps, allowing the kaolin geopolymer to be identified. The results further verified that raising the sintering temperature to 1100 °C resulted in big holes with an average size of 80 μm^3 and a layered porosity distribution in the alkali-activated kaolin geopolymer ceramic samples.

5. Advantages of Fly Ash-Based Geopolymer Concrete

Fly ash-based geopolymeric composites attract researchers universally, since their manufacturing generates 90% less CO₂ than that of the OPC system. This simply means that nine times more fly ash-based geopolymeric cement for building and infrastructure applications can be obtained for the sake of an equal quantity of CO₂ emissions [80,417]. This proves that geopolymer technology is capable of reducing CO₂ emissions in the environment [79,418], ameliorating the course of global climate modifications. Consequently, the development of geopolymer technology helps to relieve concern for the dilemma of global warming and can help for systematic fly ash waste disposal, which would otherwise fill land spaces and create health hazards, and contaminate the environment, soils, surface and subsurface waters. This innovative kind of sustainable, user- and eco-benign construction composite has proved to be a promising building material for the future. The composites possess numerous benefits such as:

- The abundant waste of fly ash will find its systematic disposal;
- Necessitates 60% less energy than OPC and only needs a low, or room temperature, as well as low atmospheric pressure, to be produced;
- Emits nine times less carbon dioxide as compared to OPC [419,420];
- Even short curing periods at room temperature can achieve analogous strength to OPC composites [419,420];
- The formation of fly ash-based geopolymers is trouble-free, since they can be obtained directly through mixing alumina silicates and alkaline activator solutions [421,422];
- Suffers 80% less shrinkage than OPC [419,420];
- Does not drop functionality even at 1000–1200 °C, proving its low thermal conductivity and excellent resistance to fire [100,419,420];
- It is effectively employed for residential buildings, pedestrian driveways, etc., due to its light weight;
- Exhibits brilliant durability and strength, sustainability, immobilization of toxic waste, relief from global warming by lowering emissions of GHG, and the organized solution of the disposal of diverse wastes by consuming them for their manufacturing; otherwise, they would fill land spaces and pollute the environment, soils, surface and subsurface water;
- Conservation of limited natural resources such as limestones, coals, etc., otherwise they would be exhausted by using them as either raw material or be burned up for obtaining an elevated temperature for calcination to produce OPC;
- Fly ash-based cement can be used underground as a sealant to store CO₂;
- Demonstrate excellent mechanical properties; remarkable resistance to chemicals, acid, sulphate, fire and thermal; fast curing speed; and high interfacial binding force, etc.;
- CFA-based adsorbents are efficient and eco-benevolent in comparison with commercial adsorbents, and they are utilized to clean up real wastewaters containing dyes, petroleum compounds, heavy metals, agricultural nutrients, radionuclides, etc.;
- The radiological characteristic of fly ash is an important parameter. Research on uses of radioactive fly ash for mine acid water or the fixation of radioactive elements could be of interest in terms of applicability, as mine locations are usually far from residences.

According to the World Bank, global metropolitan areas generate around 3.5 million tons of MSW every day, with this figure expected to rise to 6.1 million tons by 2025 [423]. In 2017, the quantity of MSW that was generated per capita in the EU, Australia, and the United States was 482, 558, and 742 kg, respectively [424]. The planet is anticipated to create 3.4 billion tons of municipal solid garbage per year by 2050 [425]. Waste management has evolved into a set of issues across the world. MSWI FA-based geopolymer maintained remarkable durability in acidic or alkaline environments. The use of MSWI FA as a precursor in geopolymers can significantly minimize or even eliminate environmental problems. It also allows MSWI FA resource usage, while avoiding the constraint of limited landfill disposal space.

6. Conclusions and Discussion

This comprehensive review on a geopolymer based on fly ash leads to the conclusion that the development of novel and ultramodern geopolymer technology, together with relevant advanced research in the past couple of decades, has revolutionized the geopolymeric constructions and infrastructure industries. Consequently, a modern era of green building materials through the feasible replacement of ordinary Portland cement (OPC) with geopolymer cement (GPC) has commenced. Moreover, this innovative, user and an eco-benevolent inorganic class of geopolymeric materials has a low carbon footprint and can be synthesized with a straightforward process at a low temperature, and with lower energy at atmospheric pressure, in comparison with present OPC production. This is why higher energy or elevated temperature reactions are no longer necessary, as found in the case of the OPC system. The unique attribute of ninefold lower carbon dioxide emissions also provides relief to the gigantic dilemma of global warming. Not only this, the quandary of the degradation of natural confined resources such as limestones, coals, etc., will be addressed and, thus, geopolymer technology will save natural resources that are necessary to consume as raw materials for producing OPC construction composites. At this juncture, the coal fly ash—an industrial waste—can be employed as a source of aluminosilicate to manufacture fly ash-based geopolymers productively. It is not only highly accessible and low-priced, but also found with a pozzolanic nature. The size, spherical shape and fineness of fly ash particles are the key parameters found to noticeably impact the properties of eventual geopolymers based on fly ash. The finer size of fly ash particles helps to develop the strength of the geopolymer, and the coarser size particles possess definite constructive performances. Remarkably, when both finer and coarser particles are employed collectively in the proper ratio, the strength and durability attributes of an ultimate geopolymer composite based on fly ash are improved. Additionally, extremely amorphous fly ashes are more efficient in picking up the pace of the pozzolanic reaction. Fly ash with a low calcium content reacts slowly because of the existence of more crystalline phases, which are considered as chemically inert. Green geopolymer based on fly ash; paste, mortar and concrete envelop a wide range of possible future materials for construction. Moreover, the organized disposal of copious wastes of fly ash by utilizing “the Best from the Wastes” strategy makes it cost-effective too. Not only this, the application of fly ash for manufacturing fly ash-based geopolymers and as supplementary cementitious material will reduce the pollution of the environment, soils, surface and sub-surface waters, owing to their heaps filling land spaces. The excellent attributes of fly ash in particular and fly ash-based geopolymers such as sealant for storing CO₂ in the underground; the immobilization of heavy metals containing compounds; fast curing rate, greater force of interfacial binding; low emissions of gaseous pollutants such as CO₂, SO₂, H₂SO₄, H₂S, NO, Hg, BTX, etc., have altogether proved outstandingly beneficial. More recently, the use of the categorization tools viz., X-ray diffractometer, scanning electron microscopy, Fourier transform infrared analyzer, thermo-gravimetric analyzer, etc., has returned favourable results regarding the physical and chemical characteristics of fly ash-based geopolymers, enabling them to be employed more competently. The penetration rate of chloride reduced with the increase in the concentration of NaOH activator liquid that was employed during the geopolymerization, owing to the enhancement of the pore structure. This is attributed to the reaction of polycondensation. Fly ash supports the production of more porous NASH gels, which decrease chloride resistance. Even though geopolymer was more porous compared to the OPC system, the geopolymer still showed improved chloride resistance. Noteworthy, the synthesis of the geopolymer, whereby NaOH was used as an activator, displayed the highest resistance to sulphate because of its more steady cross-linked structure. Moreover, the influence of silica fume and calcium on the resistance to acid by fly ash-based geopolymer is quite significant. Furthermore, curing at an elevated temperature is noted to be advantageous in the case of the geopolymer’s resistance to acid. While the geopolymer based on the fly ash is exposed to very high temperatures, it undergoes a shrinkage in the amount of water that is evaporated from its structure. There were no signs

of spalling, and only insignificant surface cracking was found in the case of geopolymer concrete that was formed by fly ash. Extraordinarily, fly ash-formed geopolymer did not indicate deterioration, even following 150 freeze–thaw cycles. The efflorescent nature of fly ash-based geopolymers is very much dependent on the type of alkali activator liquid solution, the content of calcium and the curing temperature. Fascinatingly, fly ash-based geopolymer concrete is noticeably vulnerable to a smaller quantity of ASR than its OPC counterpart. Overall, the chief factors that are found to affect the mechanical performances of geopolymer concrete based on fly ash are: the interactions between the aluminosilicate framework; alkali cations; aggregates, additives, etc. The size of the aggregates also influences the performances of the geopolymer concrete that is formed with fly ash. The thermal incompatibility among the aggregates and the matrix of the geopolymer resulted in a loss in strength for geopolymer concrete at very high temperatures. The bigger aggregates size of more than 10 mm showed superior performances concerning the strength at ambient temperature, as well as elevated temperatures, while those with a size that was smaller than 10 mm supported both the spalling and extensive cracking at an elevated temperature. Likewise, the inferior permeability of geopolymer based on fly ash proved to be competent enough to proficiently seal the leakage of CO₂. The geopolymer cement based on fly ash has huge potential for its application in the storage of carbon. The chemistry and microstructure of geopolymer composites based on fly ash are controlled through the particle size distribution analysis, a mineralogical component of the primary fly ash, the type of activator and a few other variables. The SEM images of fly ash-based geopolymer composites, along with EDS, exhibit the composition of numerous hydrated products. The case of low calcium fly ash-based concrete after 28 days shows non-reacted fly ash and non-hydrated spots, while the cases with higher calcium are less sensitive to unsatisfactory curing and react more swiftly to contribute enhanced early age strength. Fly ash-based geopolymers are excellent-quality binders and, hence, could be employed as cement to bind with aggregates with a view to manufacture the fly ash-based geopolymer concrete. Geopolymer concrete based on fly ash has a denser microstructure with an inferior chloride ion diffusion, as well as low porosity, as compared to OPC concrete. The fly ash/sand ratio accelerates the flow-value of the geopolymer mortar. The flowability and uniformity of the geopolymer mortar enhances with augmenting the ratio of SiO₂ to Na₂O ratio. The uniformity and flowability of the mortar are found to be affected by the particle size and grading of the aggregate. The ratio of binder/sand impacts the compressive strength property of geopolymer mortars. The geopolymer mortar based on fly ash is normally considered to have exceptional performance under the loading action of a compressive type. The kinds of alkali activator solutions and curing temperature are worth mentioning due to their impact on the tensile strength of geopolymer mortars. The kinds of alkali activator solution and curing temperature considerably affect the flexural strength property of geopolymer mortar. An inclusion of nano silica showed a momentous effect on the flexural strength of the geopolymer mortars. In the context of the good-quality compressive strength property of geopolymer paste formed by fly ash, the optimum ratio of silicon/aluminium was found to range from 3.5 to 4.0. In the case of water absorption in the context of the geopolymer paste and mortar of an analogous density, acceleration with regard to the curing temperature was observed as inferior. When the ratio of Na-Si/NaOH was elevated, the result of the water absorption was much higher; however, the reduction in density could be observed. The lower shrinkage and the higher tensile strength that were demonstrated by geopolymer composites based on fly ash provides technical advantages over the traditional counterpart of the OPC system—in particular, in structural components that are subject to exterior restraint, proving them a workable alternative solution to their counterpart of a conventional system, and contributing to systematic fly ash waste management. The compressive strength property of geopolymers based on fly ash is found to be influenced by Si/Al ratios, the type of alkali activators, the content of calcium, selection of additives, the process of separate activation, the co-existence gels of NASH and CSH, as well as the curing temperature and age. The elevated ratios of Si to Al increase the magnitude of the –Si–O–Si–

bond, obtaining an improved compressive strength of an entirely condensed structural geopolymer matrix. This is because the -Si-O-Si- bonds are authentically stronger than the -Al-O-Al- and -Si-O-Al- bonds. A slow but sure plunge in the tensile strength property of geopolymer based on fly ash is evidenced through augmenting the ratio of sand/fly ash. While the splitting tensile strength of geopolymer concrete that is formed with fly ash is similar to the design values that are provided by the ACI standard, on the other hand, the flexural strength performance of geopolymer concrete based on fly ash is found to be influenced by the kind of additive that is utilized with fly ash. Additives of calcium hydroxide and GGBFS are compatible with the OPC supplement by fly ash to increase the flexural strength of geopolymer concrete-based fly ash. The potential applications of a typical type of structure of geopolymer based on fly ash, i.e., silicon tetrahedral and aluminium tetrahedral, form ring chain type structures such as closed cage cavity, which favours its application as a building material. Geopolymer composites that are formed with fly ash come in various forms viz., fly ash-based geopolymer paste, mortar, binder and concrete, all of which offer a facile approach for fly ash utilization and have attracted researchers, and construction and infrastructure industries universally. This is because their manufacturing generates 90% less CO_2 than that of the OPC system, helping to relieve concern for the dilemma of global warming, and offering a method of systematic fly ash waste disposal management—otherwise, it would fill land spaces, create health hazards, and contaminate the environment, soils, surface and sub surface waters. Other advantages of geopolymer composites are as follows: they are an innovative kind of sustainable material, user- and eco-benign construction composites; necessitate 60% less energy than OPC and only need low (as low as room) temperature and atmospheric pressure for a simple and trouble free synthesis process; the accelerated polymerization places a supplement in the amorphous content, which augments the strength performance of GPC that is prepared with fly ash; even short curing periods at room temperature can achieve equivalent strength to OPC composites; they suffer an 80% lower shrinkage than the OPC system; they are not found to drop in functionality, even at 1000–1200 °C, proving their low thermal conductivity and excellent resistance to fire and championing them as exceptional heat-insulating materials; they can be efficiently utilized for residential buildings, pedestrian driveways, etc., on account of their light weight; they exhibit brilliant durability, strength and sustainability because of their inorganic origin and generally content of massive minerals of zeolitic nature viz., sodalite, analcime, etc.; they can immobilize toxic waste; they have an extremely low level of creep and permeability; inferior shrinkage, no water curing requisite; conservation of natural restricted resources such as limestones, coals, etc.; fly ash-based geopolymer binder can be utilized as a sealant to store carbon dioxide in the underground; they have outstanding mechanical properties such as high early strength due to the quicker speed of curing and higher interfacial binding force with the rapid development of gel and fast dehydration in comparison with OPC system, contributing sustainable composites; they show extraordinary resistance to chemicals, acid, sulphate and chemicals on account of possessing the Si-O and Al-O bonding; swift curing; higher interfacial binding force, etc.; their adsorbents are competent and enough in comparison with commercial adsorbents and utilized to clean up real waste-waters enclosing dyes, heavy metals, petroleum compounds, radionuclides, agricultural nutrients, etc.; radioactive fly ash either for mine acid water or fixation of radioactive elements and thus, proving competent enough to immobilize even peril wastes of radioactive type into geopolymer matrix; they have an exceptional resistance to freeze–thaw conditions, providing evidence of being a structurally steady and intact material even under severe conditions, owing to a special 3D network structure of aluminosilicate and a network framework of $[\text{-Si-O-Al-O}]_n$ bonding that is equivalent to zeolites (as this structure does not depend on lower strength bonds, as found with the OPC system); their hardening mechanism is swifter and at lower temperatures; they are found to be strongly bonded to aggregate; they have a lower cost and extensive sources of fly ash rich in silica plus alumina; and their pozzolanic nature, etc. Nevertheless, advanced research and examinations of fly ash-based geopolymeric materials concerning their properties are

still needed to establish them as proper substitutes of OPC-based counterpart composites. The production of geopolymers based on fly ash with advanced inputs on a huge industrial scale, as well as their latest applications, are worth exploring and desirable. Nevertheless, while prepared through employing profusely accessible economical precursors, activators and supplementary cementitious materials under the acceptable and necessitated quality control of diverse attributes—chiefly strength, durability and low carbon footmarks of fly ash-based geopolymers—are a significant potential component of the future toolbox of sustainable and affordable construction materials. The all-embracing applications of fly ash-based geopolymers, especially in the context of construction and infrastructure industries, have proved to be acceptable. Furthermore, these excellent attributes and advantages of fly ash-based geopolymeric composites have not merely attracted researchers but also established them as the “promising construction materials of very near future to “go green”! However, establishing and promoting the feasibility of geopolymer based on fly ash as a most promising, durable, sustainable, affordable, green, user and eco-friendly building composite necessitates full awareness and promotion of these innovative materials, in order to offer full confidence to construction and infrastructure-related persons and engineers. Eventually, it can be said that fly ash-based geopolymer technology has enough potential competencies to establish it as a fully durable, sustainable, cost-effective and promising one. It has proved to be a great strategy of “convert the waste for the best”, which is a need of the hour for the novel concept of “Go Green and Live Green”!

Author Contributions: Conceptualization, S.L. and I.L.; methodology, S.L.; validation, S.L. and I.L.; formal analysis, I.L.; investigation, S.L. and I.L.; resources, I.L.; writing—original draft preparation, S.L. and I.L.; writing—review and editing, I.L.; visualization, I.L. and S.L. All authors have read and agreed to the published version of the manuscript.

Funding: This research received no external funding.

Institutional Review Board Statement: Not applicable.

Informed Consent Statement: Not applicable.

Data Availability Statement: Not applicable.

Conflicts of Interest: The authors declare no conflict of interest.

References

1. Imbabi, M.S.; Carrigan, C.; McKenna, S. Trends and developments in green cement and concrete technology. *Int. J. Sustain. Built Environ.* **2012**, *1*, 194–216. [[CrossRef](#)]
2. Zaidi, F.H.A.; Ahmad, R.; Abdullah, M.M.A.B.; Wan Ibrahim, W.A.N.; Aziz, I.H.; Junaidi, S. Assessment of Geopolymer Concrete for Underwater Concreting Properties. *Arch. Metall. Mater.* **2022**, *2*, 677–684.
3. Arokiasamy, P.; Abdullah, M.M.A.B.; Abd Rahim, S.Z.; Sandu, A.V.; Jamil, N.H.; Nabiałek, M. Synthesis methods of hydroxyapatite from natural sources: A review. *Ceram. Int.* **2022**, *48*, 14959–14979. [[CrossRef](#)]
4. Petrillo, A.; Farina, I.; Travagliani, M.; Salzano, C.; Puca, S.; Ramondo, A.; Olivares, R.; Cossentino, L.; Cioffi, R. Opportunities and future challenges of geopolymer mortars for sustainable development. In *Handbook of Sustainable Concrete and Industrial Waste Management*; Woodhead Publishing: Sawston, UK, 2022; pp. 661–686. [[CrossRef](#)]
5. Luhar, I.; Luhar, S.; Abdullah, M.M.A.B.; Razak, R.A.; Vizureanu, P.; Sandu, A.V.; Matasaru, P.-D. A State-of-the-Art Review on Innovative Geopolymer Composites Designed for Water and Wastewater Treatment. *Materials* **2021**, *14*, 7456. [[CrossRef](#)] [[PubMed](#)]
6. Antunes, M.; Santos, R.L.; Pereira, J.; Rocha, P.; Horta, R.B.; Colaço, R. Alternative Clinker Technologies for Reducing Carbon Emissions in Cement Industry: A Critical Review. *Materials* **2021**, *15*, 209. [[CrossRef](#)] [[PubMed](#)]
7. Luhar, S.; Luhar, I. Additive Manufacturing in the Geopolymer Construction Technology: A Review. *Open Constr. Build. Technol. J.* **2020**, *14*, 150–161. [[CrossRef](#)]
8. Andrew, R.M. Global CO₂ emissions from cement production, 1928–2018. *Earth Syst. Sci. Data* **2019**, *11*, 1675–1710. [[CrossRef](#)]
9. McCaffrey, R. Climate Change and the Cement Industry. *Glob. Cem. Lime Mag.* **2022**, *15*, 19.
10. Nanthagopalan, P.; Santhanam, M. Fresh and hardened properties of self-compacting concrete produced with Manufactured sand. *Cem. Concr. Compos.* **2011**, *33*, 353–358. [[CrossRef](#)]
11. Pacheco-Torgal, F.; Shasavandi, A.; Jalali, S. Eco-Efficient Concrete Using Industrial Wastes: A Review. *Mater. Sci. Forum* **2012**, *730–732*, 581–586. [[CrossRef](#)]

12. Luhar, S.; Luhar, I.; Shaikh, F.U.A. A Review on the Performance Evaluation of Autonomous Self-Healing Bacterial Concrete: Mechanisms, Strength, Durability, and Microstructural Properties. *J. Compos. Sci.* **2022**, *6*, 23. [[CrossRef](#)]
13. Luhar, I.; Luhar, S.; Savva, P.; Theodosiou, A.; Petrou, M.F.; Nicolaidis, D. Light Transmitting Concrete: A Review. *Buildings* **2021**, *11*, 480. [[CrossRef](#)]
14. Luhar, S.; Luhar, I.; Abdullah, M.M.A.B.; Hussin, K. Challenges and prospective trends of various industrial and solid wastes incorporated with sustainable green concrete. In *Advances in Organic Farming*; Woodhead Publishing: Sawston, UK, 2021; pp. 223–240. [[CrossRef](#)]
15. Dananjayan, R.R.T.; Kandasamy, P.; Andimuthu, R. Direct mineral carbonation of coal fly ash for CO₂ sequestration. *J. Clean. Prod.* **2016**, *112*, 4173–4182. [[CrossRef](#)]
16. Ukwattage, N.L.; Ranjith, P.G.; Yellishetty, M.; Bui, H.H.; Xu, T. A laboratory-scale study of the aqueous mineral carbonation of coal fly ash for CO₂ sequestration. *J. Clean. Prod.* **2015**, *103*, 665–674. [[CrossRef](#)]
17. Bai, Y.; Guo, W.; Wang, X.; Pan, H.; Zhao, Q.; Wang, D. Utilization of municipal solid waste incineration fly ash with red mud-carbide slag for eco-friendly geopolymer preparation. *J. Clean. Prod.* **2022**, *340*, 130820. [[CrossRef](#)]
18. Nurrudin, M.F.; Sani, H.; Mohammed, B.S.; Shaaban, I. Methods of curing geopolymer concrete: A review. *Int. J. Adv. Appl. Sci.* **2018**, *5*, 31–36. [[CrossRef](#)]
19. Luhar, S.; Luhar, I. Rubberized Geopolymer Concrete: Application of Taguchi Method for Various Factors. *Int. J. Recent Technol. Eng.* **2020**, *8*, 1167–1174. [[CrossRef](#)]
20. Luhar, S.; Luhar, I. Application of artificial neural network for predicting compressive strength of geopolymer concrete. *Indian Concr. J.* **2019**, *93*, 38–43.
21. Luhar, S.; Luhar, I. Application of Seawater and Sea Sand to Develop Geopolymer Composites. *Int. J. Recent Technol. Eng.* **2020**, *8*, 5625–5633. [[CrossRef](#)]
22. Huseien, G.F.; Mirza, J.; Ismail, M.; Ghoshal, S.; Hussein, A.A. Geopolymer mortars as sustainable repair material: A comprehensive review. *Renew. Sustain. Energy Rev.* **2017**, *80*, 54–74. [[CrossRef](#)]
23. Liew, Y.-M.; Heah, C.-Y.; Mohd Mustafa, A.B.; Kamarudin, H. Structure and properties of clay-based geopolymer cements: A review. *Prog. Mater. Sci.* **2016**, *83*, 595–629. [[CrossRef](#)]
24. Ambaye, T.G.; Vaccari, M.; Bonilla-Petriciolet, A.; Prasad, S.; van Hullebusch, E.D.; Rtimi, S. Emerging technologies for biofuel production: A critical review on recent progress, challenges and perspectives. *J. Environ. Manag.* **2021**, *290*, 112627. [[CrossRef](#)]
25. Hasanbeigi, A.; Price, L.; Lin, E. Emerging energy-efficiency and CO₂ emission-reduction technologies for cement and concrete production: A technical review. *Renew. Sustain. Energy Rev.* **2012**, *16*, 6220–6238. [[CrossRef](#)]
26. Luhar, S.; Khandelwal, U. A study on durability of dredged marine sand concrete. *Int. J. Eng. Res. Rev.* **2015**, *3*, 56–76.
27. Roy, D.M.; Jiang, W.; Silsbee, M.R. Chloride diffusion in ordinary, blended, and alkali-activated cement pastes and its relation to other properties. *Cem. Concr. Res.* **2000**, *30*, 1879–1884. [[CrossRef](#)]
28. Bakharev, T.; Sanjayan, J.; Cheng, Y.-B. Sulfate attack on alkali-activated slag concrete. *Cem. Concr. Res.* **2002**, *32*, 211–216. [[CrossRef](#)]
29. Puertas, F.; Gutierrez, R.D.; Fernández-Jiménez, A.; Delvasto, S.; Maldonado, J. Alkaline cement mortars. Chemical resistance to sulfate and seawater attack. *Mater. Constr.* **2002**, *52*, 55–71. [[CrossRef](#)]
30. Fernandez-Jimenez, A.; Garcia-Lodeiro, I.; Palomo, A. Durability of alkali-activated fly ash cementitious materials. *J. Mater. Sci.* **2006**, *42*, 3055–3065. [[CrossRef](#)]
31. Luhar, S.; Luhar, I.; Gupta, R. Durability performance evaluation of green geopolymer concrete. *Eur. J. Environ. Civ. Eng.* **2020**, *26*, 4297–4345. [[CrossRef](#)]
32. Shi, C.; Stegemann, J.A. Acid corrosion resistance of different cementing materials. *Cem. Concr. Res.* **2000**, *30*, 803–808. [[CrossRef](#)]
33. Pu, X.; Yang, C.; Liu, F. Studies on resistance of alkali activated slag concrete to acid attack. In *Proceedings of the 2nd International Conference on Alkaline Cements and Concretes*; VIPOL Stock Company: Kiev, Ukraine, 1999; pp. 717–721.
34. Luhar, S. Performance Evaluation of Rubberized Geopolymer Concrete and Fly Ash based Geopolymer Mortar. Ph.D. Thesis, MNIT, Jaipur, India, 2018.
35. Puertas, F.; Amat, T.; Fernández-Jiménez, A.; Vázquez, T. Mechanical and durable behaviour of alkaline cement mortars reinforced with polypropylene fibres. *Cem. Concr. Res.* **2003**, *33*, 2031–2036. [[CrossRef](#)]
36. Luhar, S.; Luhar, I.; Nicolaidis, D.; Gupta, R. Durability Performance Evaluation of Rubberized Geopolymer Concrete. *Sustainability* **2021**, *13*, 5969. [[CrossRef](#)]
37. Shi, C. Corrosion resistance of alkali-activated slag cement. *Adv. Cem. Res.* **2003**, *15*, 77–81. [[CrossRef](#)]
38. Jimenez, A.M.F.; Palomo, J.; Puertas, F. Alkali-activated slag mortars: Mechanical strength behaviour. *Cem. Concr. Res.* **1999**, *29*, 1313–1321. [[CrossRef](#)]
39. Krizan, D.; Zivanovic, B. Effects of dosage and modulus of waterglass on early hydration of alkali-slag cements. *Cem. Concr. Res.* **2002**, *32*, 1181–1188. [[CrossRef](#)]
40. Luhar, S.; Luhar, I. Effect of different variables on fly ash based geopolymer concrete. *Indian Concr. J.* **2020**, *94*, 62–68.
41. Escalante-García, J.I.; Fuentes, A.F.; Gorokhovskiy, A.; Fraire-Luna, P.E.; Mendoza-Suarez, G. Hydration Products and Reactivity of Blast-Furnace Slag Activated by Various Alkalis. *J. Am. Ceram. Soc.* **2003**, *86*, 2148–2153. [[CrossRef](#)]
42. Fernández-Jiménez, A.; Puertas, F.; Sobrados, I.; Sanz, J. Structure of calcium silicate hydrates formed in alkaline-activated slag: Influence of the type of alkaline activator. *J. Am. Ceram. Soc.* **2003**, *86*, 1389–1394. [[CrossRef](#)]

43. Puertas, F.; Fernández-Jiménez, A.; Blanco-Varela, M. Pore solution in alkali-activated slag cement pastes. Relation to the composition and structure of calcium silicate hydrate. *Cem. Concr. Res.* **2004**, *34*, 139–148. [[CrossRef](#)]
44. Luhar, S.; LUHAR, I. Durability performance of Green Concrete Incorporating Various Wastes: A Review. *J. Mater. Eng. Struct.* **2019**, *6*, 469–484.
45. Zhang, Z.; Provis, J.L.; Reid, A.; Wang, H. Geopolymer foam concrete: An emerging material for sustainable construction. *Constr. Build. Mater.* **2014**, *56*, 113–127. [[CrossRef](#)]
46. Pérez-Villarejo, L.; Bonet-Martínez, E.; Eliche-Quesada, D.; Sánchez-Soto, P.; Rincón-López, J.; Galiano, E.C. Biomass fly ash and aluminium industry slags-based geopolymers. *Mater. Lett.* **2018**, *229*, 6–12. [[CrossRef](#)]
47. Luhar, S.; Luhar, I.; Shaikh, F. Review on Performance Evaluation of Autonomous Healing of Geopolymer Composites. *Infrastructures* **2021**, *6*, 94. [[CrossRef](#)]
48. Zhang, Z.; Zhu, H.; Zhou, C.; Wang, H. Geopolymer from kaolin in China: An overview. *Appl. Clay Sci.* **2015**, *119*, 31–41. [[CrossRef](#)]
49. Singh, N.; Kumar, M.; Rai, S. Geopolymer cement and concrete: Properties. *Mater. Today Proc.* **2020**, *29*, 743–748. [[CrossRef](#)]
50. Luhar, I.; Luhar, S. Rubberized Geopolymer Composites: Value-Added Applications. *J. Compos. Sci.* **2021**, *5*, 312. [[CrossRef](#)]
51. Albitar, M.; Ali, M.M.; Visintin, P. Experimental study on fly ash and lead smelter slag-based geopolymer concrete columns. *Constr. Build. Mater.* **2017**, *141*, 104–112. [[CrossRef](#)]
52. Hajimohammadi, A.; Ngo, T.; Kashani, A. Glass waste versus sand as aggregates: The characteristics of the evolving geopolymer binders. *J. Clean. Prod.* **2018**, *193*, 593–603. [[CrossRef](#)]
53. Davidovits, J. *Geopolymer Chemistry and Applications*; Geopolymer Institute: Saint-Quentin, France, 2008.
54. Guo, B.; Liu, B.; Yang, J.; Zhang, S. The mechanisms of heavy metal immobilization by cementitious material treatments and thermal treatments: A review. *J. Environ. Manag.* **2017**, *193*, 410–422. [[CrossRef](#)]
55. Yakubu, Y.; Zhou, J.; Ping, D.; Shu, Z.; Chen, Y. Effects of pH dynamics on solidification/stabilization of municipal solid waste incineration fly ash. *J. Environ. Manag.* **2017**, *207*, 243–248. [[CrossRef](#)]
56. Sarker, P.; Haque, R.; Ramgolam, K.V. Fracture behaviour of heat cured fly ash based geopolymer concrete. *Mater. Des.* **2013**, *44*, 580–586. [[CrossRef](#)]
57. Rabiaa, E.; Mohamed, R.A.S.; Sofi, W.H.; Tawfik, T.A. Developing Geopolymer Concrete Properties by Using Nanomaterials and Steel Fibers. *Adv. Mater. Sci. Eng.* **2020**, *2020*, 5186091. [[CrossRef](#)]
58. Verma, M.; Dev, N.; Rahman, I.; Nigam, M.; Ahmed, M.; Mallick, J. Geopolymer Concrete: A Material for Sustainable Development in Indian Construction Industries. *Crystals* **2022**, *12*, 514. [[CrossRef](#)]
59. Luhar, S.; Rajamane, N.P.; Corbu, O.; Luhar, I. Impact of incorporation of volcanic ash on geopolymerization of eco-friendly geopolymer composites: A review. In Proceedings of the IOP Conference Series: Materials Science and Engineering, Iasi, Romania, 16–17 May 2019; IOP Publishing: Bristol, UK, 2019; Volume 572, p. 012001. [[CrossRef](#)]
60. Siddika, A.; Hajimohammadi, A.; Mamun, M.A.A.; Alyousef, R.; Ferdous, W. Waste Glass in Cement and Geopolymer Concretes: A Review on Durability and Challenges. *Polymers* **2021**, *13*, 2071. [[CrossRef](#)] [[PubMed](#)]
61. Manikandan, P.; Vasugi, V. A Critical Review of Waste Glass Powder as an Aluminosilicate Source Material for Sustainable Geopolymer Concrete Production. *Silicon* **2021**, *13*, 3649–3663. [[CrossRef](#)]
62. Sulthan, F. Literature Review On Geopolymer Mortar Using Agricultural Waste As Precursor. *Int. J. Sci. Technol. Res.* **2019**, *8*, 232–236.
63. Turner, L.K.; Collins, F.G. Carbon dioxide equivalent (CO₂-e) emissions: A comparison between geopolymer and OPC cement concrete. *Constr. Build. Mater.* **2013**, *43*, 125–130. [[CrossRef](#)]
64. Verdolotti, L.; Iannace, S.; Lavorgna, M.; Lamanna, R. Geopolymerization reaction to consolidate incoherent pozzolanic soil. *J. Mater. Sci.* **2007**, *43*, 865–873. [[CrossRef](#)]
65. Luhar, S.; Cheng, T.W. Impact of Integration of Industrial Wastes on Microstructural Properties of Geopolymer Composites—A Review. *Int. J. Mech. Prod. Eng.* **2020**, *8*, 1–6.
66. Luhar, S.; Chaudhary, S.; Luhar, I. Development of rubberized geopolymer concrete: Strength and durability studies. *Constr. Build. Mater.* **2019**, *204*, 740–753. [[CrossRef](#)]
67. Khan, M.A.; Memon, S.A.; Farooq, F.; Javed, M.F.; Aslam, F.; Alyousef, R. Compressive Strength of Fly-Ash-Based Geopolymer Concrete by Gene Expression Programming and Random Forest. *Adv. Civ. Eng.* **2021**, *2021*, 6618407. [[CrossRef](#)]
68. Hardjito, D. Studies of Fly Ash-based Geopolymer Concrete. Ph.D. Dissertation, Curtin University, Bentley, WA, Australia, 2005.
69. Zhang, Z.; Provis, J.L.; Reid, A.; Wang, H. Mechanical, thermal insulation, thermal resistance and acoustic absorption properties of geopolymer foam concrete. *Cem. Concr. Compos.* **2015**, *62*, 97–105. [[CrossRef](#)]
70. Palomo, A.; Blanco-Varela, M.; Granizo, M.; Puertas, F.; Vazquez, T.; Grutzeck, M. Chemical stability of cementitious materials based on metakaolin. *Cem. Concr. Res.* **1999**, *29*, 997–1004. [[CrossRef](#)]
71. Choudhary, V.; Luhar, S. Fly Ash Utilization: A Review. *Int. J. Civ. Eng. Technol.* **2017**, *8*, 301–312.
72. Luhar, S.; Dave, U. Investigations on mechanical properties of fly ash and slag based geopolymer concrete. *Ind. Concr. J.* **2016**, *2*, 34–41.
73. Barbosa, V.F.; MacKenzie, K.J.; Thaumaturgo, C. Synthesis and characterisation of materials based on inorganic polymers of alumina and silica: Sodium polysialate polymers. *Int. J. Inorg. Mater.* **2000**, *2*, 309–317. [[CrossRef](#)]
74. Xu, H.; Deventer, J.S. The geopolymerisation of aluminosilicate minerals. *Int. J. Miner. Process.* **2000**, *59*, 247–266. [[CrossRef](#)]

75. Jaarsveld, V.; Deventer, V.; Lorenzen, L. The potential use of geopolymeric materials to immobilise toxic metals: Part I. Theory and applications. *Miner. Eng.* **1997**, *10*, 659–669. [[CrossRef](#)]
76. Falah, M.; Ohenoja, K.; Obenaus-Emler, R.; Kinnunen, P.; Illikainen, M. Improvement of mechanical strength of alkali-activated materials using micro low-alumina mine tailings. *Constr. Build. Mater.* **2020**, *248*, 118659. [[CrossRef](#)]
77. Davidovits, J.; Orlinski, J. *Proceedings Geopolymer*; Geopolymer Institute: Saint-Quentin, France, 1988.
78. Mierzwiński, D.; Walter, J. Autoclaving of alkali-activated materials. In Proceedings of the IOP Conference Series: Materials Science and Engineering, Montevideo, Uruguay, 28–29 November 2019; IOP Publishing: Bristol, UK, 2019; Volume 706, p. 012012.
79. Davidovits, J. Global Warming effect on cement and aggregate industries. *Worlds Resour. Rev.* **1994**, *6*, 263–278.
80. Davidovits, J. Environmentally Driven Geopolymer Cement Applications. In Proceedings of the Geopolymer Conference, Melbourne, Australia, 28–29 October 2002.
81. Provis, J.L.; Lukey, A.G.C.; van Deventer, J.S.J. Do Geopolymers Actually Contain Nanocrystalline Zeolites? A Reexamination of Existing Results. *Chem. Mater.* **2005**, *17*, 3075–3085. [[CrossRef](#)]
82. Davidovits, J. Geopolymers: Inorganic polymeric new materials. *J. Therm. Anal. Calorim.* **1991**, *37*, 1633–1656. [[CrossRef](#)]
83. Davidovits, J. Soft Mineralurgy and Geopolymers. In Proceedings of the the Geopolymer 88, First European Conference on Soft Mineralurgy, Compiègne, France, 1–3 June 1988.
84. Davidovits, J. Geopolymer Chemistry and Properties. In Proceedings of the the Geopolymer 88, First European Conference on Soft Mineralurgy, Compiègne, France, 1–3 June 1988.
85. Jaarsveld, V.; Deventer, V.; Lukey, G.C. The effect of composition and temperature on the properties of fly ash- and kaolinite-based geopolymers. *Chem. Eng. J.* **2002**, *89*, 63–73. [[CrossRef](#)]
86. Lan, T.; Meng, Y.; Ju, T.; Chen, Z.; Du, Y.; Deng, Y.; Song, M.; Han, S.; Jiang, J. Synthesis and application of geopolymers from municipal waste incineration fly ash (MSWI FA) as raw ingredient—A review. *Resour. Conserv. Recycl.* **2022**, *182*, 106308. [[CrossRef](#)]
87. Weng, L.; Sagoe-Crentsil, K. Dissolution processes, hydrolysis and condensation reactions during geopolymer synthesis: Part I—Low Si/Al ratio systems. *J. Mater. Sci.* **2007**, *42*, 2997–3006. [[CrossRef](#)]
88. Mackenzie, K.J.D. What are these things called geopolymers? A physico-chemical perspective. *Ceram. Trans.* **2003**, *153*, 175–186.
89. EUR 7716; Davidovits, J. *The Need to Create a New Technical Language for the Transfer of Basic Scientific Information. Transfer and Exploitation of Scientific and Technical Information*; Commission of the European Communities: Luxembourg, 1982.
90. Davidovits, J. Properties of geopolymer cements. In Proceedings of the First International Conference on Alkaline Cements and Concretes; Kiev State Technical University, Scientific Research Institute on Binders and Materials: Kiev, Ukraine, 1994; Volume 1, pp. 131–149.
91. Chanh, N.V.; Trung, D.B.; Tuan, D.V. Recent Research Geopolymer Concrete. In Proceedings of the 3rd ACF International Conference, Ho Chi Minh City, Vietnam, 11–13 November 2008.
92. Luhar, S.; Nicolaidis, D.; Luhar, I. Fire Resistance Behaviour of Geopolymer Concrete: An Overview. *Buildings* **2021**, *11*, 82. [[CrossRef](#)]
93. He, R.; Dai, N.; Wang, Z. Thermal and Mechanical Properties of Geopolymers Exposed to High Temperature: A Literature Review. *Adv. Civ. Eng.* **2020**, *2*, 7532703. [[CrossRef](#)]
94. Rangan, B.V.; Hardjito, D.; Wallah, S.E.; Sumajouw, D.M.J. Studies on Fly Ash Based Geopolymer Concrete. In *Green Chemistry and Sustainable Development Solutions*, 1st ed.; Geopolymer: Saint-Quentin, France, 2005.
95. Thaarrini, J.; Dhivya, S. Comparative study on the production cost of geopolymer and conventional concretes. *Int. J. Civ. Eng. Res.* **2016**, *7*, 117–124.
96. Bhavin, B.; Pitroda, J.; Bhavsar, J.J. Geopolymer concrete and its feasibility in India. In Proceedings of the National Conference CRDCE13, Vasad, India, 20–21 December 2013; pp. 20–21.
97. Timmons, S.F. Cementitious composition. U.S. Patent 7,442,248, 28 October 2008.
98. Gourley, J.T. Geopolymers; Opportunities for Environmentally Friendly Construction Materials. In Proceedings of the Materials 2003 Conference: Adaptive Materials for a Modern Society, Sydney, Australia, 1–3 October 2003.
99. Gourley, J.T.; Johnson, G.B. Developments in Geopolymer Precast Concrete. In Proceedings of the International Workshop on Geopolymers and Geopolymer Concrete, Perth, Australia, 28–29 September 2005.
100. Ganesan, N.; Indira, P.V.; Santhakumar, A. Prediction of ultimate strength of reinforced geopolymer concrete wall panels in one-way action. *Constr. Build. Mater.* **2013**, *48*, 91–97. [[CrossRef](#)]
101. Dawczyński, S.; Krzywon, R.; Orski, M.G.; Dubińska, W.; Samoszuk, M. Geopolymer concrete—Applications in civil engineering. In Proceedings of the XXXI Salon Tecnológico de la Construcción—EXCO 2017, Valencia, Spain, 20–24 February 2017.
102. Ober, J.A. *Mineral Commodity Summaries*; US Geological Survey: Reston, VA, USA, 2018.
103. Ma, C.-K.; Awang, A.Z.; Omar, W. Structural and material performance of geopolymer concrete: A review. *Constr. Build. Mater.* **2018**, *186*, 90–102. [[CrossRef](#)]
104. Pilehvar, S.; Cao, V.D.; Szczotok, A.M.; Valentini, L.; Salvioni, D.; Magistri, M.; Pamies, R.; Kjøniksen, A.-L. Mechanical properties and microscale changes of geopolymer concrete and Portland cement concrete containing micro-encapsulated phase change materials. *Cem. Concr. Res.* **2017**, *100*, 341–349. [[CrossRef](#)]
105. Zuhua, Z.; Xiao, Y.; Huajun, Z.; Yue, C. Role of water in the synthesis of calcined kaolin-based geopolymer. *Appl. Clay Sci.* **2009**, *43*, 218–223. [[CrossRef](#)]

106. Cao, V.D.; Pilehvar, S.; Salas-Bringas, C.; Szczotok, A.M.; Valentini, L.; Carmona, M.; Rodriguez, J.F.; Kjøniksen, A.-L. Influence of microcapsule size and shell polarity on thermal and mechanical properties of thermoregulating geopolymer concrete for passive building applications. *Energy Convers. Manag.* **2018**, *164*, 198–209. [[CrossRef](#)]
107. Cao, V.D.; Pilehvar, S.; Salas-Bringas, C.; Szczotok, A.M.; Bui, T.Q.; Carmona, M.; Rodriguez, J.F.; Kjøniksen, A.-L. Thermal performance and numerical simulation of geopolymer concrete containing different types of thermoregulating materials for passive building applications. *Energy Build.* **2018**, *173*, 678–688. [[CrossRef](#)]
108. Zeyad, A.M.; Johari, M.A.M.; Abutaleb, A.; Tayeh, B.A. The effect of steam curing regimes on the chloride resistance and pore size of high-strength green concrete. *Constr. Build. Mater.* **2021**, *280*, 122409. [[CrossRef](#)]
109. Zeyad, A.M.; Johari, M.A.M.; Alharbi, Y.R.; Abadel, A.A.; Amran, Y.M.; Tayeh, B.A.; Abutaleb, A. Influence of steam curing regimes on the properties of ultrafine POFA-based high-strength green concrete. *J. Build. Eng.* **2021**, *38*, 102204. [[CrossRef](#)]
110. Humphreys, K.; Mahasen, M. *Toward a Sustainable Cement Industry. Substudy 8, Climate Change 2*; World Business Council for Sustainable Development: Geneva, Switzerland, 2002.
111. Panda, B.; Unluer, C.; Tan, M.J. Investigation of the rheology and strength of geopolymer mixtures for extrusion-based 3D printing. *Cem. Concr. Compos.* **2018**, *94*, 307–314. [[CrossRef](#)]
112. Bernal, S.A.; Provis, J.; Rose, V.; De Gutierrez, R.M. Evolution of binder structure in sodium silicate-activated slag-metakaolin blends. *Cem. Concr. Compos.* **2011**, *33*, 46–54. [[CrossRef](#)]
113. Wang, C.; Xu, G.; Gu, X.; Gao, Y.; Zhao, P. High value-added applications of coal fly ash in the form of porous materials: A review. *Ceram. Int.* **2021**, *47*, 22302–22315. [[CrossRef](#)]
114. Zhang, X.; Bai, C.; Qiao, Y.; Wang, X.; Jia, D.; Li, H.; Colombo, P. Porous geopolymer composites: A review. *Compos. Part A Appl. Sci. Manuf.* **2021**, *150*, 106629. [[CrossRef](#)]
115. Jeremiah, J.J.; Abbey, S.J.; Booth, C.A.; Kashyap, A. Geopolymers as Alternative Sustainable Binders for Stabilisation of Clays—A Review. *Geotechnics* **2021**, *1*, 439–459. [[CrossRef](#)]
116. Paz-Gómez, D.C.; Vilarinho, I.S.; Pérez-Moreno, S.M.; Carvalheiras, J.; Guerrero, J.L.; Novais, R.M.; Seabra, M.P.; Ríos, G.; Bolívar, J.P.; Labrincha, J.A. Immobilization of Hazardous Wastes on One-Part Blast Furnace Slag-Based Geopolymers. *Sustainability* **2021**, *13*, 13455. [[CrossRef](#)]
117. Amran, M.; Al-Fakih, A.; Chu, S.H.; Fediuk, R.; Haruna, S.; Azevedo, A.; Vatin, N. Long-term durability properties of geopolymer concrete: An in-depth review. *Case Stud. Constr. Mater.* **2021**, *15*, e00661. [[CrossRef](#)]
118. Cong, P.; Cheng, Y. Advances in geopolymer materials: A comprehensive review. *J. Traffic Transp. Eng.* **2021**, *8*, 283–314. [[CrossRef](#)]
119. Ganesh, A.C.; Muthukannan, M. Development of high performance sustainable optimized fiber reinforced geopolymer concrete and prediction of compressive strength. *J. Clean. Prod.* **2021**, *282*, 124543. [[CrossRef](#)]
120. Han, Q.; Zhang, P.; Wu, J.; Jing, Y.; Zhang, D.; Zhang, T. Comprehensive review of the properties of fly ash-based geopolymer with additive of nano-SiO₂. *Nanotechnol. Rev.* **2022**, *11*, 1478–1498. [[CrossRef](#)]
121. Hardjito, W.; Sumajouw, R. Fly ash-based geopolymer concrete. *Aust. J. Struct. Eng.* **2015**, *73*, 77–86. [[CrossRef](#)]
122. Heah, C.; Kamarudin, H.; Al Bakri, A.M.; Binhussain, M.; Luqman, M.; Nizar, I.K.; Ruzaidi, C.; Liew, Y. Effect of Curing Profile on Kaolin-based Geopolymers. *Phys. Procedia* **2011**, *22*, 305–311. [[CrossRef](#)]
123. Rovnaník, P. Effect of curing temperature on the development of hard structure of metakaolin-based geopolymer. *Constr. Build. Mater.* **2010**, *24*, 1176–1183. [[CrossRef](#)]
124. Ranjbar, N.; Kuenzel, C.; Spangenberg, J.; Mehrali, M. Hardening evolution of geopolymers from setting to equilibrium: A review. *Cem. Concr. Compos.* **2020**, *114*, 103729. [[CrossRef](#)]
125. Farooq, F.; Jin, X.; Javed, M.F.; Akbar, A.; Shah, M.I.; Aslam, F.; Alyousef, R. Geopolymer concrete as sustainable material: A state of the art review. *Constr. Build. Mater.* **2021**, *306*, 124762. [[CrossRef](#)]
126. Shehata, N.; Mohamed, O.; Sayed, E.T.; Abdelkareem, M.A.; Olabi, A. Geopolymer concrete as green building materials: Recent applications, sustainable development and circular economy potentials. *Sci. Total Environ.* **2022**, *836*, 155577. [[CrossRef](#)] [[PubMed](#)]
127. Cui, Y.; Wang, D. Effects of Water on Pore Structure and Thermal Conductivity of Fly Ash-Based Foam Geopolymers. *Adv. Mater. Sci. Eng.* **2019**, *2019*, 3202794. [[CrossRef](#)]
128. Promoda Kumar Behera. Influence of High Temperatures on Properties of Geopolymers Filled by Inorganic Fibrous Particles. Masters's Thesis, Technical University of Liberec, Liberec, Czechia, 2019.
129. Aleem, M.A.; Arumairaj, P.D. Geopolymer concrete—A review. *Int. J. Eng. Sci. Emerg. Technol.* **2012**, *1*, 118–122. [[CrossRef](#)]
130. Ahmaruzzaman, M. A review on the utilization of fly ash. *Prog. Energy Combust. Sci.* **2010**, *36*, 327–363. [[CrossRef](#)]
131. Gorai, B.; Jana, R.K.; Premchand. Characteristics and utilization of copper slag a review. *Resour. Conserv. Recycl.* **2006**, *39*, 299–313. [[CrossRef](#)]
132. *International Energy Outlook*; U.S. Energy Information Administration: Washington, DC, USA, 2018.
133. Klima, K.; Schollbach, K.; Brouwers, H.; Yu, Q. Thermal and fire resistance of Class F fly ash based geopolymers—A review. *Constr. Build. Mater.* **2022**, *323*, 126529. [[CrossRef](#)]
134. Querol, X.; Juan, R.; Lopez-Soler, A.; Fernandez-Turiel, J.; Ruiz, C.R. Mobility of trace elements from coal and combustion wastes. *Fuel* **1996**, *75*, 821–838. [[CrossRef](#)]
135. Jegadeesan, G.; Al-Abed, S.R.; Pinto, P. Influence of trace metal distribution on its leachability from coal fly ash. *Fuel* **2008**, *87*, 1887–1893. [[CrossRef](#)]

136. Huggins, F.; Rezaee, M.; Honaker, R.; Hower, J. On the removal of hexavalent chromium from a Class F fly ash. *Waste Manag.* **2016**, *51*, 105–110. [[CrossRef](#)] [[PubMed](#)]
137. Yao, Z.T.; Ji, X.S.; Sarker, P.K.; Tang, J.H.; Ge, L.Q.; Xia, M.S.; Xi, Y.Q. A comprehensive review on the applications of coal fly ash. *Earth-Sci. Rev.* **2015**, *141*, 105–121. [[CrossRef](#)]
138. Bhattacharjee, U.; Kandpal, T.C. Potential of fly ash utilisation in India. *Energy* **2002**, *27*, 151–166. [[CrossRef](#)]
139. European Coal Combustion Products Association. *Production and Utilisation of CCPs in 2016 in Europe (EU 15)*; European Coal Combustion Products Association: Essen, Germany, 2016.
140. American Coal Ash Association. *Coal Combustion Products Production & Use Reports*; American Coal Ash Association: Denver, CO, USA, 2020.
141. Moreno, N.; Querol, X.; Ayora, C.; Pereira, C.F.; Janssen-Jurkovicová, M. Utilization of Zeolites Synthesized from Coal Fly Ash for the Purification of Acid Mine Waters. *Environ. Sci. Technol.* **2001**, *35*, 3526–3534. [[CrossRef](#)] [[PubMed](#)]
142. Mukherjee, A.B.; Zevenhoven, R.; Bhattacharya, P.; Sajwan, K.S.; Kikuchi, R. Mercury flow via coal and coal utilization by-products: A global perspective. *Resour. Conserv. Recycl.* **2008**, *52*, 571–591. [[CrossRef](#)]
143. Sibanda, V.; Ndlovu, S.; Dombo, G.; Shemi, A.; Rampou, M. Towards the Utilization of Fly Ash as a Feedstock for Smelter Grade Alumina Production: A Review of the Developments. *J. Sustain. Met.* **2016**, *2*, 167–184. [[CrossRef](#)]
144. Yao, Z.; Xia, M.; Sarker, P.; Chen, T. A review of the alumina recovery from coal fly ash, with a focus in China. *Fuel* **2014**, *120*, 74–85. [[CrossRef](#)]
145. Belviso, C. State-of-the-art applications of fly ash from coal and biomass: A focus on zeolite synthesis processes and issues. *Prog. Energy Combust. Sci.* **2018**, *65*, 109–135. [[CrossRef](#)]
146. Belviso, C.; Cavalcante, F.; Fiore, S. Synthesis of zeolite from Italian coal fly ash: Differences in crystallization temperature using seawater instead of distilled water. *Waste Manag.* **2010**, *30*, 839–847. [[CrossRef](#)]
147. Belviso, C.; Cavalcante, F.; Ragone, P.; Fiore, S. Immobilization of Ni by synthesising zeolite at low temperatures in a polluted soil. *Chemosphere* **2010**, *78*, 1172–1176. [[CrossRef](#)]
148. Belviso, C.; Cavalcante, F.; Lettino, A.; Fiore, S. Effects of ultrasonic treatment on zeolite synthesized from coal fly ash. *Ultrason. Sonochemistry* **2011**, *18*, 661–668. [[CrossRef](#)] [[PubMed](#)]
149. Belviso, C.; Cavalcante, F.; Ragone, P.; Fiore, S. Immobilization of Zn and Pb in Polluted Soil by In Situ Crystallization Zeolites from Fly Ash. *Water Air Soil Pollut.* **2012**, *223*, 5357–5364. [[CrossRef](#)]
150. Wang, P.; Hu, Y.; Cheng, H. Municipal solid waste (MSW) incineration fly ash as an important source of heavy metal pollution in China. *Environ. Pollut.* **2019**, *252*, 461–475. [[CrossRef](#)] [[PubMed](#)]
151. Havlica, J.; Brandstettr, J.; Odler, I. Possibilities of Utilizing Solid Residues from Pressured Fluidized Bed Coal Combustion (PSBC) for the Production of Blended Cements. *Cem. Concr. Res.* **1998**, *28*, 299–307. [[CrossRef](#)]
152. Li, X.-G.; Chen, Q.-B.; Ma, B.-G.; Huang, J.; Jian, S.-W.; Wu, B. Utilization of modified CFBC desulfurization ash as an admixture in blended cements: Physico-mechanical and hydration characteristics. *Fuel* **2012**, *102*, 674–680. [[CrossRef](#)]
153. Brandštetr, J.; Havlica, J. Phase composition of solid residues of fluidized bed coal combustion, quality tests, and application possibilities. *Chem. Pap.* **1996**, *50*, 188–194.
154. Kaewmanee, K.; Krammart, P.; Sumranwanich, T.; Choktaweekarn, P.; Tangtermsirikul, S. Effect of free lime content on properties of cement-fly ash mixtures. *Constr. Build. Mater.* **2013**, *38*, 829–836. [[CrossRef](#)]
155. Dvořák, R.; Chlápek, P.; Jecha, D.; Puchýř, R.; Stehlík, P. New approach to common removal of dioxins and NO_x as a contribution to environmental protection. *J. Clean. Prod.* **2010**, *18*, 881–888. [[CrossRef](#)]
156. Brendel, G.F.; Bonetti, J.E.; Rathbone, R.F.; Frey, R.N.F., Jr. *Investigation of Ammonia Adsorption on Fly Ash Due to the Installation of Selective Catalytic Reduction Systems*; U.S. Department of Energy, Office of Scientific and Technical Informatio: Pittsburgh, PA, USA, 2000.
157. Mazur, M.; Janda, T.; Zukowski, W. Chemical and Thermal Methods for Removing Ammonia from Fly Ashes. *Tech. Trans.* **2017**, *6*, 31–50.
158. Michalik, A.; Babińska, J.; Chyliński, F.; Piekarczyk, A. Ammonia in Fly Ashes from Flue Gas Denitrification Process and its Impact on the Properties of Cement Composites. *Buildings* **2019**, *9*, 225. [[CrossRef](#)]
159. Procházka, L.; Boháčová, J.; Vojvodíková, B. Influence of Fly Ash Denitrification on Properties of Hybrid Alkali-Activated Composites. *Crystals* **2022**, *12*, 633. [[CrossRef](#)]
160. Jimenez, A.M.F.; Garcia-Lodeiro, I.; Maltseva, O.; Palomo, A. Mechanical-Chemical Activation of Coal Fly Ashes: An Effective Way for Recycling and Make Cementitious Materials. *Front. Mater.* **2019**, *6*, 51. [[CrossRef](#)]
161. Pavithra, P.; Reddy, M.S.; Dinakar, P.; Rao, B.H.; Satpathy, B.; Mohanty, A. A mix design procedure for geopolymer concrete with fly ash. *J. Clean. Prod.* **2016**, *133*, 117–125. [[CrossRef](#)]
162. Kurtoglu, A.E.; Alzebaree, R.; Aljumaili, O.; Nis, A.; Gulsan, M.E.; Humur, G.; Cevik, A. Mechanical and durability properties of fly ash and slag based geopolymer concrete. *Adv. Concr. Constr.* **2018**, *6*, 345.
163. Okoye, F.; Durgaprasad, J.; Singh, N. Effect of silica fume on the mechanical properties of fly ash based-geopolymer concrete. *Ceram. Int.* **2016**, *42*, 3000–3006. [[CrossRef](#)]
164. Xie, T.; Ozbakkaloglu, T. Behavior of low-calcium fly and bottom ash-based geopolymer concrete cured at ambient temperature. *Ceram. Int.* **2015**, *41*, 5945–5958. [[CrossRef](#)]

165. Assi, L.; Ghahari, S.; Deaver, E.; Leaphart, D.; Ziehl, P. Improvement of the early and final compressive strength of fly ash-based geopolymers at ambient conditions. *Constr. Build. Mater.* **2016**, *123*, 806–813. [[CrossRef](#)]
166. Hager, I.; Sitarz, M.; Mróz, K. Fly-ash-based geopolymer mortar for high-temperature application—Effect of slag addition. *J. Clean. Prod.* **2021**, *316*, 128168. [[CrossRef](#)]
167. Embong, R.; Kusbiantoro, A.; Shafiq, N.; Nuruddin, M.F. Strength and microstructural properties of fly ash based geopolymer concrete containing high-calcium and water-absorptive aggregate. *J. Clean. Prod.* **2016**, *112*, 816–822. [[CrossRef](#)]
168. Sreevidya, V.; Anuradha, R.; Dinakar, D.; Venkatasubramani, R. Acid resistance of flyash based geopolymer mortar under ambient curing and heat curing. *Int. J. Eng. Sci. Technol.* **2012**, *4*, 681–684.
169. Duan, P.; Yan, C.; Luo, W.; Zhou, W. Effects of adding nano-TiO₂ on compressive strength, drying shrinkage, carbonation and microstructure of fluidized bed fly ash based geopolymer paste. *Constr. Build. Mater.* **2016**, *106*, 115–125. [[CrossRef](#)]
170. Rajak, M.; Rai, B. Effect of Micro Polypropylene Fibre on the Performance of Fly Ash-Based Geopolymer Concrete. *J. Appl. Eng. Sci.* **2019**, *9*, 97–108. [[CrossRef](#)]
171. Liu, M.Y.J.; Alengaram, U.J.; Santhanam, M.; Jumaat, M.Z.; Mo, K.H. Microstructural investigations of palm oil fuel ash and fly ash based binders in lightweight aggregate foamed geopolymer concrete. *Constr. Build. Mater.* **2016**, *120*, 112–122. [[CrossRef](#)]
172. Park, Y.; Abolmaali, A.; Kim, Y.H.; Ghahremannejad, M. Compressive strength of fly ash-based geopolymer concrete with crumb rubber partially replacing sand. *Constr. Build. Mater.* **2016**, *118*, 43–51. [[CrossRef](#)]
173. Khan, M.; Castel, A.; Akbarnezhad, A.; Foster, S.; Smith, M. Utilisation of steel furnace slag coarse aggregate in a low calcium fly ash geopolymer concrete. *Cem. Concr. Res.* **2016**, *89*, 220–229. [[CrossRef](#)]
174. Assaedi, H.; Shaikh, F.U.A.; Low, I.M. Influence of mixing methods of nano silica on the microstructural and mechanical properties of flax fabric reinforced geopolymer composites. *Constr. Build. Mater.* **2016**, *123*, 541–552. [[CrossRef](#)]
175. Gunasekara, C.; Law, D.; Setunge, S. Long term permeation properties of different fly ash geopolymer concretes. *Constr. Build. Mater.* **2016**, *124*, 352–362. [[CrossRef](#)]
176. Leong, H.Y.; Ong, D.E.L.; Sanjayan, J.; Nazari, A. Suitability of Sarawak and Gladstone fly ash to produce geopolymers: A physical, chemical, mechanical, mineralogical and microstructural analysis. *Ceram. Int.* **2016**, *42*, 9613–9620. [[CrossRef](#)]
177. Huiskes, D.M.A.; Keulen, A.; Yu, Q.L.; Brouwers, H.J.H. Design and performance evaluation of ultra-lightweight geopolymer concrete. *Mater. Des.* **2016**, *89*, 516–526. [[CrossRef](#)]
178. Zeng, S.; Wang, J. Characterization of mechanical and electric properties of geopolymers synthesized using four locally available fly ashes. *Constr. Build. Mater.* **2016**, *121*, 386–399. [[CrossRef](#)]
179. Tho-In, T.; Sata, V.; Boonserm, K.; Chindapasirt, P. Compressive strength and microstructure analysis of geopolymer paste using waste glass powder and fly ash. *J. Clean. Prod.* **2018**, *172*, 2892–2898. [[CrossRef](#)]
180. Das, S.; Yang, P.; Singh, S.S.; Mertens, J.C.; Xiao, X.; Chawla, N.; Neithalath, N. Effective properties of a fly ash geopolymer: Synergistic application of X-ray synchrotron tomography, nanoindentation, and homogenization models. *Cem. Concr. Res.* **2015**, *78*, 252–262. [[CrossRef](#)]
181. Pilehvar, S.; Cao, V.D.; Szczotok, A.M.; Carmona, M.; Valentini, L.; Lanzón, M.; Pamies, R.; Kjøniksen, A.-L. Physical and mechanical properties of fly ash and slag geopolymer concrete containing different types of micro-encapsulated phase change materials. *Constr. Build. Mater.* **2018**, *173*, 28–39. [[CrossRef](#)]
182. Blissett, R.S.; Rowson, N.A. A review of the multi-component utilisation of coal fly ash. *Fuel* **2012**, *97*, 1–23. [[CrossRef](#)]
183. Bhatt, A.; Priyadarshini, S.; Mohanakrishnan, A.A.; Abri, A.; Sattler, M.; Techapaphawit, S. Physical, chemical, and geotechnical properties of coal fly ash: A global review. *Case Stud. Constr. Mater.* **2019**, *11*, e00263, Erratum in *Case Stud. Constr. Mater.* **2021**, *14*, e00486. [[CrossRef](#)]
184. Korniejenko, K.; Halyag, N.P.; Mucsi, G. Fly ash as a raw material for geopolymerisation—chemical composition and physical properties. *IOP Conf. Ser. Mater. Sci. Eng.* **2019**, *706*, 012002. [[CrossRef](#)]
185. Chindapasirt, P.; Phoo-Ngernkham, T.; Hanjitsuwan, S.; Horpibulsuk, S.; Poowancum, A.; Injorhor, B. Effect of calcium-rich compounds on setting time and strength development of alkali-activated fly ash cured at ambient temperature. *Case Stud. Constr. Mater.* **2018**, *9*, e00198. [[CrossRef](#)]
186. Yadav, V.K.; Fulekar, M.H. Advances in Methods for Recovery of Ferrous, Alumina, and Silica Nanoparticles from Fly Ash Waste. *Ceramics* **2020**, *3*, 384–420. [[CrossRef](#)]
187. Nyale, S.M.; Eze, C.P.; Akinyeye, R.O.; Gitari, W.M.; Akinyemi, S.A.; Fatoba, O.O.; Petrik, L.F. The leaching behaviour and geochemical fractionation of trace elements in hydraulically disposed weathered coal fly ash. *J. Environ. Sci. Health Part A* **2013**, *49*, 233–242. [[CrossRef](#)]
188. Tiwari, M.; Sahu, S.K.; Bhangare, R.C.; Ajmal, P.Y.; Pandit, G.G. Elemental characterization of coal, fly ash, and bottom ash using an energy dispersive X-ray fluorescence technique. *Appl. Radiat. Isot.* **2014**, *90*, 53–57. [[CrossRef](#)]
189. Neupane, G.; Donahoe, R.J. Leachability of elements in alkaline and acidic coal fly ash samples during batch and column leaching tests. *Fuel* **2013**, *104*, 758–770. [[CrossRef](#)]
190. Shibayama, A.; Kim, Y.; Harjanto, S.; Sugai, Y.; Okada, K.; Fujita, T. Remediation of contaminated soil by fly ash containing dioxins from incineration by using flotation. *Mater. Trans.* **2005**, *46*, 990–995. [[CrossRef](#)]
191. Nomura, Y.; Fujiwara, K.; Terada, A.; Nakai, S.; Hosomi, M. Prevention of lead leaching from fly ashes by mechanochemical treatment. *Waste Manag.* **2010**, *30*, 1290–1295. [[CrossRef](#)] [[PubMed](#)]
192. Slanička, Š. The influence of fly ash fineness on the strength of concrete. *Cem. Concr. Res.* **1991**, *21*, 285–296. [[CrossRef](#)]

193. Erdoğdu, K.; Türker, P. Effects of fly ash particle size on strength of portland cement fly ash mortars. *Cem. Concr. Res.* **1998**, *28*, 1217–1222. [[CrossRef](#)]
194. Chindapasirt, P.; Chotithanorm, C.; Cao, H.; Sirivivatnanon, V. Influence of fly ash fineness on the chloride penetration of concrete. *Constr. Build. Mater.* **2007**, *21*, 356–361. [[CrossRef](#)]
195. Chindapasirt, P.; Jaturapitakkul, C.; Sinsiri, T. Effect of fly ash fineness on microstructure of blended cement paste. *Constr. Build. Mater.* **2007**, *21*, 1534–1541. [[CrossRef](#)]
196. Chindapasirt, P.; Homwuttiwong, S.; Sirivivatnanon, V. Influence of fly ash fineness on strength, drying shrinkage and sulfate resistance of blended cement mortar. *Cem. Concr. Res.* **2004**, *34*, 1087–1092. [[CrossRef](#)]
197. Jones, M.; McCarthy, A.; Booth, A.; Jones, R. Characteristics of the ultrafine component of fly ash. *Fuel* **2006**, *85*, 2250–2259. [[CrossRef](#)]
198. Yazici, S.; Arel, H.S. Effects of fly ash fineness on the mechanical properties of concrete. *Sadhana* **2012**, *37*, 389–403. [[CrossRef](#)]
199. Vassilev, S.V.; Vassileva, C.G. A new approach for the classification of coal fly ashes based on their origin, composition, properties, and behaviour. *Fuel* **2007**, *86*, 1490–1512. [[CrossRef](#)]
200. ASTM-C618-8a; *Standard Specification for Coal Fly Ash and Raw or Calcined Natural Pozzolan for Use in Concrete*; ASTM International: West Conshohocken, PA, USA, 2009.
201. Bankowski, P.; Zou, L.; Hodges, R. Reduction of metal leaching in brown coal fly ash using geopolymers. *J. Hazard. Mater.* **2004**, *114*, 59–67. [[CrossRef](#)] [[PubMed](#)]
202. Antiohos, S.; Tsimas, S. A novel way to upgrade the coarse part of a high calcium fly ash for reuse into cement systems. *Waste Manag.* **2007**, *27*, 675–683. [[CrossRef](#)]
203. Medhat, H.; Michail, D. The effect of fly ash composition on the expansion of concrete due to alkali silica reaction. *Cem. Concr. Res.* **2000**, *30*, 1063–1072.
204. Wedding, P.; Dunstan, E. A Possible Method for Identifying Fly Ashes That Will Improve the Sulfate Resistance of Concretes. *Cem. Concr. Aggregates* **1980**, *2*, 20–30. [[CrossRef](#)]
205. Smith, R. Is the available alkali test a good durability predictor for fly ash concrete incorporating reactive aggregate. In Proceedings of the MRS Symposium, Pittsburgh, PA, USA, 30 November–5 December 1988; pp. 249–256.
206. Odler, I. *Special Inorganic Cements*; CRC Press: London, UK, 2009.
207. Diamond, S. Effects of two Danish fly ashes on alkali contents of pore solutions of cement-fly ash pastes. *Cem. Concr. Res.* **1981**, *11*, 383–394. [[CrossRef](#)]
208. Joshi, R.C.; Lohtia, R.P. *Fly Ash in Concrete Production, Properties and Uses*; Gordon and Breach Science Publishers: Amsterdam, The Netherlands, 1997.
209. Temuujin, J.; Van Riessen, A. Effect of fly ash preliminary calcination on the properties of geopolymer. *J. Hazard. Mater.* **2009**, *164*, 634–639. [[CrossRef](#)] [[PubMed](#)]
210. McCarthy, G.; Solem, J.; Manz, O.; Hassett, D. *Use of a Database of Chemical, Mineralogical, and Physical Properties of North American Fly Ash to Study the Nature of Fly Ash and Its Utilization as a Mineral Admixture in Concrete*; Materials Research Society: Boston, MA, USA, 1989; p. 178.
211. Durdzinski, P.T.; Snellings, R.; Dunant, C.F.; Haha, M.B.; Scrivener, K.L. Fly ash as an assemblage of model Ca-Mg-Naealuminosilicate glasses. *Cem. Concr. Res.* **2015**, *78*, 263–272. [[CrossRef](#)]
212. Sakai, E.; Miyahara, S.; Ohsawa, S.; Lee, S.-H.; Daimon, M. Hydration of fly ash cement. *Cem. Concr. Res.* **2005**, *35*, 1135–1140. [[CrossRef](#)]
213. Tkaczewska, E. Effect of size fraction and glass structure of siliceous fly ashes on fly ash cement hydration. *J. Ind. Eng. Chem.* **2014**, *20*, 315–321. [[CrossRef](#)]
214. Malhotra, V. Durability of concrete incorporating high-volume of low-calcium (ASTM Class F) fly ash. *Cem. Concr. Compos.* **1990**, *12*, 271–277. [[CrossRef](#)]
215. Sobolev, K.; Vivian, I.F.; Saha, R.; Wasi, N.M.W.; Saltibus, N.E. The effect of fly ash on the rheological properties of bituminous materials. *Fuel* **2014**, *116*, 471–477. [[CrossRef](#)]
216. Rubel, A.; Andrews, R.; Gonzalez, R.; Groppo, J.; Robl, T. Adsorption of Hg and NO_x on coal by-products. *Fuel* **2005**, *84*, 911–916. [[CrossRef](#)]
217. Pereira, C.F.; Luna, Y.; Querol, X.; Antenucci, D.; Vale, J. Waste stabilization/solidification of an electric arc furnace dust using fly ash-based geopolymers. *Fuel* **2009**, *88*, 1185–1193. [[CrossRef](#)]
218. Ukwattage, N.; Ranjith, P.; Bouazza, M. The use of coal combustion fly ash as a soil amendment in agricultural lands (with comments on its potential to improve food security and sequester carbon). *Fuel* **2013**, *109*, 400–408. [[CrossRef](#)]
219. Teixeira, E.R.; Mateus, R.; Camões, A.; Bragança, L.; Branco, F.G. Comparative environmental life-cycle analysis of concretes using biomass and coal fly ashes as partial cement replacement material. *J. Clean. Prod.* **2016**, *112*, 2221–2230. [[CrossRef](#)]
220. Chang, H.-L.; Shih, W.-H. Synthesis of Zeolites A and X from Fly Ashes and Their Ion-Exchange Behavior with Cobalt Ions. *Ind. Eng. Chem. Res.* **2000**, *39*, 4185–4191. [[CrossRef](#)]
221. Luhar, S.; Cheng, T.W.; Nicolaidis, D.; Luhar, I.; Pnias, D.; Sakkas, K. Valorisation of glass wastes for the development of geopolymer composites—Durability, thermal and microstructural properties: A review. *Constr. Build. Mater.* **2019**, *222*, 673–687. [[CrossRef](#)]

222. Asokan, P.; Saxena, M.; Asolekar, S.R. Coal combustion residues environmental implications and recycling potentials. *Resour. Conserv. Recycl.* **2005**, *43*, 239–262. [[CrossRef](#)]
223. Heidrich, C.; Feuerborn, H.-J.; Weir, A. Coal combustion products: A global perspective. In Proceedings of the 2013 World of Coal Ash (WOCA) Conference, Lexington, KY, USA, 22–25 April 2013.
224. Kovler, K. Radiological constraints of using building materials and industrial by-products in construction. *Constr. Build. Mater.* **2009**, *23*, 246–253. [[CrossRef](#)]
225. Luhar, S.; Cheng, T.W.; Nicolaidis, D.; Luhar, I.; Panias, D.; Sakkas, K. Valorisation of glass waste for development of Geopolymer composites—Mechanical properties and rheological characteristics: A review. *Constr. Build. Mater.* **2019**, *220*, 547–564. [[CrossRef](#)]
226. McLellan, B.C.; Williams, R.P.; Lay, J.; van Riessen, A.; Corder, G.D. Costs and carbon emissions for geopolymer pastes in comparison to ordinary portland cement. *J. Clean. Prod.* **2011**, *19*, 1080–1090. [[CrossRef](#)]
227. Jen, G.; Skalamprinos, S.; Whittaker, M.; Galan, I.; Imbabi, M.S.; Glasser, F.P. The impact of intrinsic anhydrite in an experimental calcium sulfoaluminate cement from a novel, carbon-minimized production process. *Mater. Struct.* **2017**, *50*, 144. [[CrossRef](#)]
228. Şahmaran, M.; Li, V.C. Durability properties of micro-cracked ECC containing high volumes fly ash. *Cem. Concr. Res.* **2009**, *39*, 1033–1043. [[CrossRef](#)]
229. Nath, S.K.; Mukherjee, S.; Maitra, S.; Kumar, S. Kinetics study of geopolymerization of fly ash using isothermal conduction calorimetry. *J. Therm. Anal.* **2016**, *127*, 1953–1961. [[CrossRef](#)]
230. Steins, P.; Poulesquen, A.; Diat, O.; Frizon, F. Structural Evolution during Geopolymerization from an Early Age to Consolidated Material. *Langmuir* **2012**, *28*, 8502–8510. [[CrossRef](#)] [[PubMed](#)]
231. Dimas, D.; Giannopoulou, I.; Panias, D. Polymerization in sodium silicate solutions: A fundamental process in geopolymerization technology. *J. Mater. Sci.* **2009**, *44*, 3719–3730. [[CrossRef](#)]
232. Davidovits, J. 30 years of successes and failures in geopolymer applications, market trends and potential breakthroughs. In Proceedings of the Geopolymer 2002 Conference, Melbourne, Australia, 28–29 October 2002.
233. He, J.; Zhang, J.; Yu, Y.; Zhang, G. The strength and microstructure of two geopolymers derived from metakaolin and red mud fly ash admixture: A comparative study. *Constr. Build. Mater.* **2012**, *30*, 80–91. [[CrossRef](#)]
234. Duxson, P.; Provis, J.L.; Lukey, G.C.; Mallicoat, S.W.; Kriven, W.M.; van Deventer, J.S.J. Understanding the relationship between geopolymer composition, microstructure and mechanical properties. *Colloids Surf. A Physicochem. Eng. Asp.* **2005**, *269*, 47–58. [[CrossRef](#)]
235. Kriven, W.M.; Bell, J.L.; Gordon, M. Microstructure and Microchemistry of Fully-Reacted Geopolymers and Geopolymer Matrix Composites. *Ceram. Trans.* **2006**, *153*, 227–250.
236. Xu, H.; van Deventer, J.S.J. The geopolymerisation of natural alumino-silicates. In Proceedings of the 2nd International Conference on Geopolymer, Saint-Quentin, France, 30 June–2 July 1999; pp. 43–63.
237. Lizcano, M.; Kim, H.S.; Basu, S.; Radovic, M. Mechanical properties of sodium and potassium activated metakaolin-based geopolymers. *J. Mater. Sci.* **2011**, *47*, 2607–2616. [[CrossRef](#)]
238. Duxson, P.; Lukey, G.C.; Separovic, F.; van Deventer, J.S.J. Effect of Alkali Cations on Aluminum Incorporation in Geopolymeric Gels. *Ind. Eng. Chem. Res.* **2005**, *44*, 832–839. [[CrossRef](#)]
239. Ma, Y.; Hu, J.; Ye, G. The pore structure and permeability of alkali activated fly ash. *Fuel* **2013**, *104*, 771–780. [[CrossRef](#)]
240. Rattanasak, U.; Pankhet, K.; Chindaprasirt, P. Effect of chemical admixtures on properties of high-calcium fly ash geopolymer. *Int. J. Miner. Met. Mater.* **2011**, *18*, 364–369. [[CrossRef](#)]
241. Diaz, E.; Allouche, E.; Eklund, S. Factors affecting the suitability of fly ash as source material for geopolymers. *Fuel* **2010**, *89*, 992–996. [[CrossRef](#)]
242. Geetha, S.; Ramamurthy, K. Properties of geopolymerised low-calcium bottom ash aggregate cured at ambient temperature. *Cem. Concr. Compos.* **2013**, *43*, 20–30. [[CrossRef](#)]
243. Hanjitsuwan, S.; Hunpratub, S.; Thongbai, P.; Maensiri, S.; Sata, V.; Chindaprasirt, P. Effects of NaOH concentrations on physical and electrical properties of high calcium fly ash geopolymer paste. *Cem. Concr. Compos.* **2014**, *45*, 9–14. [[CrossRef](#)]
244. Hardjito, D.; Wallah, S.; Sumajouw, D.; Rangan, B. On the development of fly ash-based geopolymer concrete. *ACI Mater. J.* **2004**, *101*, 467–472.
245. Li, Z.; Liu, S. Influence of Slag as Additive on Compressive Strength of Fly Ash-Based Geopolymer. *J. Mater. Civ. Eng.* **2007**, *19*, 470–474. [[CrossRef](#)]
246. Idawati, I.; Bernal, S.A.; Provis, J.L.; Nicolas, S.R.; Hamdan, S.; van Deventer, J.S.J. Modification of phase evolution in alkali-activated blast furnace slag by the incorporation of fly ash. *Cem. Concr. Compos.* **2014**, *45*, 125–135.
247. Kumar, S.; Kumar, R.; Mehrotra, S.P. Influence of granulated blast furnace slag on the reaction, structure and properties of fly ash based geopolymer. *J. Mater. Sci.* **2010**, *45*, 607–615. [[CrossRef](#)]
248. Yang, T.; Yao, X.; Zhang, Z.; Wang, H. Mechanical property and structure of alkali-activated fly ash and slag blends. *J. Sustain. Cem. Mater.* **2012**, *1*, 167–178. [[CrossRef](#)]
249. Piga, F.P.; Stoppa, L. Recovering metals from red mud generated during alumina production. *JOM* **1993**, *45*, 55–59. [[CrossRef](#)]
250. Fu, Q.; Xu, W.; Zhao, X.; Bu, M.; Yuan, Q.; Niu, D. The microstructure and durability of fly ash-based geopolymer concrete: A review. *Ceram. Int.* **2021**, *47*, 29550–29566. [[CrossRef](#)]

251. De Vargas, A.S.; Dal Molin, D.C.C.; Vilela, A.C.F.; da Silva, F.J.; Pavão, B.; Veit, H. The effects of Na₂O/SiO₂ molar ratio, curing temperature and age on compressive strength, morphology and microstructure of alkali-activated fly ash-based geopolymers. *Cem. Concr. Compos.* **2011**, *33*, 653–660. [[CrossRef](#)]
252. Helmy, A.I.I. Intermittent curing of fly ash geopolymer mortar. *Constr. Build. Mater.* **2016**, *110*, 54–64. [[CrossRef](#)]
253. Criado, M.; Palomo, A.; Jimenez, A.M.F. Alkali activation of fly ashes. Part 1: Effect of curing conditions on the carbonation of the reaction products. *Fuel* **2005**, *84*, 2048–2054. [[CrossRef](#)]
254. Rattanasak, U.; Chindaprasirt, P. Influence of NaOH solution on the synthesis of fly ash geopolymer. *Miner. Eng.* **2009**, *22*, 1073–1078. [[CrossRef](#)]
255. Yang, T.; Yao, X.; Zhang, Z. Geopolymer prepared with high-magnesium nickel slag: Characterization of properties and microstructure. *Constr. Build. Mater.* **2014**, *59*, 188–194. [[CrossRef](#)]
256. Jang, J.G.; Lee, N.K.; Lee, H.K. Fresh and hardened properties of alkali-activated fly ash/slag pastes with superplasticizers. *Constr. Build. Mater.* **2014**, *50*, 169–176. [[CrossRef](#)]
257. Wang, W.-C.; Wang, H.-Y.; Lo, M.-H. The fresh and engineering properties of alkali activated slag as a function of fly ash replacement and alkali concentration. *Constr. Build. Mater.* **2015**, *84*, 224–229. [[CrossRef](#)]
258. Deb, P.S.; Nath, P.; Sarker, P.K. The effects of ground granulated blast-furnace slag blending with fly ash and activator content on the workability and strength properties of geopolymer concrete cured at ambient temperature. *Mater. Des.* **2014**, *62*, 32–39. [[CrossRef](#)]
259. Xu, H.; Li, Q.; Shen, L.; Zhang, M.; Zhai, J. Low-reactive circulating fluidized bed combustion (CFBC) fly ashes as source material for geopolymer synthesis. *Waste Manag.* **2010**, *30*, 57–62. [[CrossRef](#)] [[PubMed](#)]
260. Nazari, A.; Bagheri, A.; Riahi, S. Properties of geopolymer with seeded fly ash and rice husk bark ash. *Mater. Sci. Eng. A* **2011**, *528*, 7395–7401. [[CrossRef](#)]
261. Songpiriyakij, S.; Kubprasit, T.; Jaturapitakkul, C.; Chindaprasirt, P. Compressive strength and degree of reaction of biomass- and fly ash-based geopolymer. *Constr. Build. Mater.* **2010**, *24*, 236–240. [[CrossRef](#)]
262. Zhang, M.; El-Korchi, T.; Zhang, G.P.; Liang, J.Y.; Tao, M.J. Synthesis factors affecting mechanical properties, microstructure, and chemical composition of red mud-fly ash-based geopolymers. *Fuel* **2014**, *134*, 315–325. [[CrossRef](#)]
263. Schmucker, M.; Mackenzie, J.D.M. Microstructure of sodium polysialate siloxo geopolymer. *Ceram. Int.* **2005**, *31*, 433–440. [[CrossRef](#)]
264. Leung, C.K.Y.; Pheerapha, T. Very high early strength of microwave cured concrete. *Cem. Concr. Res.* **1995**, *25*, 136–146. [[CrossRef](#)]
265. Somna, K.; Jaturapitakkul, C.; Kajitvichyanukul, P.; Chindaprasirt, P. NaOH-activated ground fly ash geopolymer cured at ambient temperature. *Fuel* **2011**, *90*, 2118–2124. [[CrossRef](#)]
266. Nasvi, M.M.; Gamage, R.P.; Jay, S. Geopolymer as well cement and the variation of its mechanical behavior with curing temperature. *Greenh. Gases: Sci. Technol.* **2011**, *2*, 46–58. [[CrossRef](#)]
267. Kim, B.-J.; Yi, C.; Kang, K.-I. Microwave curing of alkali-activated binder using hwangtoh without calcination. *Constr. Build. Mater.* **2015**, *98*, 465–475. [[CrossRef](#)]
268. Chindaprasirt, P.; Rattanasak, U.; Taebuanhuad, S. Role of microwave radiation in curing the fly ash geopolymer. *Adv. Powder Technol.* **2013**, *24*, 703–707. [[CrossRef](#)]
269. Lee, B.; Kim, G.; Kim, R.; Cho, B.; Lee, S.; Chon, C.-M. Strength development properties of geopolymer paste and mortar with respect to amorphous Si/Al ratio of fly ash. *Constr. Build. Mater.* **2017**, *151*, 512–519. [[CrossRef](#)]
270. Zhuang, X.Y.; Chen, L.; Komarneni, S.; Zhou, C.H.; Tong, D.S.; Yang, H.M.; Yu, W.H.; Wang, H. Fly ash-based geopolymer: Clean production, properties and applications. *J. Clean. Prod.* **2016**, *125*, 253–267. [[CrossRef](#)]
271. Zhang, H.Y.; Kodur, V.; Wu, B.; Cao, L.; Wang, F. Thermal behavior and mechanical properties of geopolymer mortar after exposure to elevated temperatures. *Constr. Build. Mater.* **2016**, *109*, 17–24. [[CrossRef](#)]
272. Adak, D.; Sarker, M.; Mandal, S. Effect of nano-silica on strength and durability of fly ash based geopolymer mortar. *Constr. Build. Mater.* **2014**, *70*, 453–459. [[CrossRef](#)]
273. Al-Majidi, M.H.; Lampropoulos, A.; Cundy, A.; Meikle, S. Development of geopolymer mortar under ambient temperature for in situ applications. *Constr. Build. Mater.* **2016**, *120*, 198–211. [[CrossRef](#)]
274. Collins, F.; Sanjayan, J. Early Age Strength and Workability of Slag Pastes Activated by NaOH and Na₂CO₃. *Cem. Concr. Res.* **1998**, *28*, 655–664. [[CrossRef](#)]
275. Rangan, B.V. Studies on fly-ash based geopolymer concrete. *Malays. Constr. Res. J.* **2008**, *3*, 1–20.
276. Nath, P.; Sarker, P.K. Flexural strength and elastic modulus of ambient-cured blended low-calcium fly ash geopolymer concrete. *Constr. Build. Mater.* **2017**, *130*, 22–31. [[CrossRef](#)]
277. Chindaprasirt, P.; Chalee, W. Effect of sodium hydroxide concentration on chloride penetration and steel corrosion of fly ash-based geopolymer concrete under marine site. *Constr. Build. Mater.* **2014**, *63*, 303–310. [[CrossRef](#)]
278. Ismail, I.; Bernal, S.A.; Provis, J.L.; Nicolas, R.S.; Brice, D.G.; Kilcullen, A.R.; Hamdan, S.; van Deventer, J.S. Influence of fly ash on the water and chloride permeability of alkali-activated slag mortars and concretes. *Constr. Build. Mater.* **2013**, *48*, 1187–1201. [[CrossRef](#)]
279. Yang, T.; Yao, X.; Zhang, Z.H. Quantification of chloride diffusion in fly asheslag-based geopolymers by X-ray fluorescence (XRF). *Constr. Build. Mater.* **2014**, *69*, 109–115. [[CrossRef](#)]

280. Bakharev, T. Durability of geopolymer materials in sodium and magnesium sulphate solutions. *Cem. Concr. Res.* **2005**, *35*, 1233–1246. [[CrossRef](#)]
281. Sukmak, P.; De Silva, P.; Horpibulsuk, S.; Chindaprasirt, P. Sulfate Resistance of Clay-Portland Cement and Clay High-Calcium Fly Ash Geopolymer. *J. Mater. Civ. Eng.* **2015**, *27*, 04014158. [[CrossRef](#)]
282. Ismail, I.; Bernal, S.A.; Provis, J.L.; Hamdan, S.; van Deventer, J.S. Microstructural changes in alkali activated fly ash/slag geopolymers with sulfate exposure. *Mater. Struct.* **2013**, *46*, 361–373. [[CrossRef](#)]
283. Puligilla, S.; Mondal, P. Role of slag in microstructural development and hardening of fly ash-slag geopolymer. *Cem. Concr. Res.* **2013**, *43*, 70–80. [[CrossRef](#)]
284. Bakharev, T. Resistance of geopolymer materials to acid attack. *Cem. Concr. Res.* **2005**, *35*, 658–670. [[CrossRef](#)]
285. Lloyd, R.R.; Provis, J.L.; Van Deventer, J.S.J. Acid resistance of inorganic polymer binders. 1. Corrosion rate. *Mater. Struct.* **2012**, *45*, 1–14. [[CrossRef](#)]
286. Nguyen, K.; Lee, Y.H.; Lee, J.; Ahn, N. Acid Resistance and Curing Properties for Green Fly Ash-geopolymer Concrete. *J. Asian Arch. Build. Eng.* **2013**, *12*, 317–322. [[CrossRef](#)]
287. Chindaprasirt, P.; Rattanasak, U.; Taebuanhuad, S. Resistance to acid and sulfate solutions of microwave-assisted high calcium fly ash geopolymer. *Mater. Struct.* **2013**, *46*, 375–381. [[CrossRef](#)]
288. Rickard, W.D.; Williams, R.; Temuujin, J.; van Riessen, A. Assessing the suitability of three Australian fly ashes as an aluminosilicate source for geopolymers in high temperature applications. *Mater. Sci. Eng. A* **2011**, *528*, 3390–3397. [[CrossRef](#)]
289. Razak, S.N.A.; Shafiq, N.; Guillaumat, L.; Farhan, S.A.; Lohana, V.K. Fire-Exposed Fly-Ash-Based Geopolymer Concrete: Effects of Burning Temperature on Mechanical and Microstructural Properties. *Materials* **2022**, *15*, 1884. [[CrossRef](#)] [[PubMed](#)]
290. Guerrieri, M.; Sanjayan, J.G. Behavior of combined fly ash/slag-based geopolymers when exposed to high temperatures. *Fire Mater.* **2010**, *34*, 163–175. [[CrossRef](#)]
291. Rickard, W.D.A.; van Riessen, A.; Walls, P. Thermal character of geopolymers synthesized from Class F fly ash containing high concentrations of iron and alpha quartz. *Int. J. Appl. Ceram. Technol.* **2010**, *7*, 81–88. [[CrossRef](#)]
292. Kong, D.L.Y.; Sanjayan, J.G.; Sagoe-Crentsil, K. Comparative performance of geopolymers made with metakaolin and fly ash after exposure to elevated temperatures. *Cem. Concr. Res.* **2007**, *37*, 1583–1589. [[CrossRef](#)]
293. Bakharev, T. Thermal behaviour of geopolymers prepared using class F fly ash and elevated temperature curing. *Cem. Concr. Res.* **2006**, *36*, 1134–1147. [[CrossRef](#)]
294. Rickard, W.D.A.; van Riessen, A. Performance of solid and cellular structured fly ash geopolymers exposed to a simulated fire. *Cem. Concr. Compos.* **2014**, *48*, 75–82. [[CrossRef](#)]
295. Dombrowski, K.; Buchwald, A.; Weil, M. The influence of calcium content on the structure and thermal performance of fly ash based geopolymers. *J. Mater. Sci.* **2006**, *42*, 3033–3043. [[CrossRef](#)]
296. Sarker, P.K.; Kelly, S.; Yao, Z. Effect of fire exposure on cracking, spalling and residual strength of fly ash geopolymer concrete. *Mater. Des.* **2014**, *63*, 584–592. [[CrossRef](#)]
297. Hobbs, D. Concrete deterioration: Causes, diagnosis, and minimising risk. *Int. Mater. Rev.* **2001**, *46*, 117–144. [[CrossRef](#)]
298. Temuujin, J.; Minjigmaa, A.; Davaabal, B.; Bayarzul, U.; Ankhtuya, A.; Jadambaa, T.; MacKenzie, K.J.D. Utilization of radioactive high-calcium Mongolian fly ash for the preparation of alkali-activated geopolymers for safe use as construction materials. *Ceram. Int.* **2014**, *40*, 16475–16483. [[CrossRef](#)]
299. Sun, P.J.; Wu, H.C. Chemical and freeze-thaw resistance of fly ash-based inorganic mortars. *Fuel* **2013**, *111*, 740–745. [[CrossRef](#)]
300. Brooks, R.; Bahadory, M.; Tovia, F.; Rostami, H. Properties of alkali-activated fly ash: High performance to lightweight. *Int. J. Sustain. Eng.* **2010**, *3*, 211–218. [[CrossRef](#)]
301. Pacheco-Torgal, F.; Jalali, S. Influence of sodium carbonate addition on the thermal reactivity of tungsten mine waste mud based binders. *Constr. Build. Mater.* **2010**, *24*, 56–60. [[CrossRef](#)]
302. Duxson, P.; Provis, J.L.; Lukey, G.C.; van Deventer, J.S.J. ³⁹K NMR of free potassium in geopolymers. *Ind. Eng. Chem. Res.* **2006**, *45*, 9208–9210.
303. Bortnovsky, O.; Dědeček, J.; Tvaruzkova, Z.; Sobalík, Z.; Šubrt, J. Metal Ions as Probes for Characterization of Geopolymer Materials. *J. Am. Ceram. Soc.* **2008**, *91*, 3052–3057. [[CrossRef](#)]
304. Zhang, Z.; Provis, J.L.; Reid, A.; Wang, H. Fly ash-based geopolymers: The relationship between composition, pore structure and efflorescence. *Cem. Concr. Res.* **2014**, *64*, 30–41. [[CrossRef](#)]
305. Lloyd, R.R.; Provis, J.L.; van Deventer, J.S. Pore solution composition and alkali diffusion in inorganic polymer cement. *Cem. Concr. Res.* **2010**, *40*, 1386–1392. [[CrossRef](#)]
306. Schneider, M.; Romer, M.; Tschudin, M.; Bolio, H. Sustainable cement production—Present and future. *Cem. Concr. Res.* **2011**, *41*, 642–650. [[CrossRef](#)]
307. Habert, G.; de Lacaillerie, J.D.E.; Roussel, N. An environmental evaluation of geopolymer based concrete production: Reviewing current research trends. *J. Clean. Prod.* **2011**, *19*, 1229–1238. [[CrossRef](#)]
308. Reddy, D.V.; Edouard, J.B.; Sobhan, K. Durability of fly ashebased geopolymer structural concrete in the marine environment. *J. Mater. Civ. Eng.* **2013**, *25*, 781–787. [[CrossRef](#)]
309. Kupwade-Patil, K.; Allouche, E.N. Impact of Alkali Silica Reaction on Fly Ash-Based Geopolymer Concrete. *J. Mater. Civ. Eng.* **2013**, *25*, 131–139. [[CrossRef](#)]

310. Topark-Ngarm, P.; Chindaprasirt, P.; Sata, V. Setting Time, Strength, and Bond of High-Calcium Fly Ash Geopolymer Concrete. *J. Mater. Civ. Eng.* **2015**, *27*, 04014198. [[CrossRef](#)]
311. Kong, D.L.; Sanjayan, J.G. Effect of elevated temperatures on geopolymer paste, mortar and concrete. *Cem. Concr. Res.* **2010**, *40*, 334–339. [[CrossRef](#)]
312. Sata, V.; Wongsu, A.; Chindaprasirt, P. Properties of pervious geopolymer concrete using recycled aggregates. *Constr. Build. Mater.* **2013**, *42*, 33–39. [[CrossRef](#)]
313. Nuaklong, P.; Sata, V.; Chindaprasirt, P. Influence of recycled aggregate on fly ash geopolymer concrete properties. *J. Clean. Prod.* **2016**, *112*, 2300–2307. [[CrossRef](#)]
314. Nematollahi, B.; Sanjayan, J. Effect of different superplasticizers and activator combinations on workability and strength of fly ash based geopolymer. *Mater. Des.* **2014**, *57*, 667–672. [[CrossRef](#)]
315. Nasvi, M.; Ranjith, P.; Sanjayan, J. The permeability of geopolymer at down-hole stress conditions: Application for carbon dioxide sequestration wells. *Appl. Energy* **2013**, *102*, 1391–1398. [[CrossRef](#)]
316. Nasvi, M.; Ranjith, P.; Sanjayan, J.; Bui, H.H. Effect of temperature on permeability of geopolymer: A primary well sealant for carbon capture and storage wells. *Fuel* **2014**, *117*, 354–363. [[CrossRef](#)]
317. Hardjito, D.; Wallah, S.E.; Sumajouw, D.M.J.; Rangan, B.V. Fly Ash Based Geopolymer Concrete. *Aust. J. Struct. Eng.* **2005**, *6*, 77–86. [[CrossRef](#)]
318. Lloyd, N.A.; Rangan, B.V. Geopolymer Concrete with Fly Ash. In Proceedings of the Second International Conference on Sustainable Construction Materials and Technologies, Ancone, Italy, 28–30 June 2010.
319. Pnias, D.; Giannopoulou, I.P.; Perraki, T. Effect of synthesis parameters on the mechanical properties of fly ash-based geopolymers. *Colloids Surf. A Phys. Chem. Eng. Asp.* **2007**, *301*, 246–254. [[CrossRef](#)]
320. Sofi, M.; Deventer, J.; Mendis, P.; Lukey, G.C. Engineering Properties of Inorganic Polymer Concretes (IPCs). *Cem. Concr. Res.* **2007**, *37*, 251–257. [[CrossRef](#)]
321. Rangan, B.V.; Wallah, S.E. *Low Calcium Fly Ash Based Geopolymer Concrete: Long Term Properties*; Research Report GC2; Faculty of Engineering Curtin University of Technology: Perth, Australia, 2006.
322. Fernandez, J.; Palomo, A. Characterization of Fly Ash: Potential Reactivity Alkaline Cements. *Fuel* **2003**, *82*, 2259–2265. [[CrossRef](#)]
323. Neville, A.M. *Properties of Concrete*, 4th and Final ed.; Pearson Education, Longman Group: Essex, UK, 2000.
324. Hardjito, D.; Wallah, S.E.; Sumajouw, D.M.; Rangan, B.V. Introducing Fly Ash-Based Geopolymer Concrete: Manufacture and Engineering Properties. In Proceedings of the Our World in Concrete and Structures International Conference, Singapore, 23–24 August 2005.
325. Cheema, D.S.; Lloyd, N.A.; Rangan, B.V. Durability of Geopolymer Concrete Box Culverts—A Green Alternative. In Proceedings of the 34th Conference on OurWorld in Concrete and Structures, Singapore, 16–18 August 2009.
326. Adam, A.A.; Molyneaux, T.C.K.; Patnaikuni, I.; Law, D.W. Strength, sorptivity and carbonation of geopolymer concrete. In *Challenges, Opportunities and Solutions in Structural Engineering and Construction*; CRC Press: Boca Raton, FL, USA, 2009.
327. Thokchom, S.; Ghosh, P.; Ghosh, S. Performance of Fly ash Based Geopolymer Mortars in Sulphate Solution. *J. Eng. Sci. Technol. Rev.* **2010**, *3*, 36–40. [[CrossRef](#)]
328. Anurag, M. Deepika, Namrata, Manish, Nidhi and Durga, Effect of concentration of alkaline liquid and Curing time on strength and water absorption Of geopolymer concrete. *ARPJ. Eng. Appl. Sci.* **2008**, *3*, 14–18.
329. Song, S.; Jennings, H.M. Pore solution chemistry of alkali-activated ground granulated blast-furnace slag. *Cem. Concr. Res.* **1999**, *29*, 159–170. [[CrossRef](#)]
330. Sathia, R.; Babu, K.G.; Santhanam, M. Durability study of low calcium fly ash geopolymer concrete. In Proceedings of the 3rd ACF International Conference ACF, Ho Chi Minh City, Vietnam, 11–13 November 2008.
331. Bakharev, T. Heat resistance of geopolymer materials prepared using class F fly ash. *J. Aust. Ceram. Soc.* **2006**, *42*, 34–44.
332. Wallah, S.E.; Hardjito, D.; Sumajouw, D.M.; Rangan, B.V. Sulfate and acid resistance of fly ash-based geopolymer concrete. In Proceedings of the Australian Structural Engineering Conference 2005, Newcastle, NSW, Australia, 11–14 September 2005; pp. 733–742.
333. Bakharev, T.; Sanjayan, J.G.; Cheng, J.B. Resistance of alkali-activated slag concrete to acid attack. *Cem. Concr. Res.* **2003**, *33*, 1607–1611. [[CrossRef](#)]
334. Song, X.J.; Marosszeky, M.M.; Munn, R. Durability of fly ash-based Geopolymer concrete against sulphuric acid attack. In Proceedings of the International Conference on Durability of Building Materials and Components, Lyon, France, 17–20 April 2005.
335. Olivia, M.; Nikraz, H. Corrosion Performance of Embedded Steel in Fly Ash Geopolymer Concrete by Impressed Voltage Method. In Proceedings of the 21st Australian Conference on the Mechanics of Structures and Materials, Melbourne, VIC, Australia, 7–10 December 2010; pp. 781–786.
336. Roy, D.M. Alkali-activated cements Opportunities and challenges. *Cem. Concr. Res.* **1999**, *29*, 249–254. [[CrossRef](#)]
337. Wallah, S.E.; Rangan, B.V. *Low-Calcium Fly Ash-Based Geopolymer Concrete: Long Term Properties*; Research Report GC3; Faculty of Engineering, Curtin University: Perth, Australia, 2006.
338. Rashad, A.M.; Zeedan, S.R. The effect of activator concentration on the residual compressive strength of alkali-activated fly ash paste subjected to thermal load. *Constr. Build. Mater.* **2011**, *25*, 3098–3107. [[CrossRef](#)]
339. Kong, D.L.Y.; Sanjayan, J.G. Damage behavior of geopolymer composites exposed to elevated temperatures. *Cem. Concr. Compos.* **2008**, *30*, 986–991. [[CrossRef](#)]

340. Luhar, S.; Chaudhary, S.; Luhar, I. Thermal resistance of fly ash based rubberized geopolymer concrete. *J. Build. Eng.* **2018**, *19*, 420–428. [[CrossRef](#)]
341. Pan, Z.; Sanjayan, J.G.; Rangan, B.V. An investigation of the mechanisms for strength gain or loss geopolymer mortar after exposure to elevated temperature. *J. Mater. Sci.* **2009**, *44*, 1873–1880. [[CrossRef](#)]
342. Ranjbar, N.; Mehrali, M.; Alengaram, U.J.; Metselaar, H.S.C.; Jummat, M.Z. Compressive strength and microstructural analysis of fly ash/palm oil fuel ash based geopolymer mortar under elevated temperatures. *Constr. Build. Mater.* **2014**, *65*, 114–121. [[CrossRef](#)]
343. Kong, D.L.Y.; Sanjayan, J.G.; Crentsil, K.S. Factors affecting the performance of metakaolingeopolymers to elevated temperatures. *J. Mater. Sci.* **2008**, *43*, 824–831. [[CrossRef](#)]
344. Pan, Z.; Sanjayan, J.G.; Collins, F. Effect of transient creep on compressive strength of geopolymer concrete for elevated temperature exposure. *Cem. Concr. Res.* **2014**, *56*, 182–189. [[CrossRef](#)]
345. Hussain, M.W.; Bhutta, M.A.R.; Azreen, M.; Ramadhansyah, P.J.; Mirza, J. Performance of blended ash geopolymer concrete at elevated temperature. *Mater. Struct.* **2015**, *48*, 709–720. [[CrossRef](#)]
346. Fan, F. Mechanical and Thermal Properties of Fly Ash-Based Geopolymer Cement. Master's Thesis, Louisiana State University, Baton Rouge, LA, USA, 2014.
347. Omar, A.A.; Bakri, A.M.; Kamarudin, H.; Nizar, I.K.; Saif, A.A. Effect of elevated temperatures on the thermal behaviour and mechanical performance of fly ash geopolymer paste, mortar and lightweight concrete. *Constr. Build. Mater.* **2014**, *50*, 377–387.
348. Zhang, Y.; Sun, W.; Li, Z. Infrared spectroscopy study of structural nature of geopolymeric products. *J. Wuhan Univ. Technol. Sci. Ed.* **2008**, *23*, 522–527. [[CrossRef](#)]
349. Chindapasirt, P.; Chareerat, T.; Sirivivatnanon, V. Workability and strength of coarse high calcium fly ash geopolymer. *Cem. Concr. Compos.* **2007**, *29*, 224–229. [[CrossRef](#)]
350. Jumrat, S.; Chatveera, B.; Rattanadecho, P. Dielectric properties and temperature profile of fly ash-based geopolymer mortar. *Int. Commun. Heat Mass Transf.* **2011**, *38*, 242–248. [[CrossRef](#)]
351. Sukmak, P.; Horpibulsuk, S.; Shen, S.L. Strength development in clay–fly ash geopolymer. *Constr. Build. Mater.* **2013**, *40*, 566–574. [[CrossRef](#)]
352. Rifaai, Y.; Yahia, A.; Mostafa, A.; Aggoun, S.; Kadri, E.H. Rheology of fly ash-based geopolymer: Effect of NaOH concentration. *Constr. Build. Mater.* **2019**, *223*, 583–594. [[CrossRef](#)]
353. Patankar, S.V.; Ghugal, Y.M.; Jamkar, S.S. Effect of Concentration of Sodium Hydroxide and Degree of Heat Curing on Fly Ash-Based Geopolymer Mortar. *Indian J. Mater. Sci.* **2014**, *2014*, 938789. [[CrossRef](#)]
354. Bhowmick, A.; Ghosh, S. Effect of synthesizing parameters on workability and compressive strength of fly ash based geopolymer mortar. *Int. J. Civ. Struct. Eng.* **2012**, *3*, 168–177.
355. Malkawi, A.B.; Nuruddin, M.F.; Fauzi, A.; Almattarneh, H.; Mohammed, B.S. Effects of Alkaline Solution on Properties of the HCFA Geopolymer Mortars. *Procedia Eng.* **2016**, *148*, 710–717. [[CrossRef](#)]
356. Lee, N.; Kim, E.; Lee, H. Mechanical properties and setting characteristics of geopolymer mortar using styrene-butadiene (SB) latex. *Constr. Build. Mater.* **2016**, *113*, 264–272. [[CrossRef](#)]
357. Sathonsaowaphak, A.; Chindapasirt, P.; Pimraksa, K. Workability and strength of lignite bottom ash geopolymer mortar. *J. Hazard. Mater.* **2009**, *168*, 44–50. [[CrossRef](#)] [[PubMed](#)]
358. Li, Q.; Chen, C.; Shen, L.; Zhai, J. Manufacturing F-fly ash based geopolymer mortars using CFBC bottom ash as fine aggregates. *J. Chem. Soc. Pak.* **2013**, *35*, 314–319.
359. Huseien, G.F.; Mirza, J.; Ismail, M.; Hussin, M.W. Influence of different curing temperatures and alkali activators on properties of GBFS geopolymer mortars containing fly ash and palm-oil fuel ash. *Constr. Build. Mater.* **2016**, *125*, 1229–1240. [[CrossRef](#)]
360. Islam, A.; Alengaram, U.J.; Jumaat, M.Z.; Bashar, I.I. The development of compressive strength of ground granulated blast furnace slag-palm oil fuel ash-fly ash based geopolymer mortar. *Mater. Des.* **2014**, *56*, 833–841. [[CrossRef](#)]
361. Phoo-ngernkham, T.; Hanjitsuwan, S.; Li, L.Y.; Damrongwiriyanupap, N.; Chindapasirt, P. Adhesion characterisation of Portland cement concrete and alkali-activated binders. *Adv. Cem. Res.* **2019**, *31*, 69–79. [[CrossRef](#)]
362. Temuujin, J.; van Riessen, A.; MacKenzie, K.J.D. Preparation and characterization of fly ash based geopolymer mortars. *Constr. Build Mater* **2010**, *24*, 1906–1910. [[CrossRef](#)]
363. Zejak, R.; Nikolic, I.; Blecic, D.; Radmilovic, V.; Radmilovic, V. Mechanical and microstructural properties of the fly-ash-based geopolymer paste and mortar. *Mater. Technol.* **2013**, *47*, 535–540.
364. Zhang, P.; Kang, L.; Zheng, Y.; Zhang, T.; Zhang, B. Influence of SiO₂/Na₂O molar ratio on mechanical properties and durability of metakaolin-fly ash blend alkali-activated sustainable mortar incorporating manufactured sand. *J. Mater. Res. Technol.* **2022**, *18*, 3553–3563. [[CrossRef](#)]
365. Kotwal, A.R.; Kim, Y.J.; Hu, J.; Sriraman, V. Characterization and Early Age Physical Properties of Ambient Cured Geopolymer Mortar Based on Class C Fly Ash. *Int. J. Concr. Struct. Mater.* **2014**, *9*, 35–43. [[CrossRef](#)]
366. Görhan, G.; Kürklü, G. The influence of the NaOH solution on the properties of the fly ash-based geopolymer mortar cured at different temperatures. *Compos. Part B Eng.* **2014**, *58*, 371–377. [[CrossRef](#)]
367. Bashar, I.I.; Alengaram, U.J.; Jumaat, M.Z.; Islam, A. The effect of variation of molarity of alkali activator and fine aggregate content on the compressive strength of the fly ash: Palm oil fuel ash based geopolymer mortar. *Adv. Mater. Sci. Eng.* **2014**, *2014*, 245473. [[CrossRef](#)]

368. Okba, S.H.; Nasr, E.S.A.; Helmy, A.I.; Yousef, I.A.L. Effect of thermal exposure on the mechanical properties of polymer adhesives. *Constr. Build. Mater.* **2017**, *135*, 490–504. [[CrossRef](#)]
369. Li, X.; Ma, X.; Zhang, S.; Zheng, E. Mechanical Properties and Microstructure of Class C Fly Ash-Based Geopolymer Paste and Mortar. *Materials* **2013**, *6*, 1485–1495. [[CrossRef](#)] [[PubMed](#)]
370. Adam, A.A.; Horiato, X. The Effect of Temperature and Duration of Curing on the Strength of Fly Ash Based Geopolymer Mortar. *Procedia Eng.* **2014**, *95*, 410–414. [[CrossRef](#)]
371. Narayanan, A.; Shanmugasundaram, P. An Experimental Investigation on Flyash-based Geopolymer Mortar under different curing regime for Thermal Analysis. *Energy Build.* **2017**, *138*, 539–545. [[CrossRef](#)]
372. Mallikarjuna Rao, G.; Gunneswara Rao, T.D. Final setting time and compressive strength of fly ash and GGBS-based geopolymer paste and mortar. *Arab. J. Sci. Eng.* **2015**, *40*, 3067–3074. [[CrossRef](#)]
373. Algaifi, H.A.; Mustafa Mohamed, A.; Alsuhaibani, E.; Shahidan, S.; Alrshoudi, F.; Huseien, G.F.; Bakar, S.A. Optimisation of GBFS, Fly Ash, and Nano-Silica Contents in Alkali-Activated Mortars. *Polymers* **2021**, *13*, 2750. [[CrossRef](#)] [[PubMed](#)]
374. Chuah, S.; Duan, W.; Pan, Z.; Hunter, E.; Korayem, A.; Zhao, X.; Collins, F.; Sanjayan, J. The properties of fly ash based geopolymer mortars made with dune sand. *Mater. Des.* **2016**, *92*, 571–578. [[CrossRef](#)]
375. Guades, E.J. Experimental investigation of the compressive and tensile strengths of geopolymer mortar: The effect of sand/fly ash (S/FA) ratio. *Constr. Build. Mater.* **2016**, *127*, 484–493. [[CrossRef](#)]
376. Cyr, M.; Idir, R.; Pointot, T. Properties of inorganic polymer (geopolymer) mortars made of glass cullet. *J. Mater. Sci.* **2012**, *47*, 2782–2797. [[CrossRef](#)]
377. Atis, C.D.; Gorur, E.B.; Karahan, O.; Bilim, C.; Ilkentapar, S.; Luga, E. Very high strength (120 MPa) class F fly ash geopolymer mortar activated at different NaOH amount, heat curing temperature and heat curing duration. *Constr. Build Mater.* **2015**, *96*, 673–678. [[CrossRef](#)]
378. Satya, Y.S.D.; Saputra, E.; Olivia, M. Performance of Blended Fly Ash (FA) and Palm Oil Fuel Ash (POFA) Geopolymer Mortar in Acidic Peat Environment. *Mater. Sci. Forum* **2016**, *841*, 83–89. [[CrossRef](#)]
379. Olivia, M.; Wulandari, C.; Sitompul, I.R.; Darmayanti, L.; Djauhari, Z. Study of Fly Ash (FA) and Palm Oil Fuel Ash (POFA) Geopolymer Mortar Resistance in Acidic Peat Environment. *Mater. Sci. Forum* **2016**, *841*, 126–132. [[CrossRef](#)]
380. Sreevidya, V.; Anuradha, R.; Thomas, T.; Venkatasubramani, R. Durability studies on fly ash geopolymer mortar under in ambient curing condition. *Asian J. Chem.* **2013**, *25*, 2497–2499. [[CrossRef](#)]
381. Abdollahnejad, Z.; Pacheco-Torgal, F.; Aguiar, J.; Jesus, C. Durability Performance of Fly Ash Based One-Part Geopolymer Mortars. *Key Eng. Mater.* **2015**, *634*, 113–120. [[CrossRef](#)]
382. Thokchom, S.; Ghosh, P.; Ghosh, S. Acid resistance of fly ash based geopolymer mortars. *Int. J. Recent Trends Eng. Technol.* **2009**, *1*, 36–40.
383. Kürklü, G. The effect of high temperature on the design of blast furnace slag and coarse fly ash-based geopolymer mortar. *Compos. Part B Eng.* **2016**, *92*, 9–18. [[CrossRef](#)]
384. Djobo, J.N.Y.; Elimbi, A.; Tchakouté, H.K.; Kumar, S. Mechanical properties and durability of volcanic ash based geopolymer mortars. *Constr. Build. Mater.* **2016**, *124*, 606–614. [[CrossRef](#)]
385. Abdulkareem, O.A.; Al Bakri, A.M.; Kamarudin, H.; Nizar, I.K.; Saif, A.A. Strength and porosity characterizations of blended biomass wood ash-fly ash-based geopolymer mortar. *AIP Conf. Proc.* **2018**, *2045*, 020096.
386. Kumar, E.M.; Ramamurthy, K. Influence of production on the strength, density and water absorption of aerated geopolymer paste and mortar using Class F fly ash. *Constr. Build. Mater.* **2017**, *156*, 1137–1149. [[CrossRef](#)]
387. Ling, Y.; Wang, K.; Fu, C. Shrinkage behavior of fly ash based geopolymer pastes with and without shrinkage reducing admixture. *Cem. Concr. Compos.* **2019**, *98*, 74–82. [[CrossRef](#)]
388. Zuda, L.; Pavlík, Z.; Rovnanikova, P.; Bayer, P.; Černý, R. Properties of Alkali Activated Aluminosilicate Material after Thermal Load. *Int. J. Thermophys.* **2006**, *27*, 1250–1263. [[CrossRef](#)]
389. Saha, S.; Rajasekaran, C. Enhancement of the properties of fly ash based geopolymer paste by incorporating ground granulated blast furnace slag. *Constr. Build. Mater.* **2017**, *146*, 615–620. [[CrossRef](#)]
390. Chindapasirt, P.; De Silva, P.; Sagoe-Crentsil, K.; Hanjitsuwan, S. Effect of SiO₂ and Al₂O₃ on the setting and hardening of high calcium fly ash-based geopolymer systems. *J. Mater. Sci.* **2012**, *47*, 4876–4883. [[CrossRef](#)]
391. Alonso, S.; Palomo, A. Calorimetric study of alkaline activation of calcium hydroxide–metakaolin solid mixtures. *Cem. Concr. Res.* **2001**, *31*, 25–30. [[CrossRef](#)]
392. Puertas, F.; Amat, T.; Vázquez, T. Behaviour of alkaline cement mortars reinforced with acrylic and polypropylene fibres. *Mater. Constr.* **2000**, *50*, 69–84. [[CrossRef](#)]
393. Fernández-Jiménez, A.; Palomo, A. Composition and microstructure of alkali activated fly ash binder: Effect of the activator. *Cem. Concr. Res.* **2005**, *35*, 1984–1992. [[CrossRef](#)]
394. Liu, G.; Florea, M.V.A.; Brouwers, H.J.H. Waste glass as binder in alkali activated slag–fly ash mortars. *Mater. Struct.* **2019**, *52*, 101. [[CrossRef](#)]
395. Chindapasirt, P.; Rattanasak, U.; Vongvoradit, P.; Jenjirapanya, S. Thermal treatment and utilization of Al-rich waste in high calcium fly ash geopolymeric materials. *Int. J. Miner. Met. Mater.* **2012**, *19*, 872–878. [[CrossRef](#)]
396. Fletcher, R.A.; MacKenzie, K.J.; Nicholson, C.L.; Shimada, S. The composition range of aluminosilicate geopolymers. *J. Eur. Ceram. Soc.* **2005**, *25*, 1471–1477. [[CrossRef](#)]

397. De Silva, P.; Sagoe-Crenstil, K.; Sirivivatnanon, V. Kinetics of geopolymerization: Role of Al_2O_3 and SiO_2 . *Cem. Concr. Res.* **2007**, *37*, 512–518. [CrossRef]
398. Temuujin, J.; Van Riessen, A.; Williams, R. Influence of calcium compounds on the mechanical properties of fly ash geopolymer pastes. *J. Hazard. Mater.* **2009**, *167*, 82–88. [CrossRef]
399. Guo, X.; Shi, H.; Dick, W.A. Compressive strength and microstructural characteristics of class C fly ash geopolymer. *Cem. Concr. Compos.* **2010**, *32*, 142–147. [CrossRef]
400. Mehta, P.K.; Monteiro, P.J. *Concrete Microstructure, Properties and Materials*; McGraw-Hill Education: New York, NY, USA, 2017.
401. Van Deventer, J.S.; San Nicolas, R.; Ismail, I.; Bernal, S.A.; Brice, D.G.; Provis, J.L. Microstructure and durability of alkali-activated materials as key parameters for standardization. *J. Sustain. Cem. Mater.* **2015**, *4*, 116–128. [CrossRef]
402. Weir, A.J.; Abrams, G.; Adolphsen, C.E.; Alexander, J.P.; Alvarez, M.; Amidei, D.; Baden, A.R.; Barish, B.C.; Barklow, T.; Barnett, B.A.; et al. A reanalysis of $\text{B}^0\text{-}\bar{\text{B}}^0$ mixing in e^+e^- annihilation at 29 GeV. *Phys. Lett. B* **1990**, *240*, 289–296. [CrossRef]
403. Brouwers, H.J.H.; Van Eijk, R.J. Fly ash reactivity: Extension and application of a shrinking core model and thermodynamic approach. *J. Mater. Sci.* **2002**, *37*, 2129–2141. [CrossRef]
404. Phoo-ngernkham, T.; Chindaprasirt, P.; Sata, V.; Hanjitsuwan, S.; Hatanaka, S. The effect of adding nano- SiO_2 and nano- Al_2O_3 on properties of high calcium fly ash geopolymer cured at ambient temperature. *Mater. Des.* **2014**, *55*, 58–65. [CrossRef]
405. Wongsu, A.; Boonserm, K.; Waisurasingha, C.; Sata, V.; Chindaprasirt, P. Use of municipal solid waste incinerator (MSWI) bottom ash in high calcium fly ash geopolymer matrix. *J. Clean. Prod.* **2017**, *148*, 49–59. [CrossRef]
406. Adak, D.; Sarkar, M.; Mandal, S. Structural performance of nano-silica modified fly-ash based geopolymer concrete. *Constr. Build. Mater.* **2017**, *135*, 430–439. [CrossRef]
407. Salih, M.A.; Ali, A.A.A.; Farzadnia, N. Characterization of mechanical and microstructural properties of palm oil fuel ash geopolymer cement paste. *Constr. Build. Mater.* **2014**, *65*, 592–603. [CrossRef]
408. Swanepoel, J.; Strydom, C. Utilisation of fly ash in a geopolymeric material. *Appl. Geochem.* **2002**, *17*, 1143–1148. [CrossRef]
409. Ghani, U.; Hussain, S.; Imtiaz, M.; Khan, S.A. Role of calcination on geopolymerization of lateritic clay by alkali treatment. *J. Saudi Chem. Soc.* **2021**, *25*, 101198. [CrossRef]
410. Gao, K.; Lin, K.L.; Wang, D.; Hwang, C.L.; Shiu, H.S.; Chang, Y.M.; Cheng, T.W. Effects $\text{SiO}_2/\text{Na}_2\text{O}$ molar ratio on mechanical properties and the microstructure of nano- SiO_2 metakaolin-based geopolymers. *Constr. Build. Mater.* **2014**, *53*, 503–510. [CrossRef]
411. Zawrah, M.; Gado, R.; Feltin, N.; Ducourtieux, S.; Devoille, L. Recycling and utilization assessment of waste fired clay bricks (Grog) with granulated blast-furnace slag for geopolymer production. *Process Saf. Environ. Prot.* **2016**, *103*, 237–251. [CrossRef]
412. Duan, P.; Yan, C.; Zhou, W.; Luo, W. Fresh properties, mechanical strength and microstructure of fly ash geopolymer paste reinforced with sawdust. *Constr. Build. Mater.* **2016**, *111*, 600–610. [CrossRef]
413. Okoye, F.; Durgaprasad, J.; Singh, N. Mechanical properties of alkali activated flyash/Kaolin based geopolymer concrete. *Constr. Build. Mater.* **2015**, *98*, 685–691. [CrossRef]
414. Cai, J.; Jiang, J.; Gao, X.; Ding, M. Improving the Mechanical Properties of Fly Ash-Based Geopolymer Composites with PVA Fiber and Powder. *Materials* **2022**, *15*, 2363. [CrossRef]
415. Kaze, C.R.; Adesina, A.; Lecomte-Nana, G.L.; Assaedi, H.; Alomayri, T.; Kamseu, E.; Melo, U.C. Physico-mechanical and microstructural properties of geopolymer binders synthesized with metakaolin and meta-halloysite as precursors. *Clean. Mater.* **2022**, *4*, 100070. [CrossRef]
416. Ramli, M.I.I.; Salleh, M.A.A.M.; Abdullah, M.M.A.B.; Aziz, I.H.; Ying, T.C.; Shahedan, N.F.; Kockelmann, W.; Fedrigo, A.; Sandu, A.V.; Vizureanu, P.; et al. The Influence of Sintering Temperature on the Pore Structure of an Alkali-Activated Kaolin-Based Geopolymer Ceramic. *Materials* **2022**, *15*, 2667. [CrossRef] [PubMed]
417. Kalombe, R.M.; Ojumu, V.T.; Eze, C.P.; Nyale, S.M.; Kevern, J.; Petrik, L.F. Fly Ash-Based Geopolymer Building Materials for Green and Sustainable Development. *Materials* **2020**, *13*, 5699. [CrossRef]
418. Luhar, S.; Chaudhary, S.; Dave, U.V. Effect of different type of curing on fly ash and Slag based geopolymer concrete. *Int. J. Civ. Struct. Environ. Infrastr. Eng. Res. Dev* **2016**, 69–78. Available online: https://www.researchgate.net/publication/309766349_Effect_of_Different_type_of_curing_on_fly_ash_and_slag_based_geopolymer_concrete (accessed on 20 April 2022).
419. Sanni, S.H.; Khadiranaikar, R.B. Performance of geopolymer concrete under severe environmental conditions. *Int. J. Civ. Struct. Eng.* **2012**, *3*, 396.
420. Luhar, S. *Fly Ash and Slag Based Geopolymer Concrete: Experimental Facts*; LAP Lambert Academic Publishing: Sunnysvale, CA, USA, 2016.
421. Cheng, T.W.; Chiu, J.P. Fire-resistant geopolymer produced by granulated blast furnace slag. *Miner. Eng.* **2003**, *16*, 205–210. [CrossRef]
422. World Bank. *Solid Waste Manage*; The World Bank Group: Washington, DC, USA, 2013.
423. European Union. *The EU in the World- Environment*, 2020th ed.; European Union, Ed.; Eurostat: Luxembourg City, Luxembourg, 2020.
424. Krautwurst, N.; Nicoleau, L.; Dietzsch, M.; Lieberwirth, I.; Labbez, C.; Fernandez- Martinez, A.; Van Driessche, A.E.S.; Barton, B.; Leukel, S.; Tremel, W. Twostep nucleation process of calcium silicate hydrate, the nanobrick of cement. *Chem. Mater.* **2018**, *30*, 2895–2904. [CrossRef]
425. Korniejenko, K.; Kozub, B.; Bağ, A.; Balamurugan, P.; Uthayakumar, M.; Furtos, G. Tackling the Circular Economy Challenges—Composites Recycling: Used Tyres, Wind Turbine Blades, and Solar Panels. *J. Compos. Sci.* **2021**, *5*, 243. [CrossRef]